Democratic Republic of Algeria and popular ministry of superior education and scientific research

Amar Thelidji-Laghouat University

Faculty of Science and Technology

Department of Mechanical Engineering

Industrial maintenance

Master memory

Theme

Mass Unbalance Default with Daubechies Wavelet

Submitted by:

- Benarous ali haroun
- Briki ibrahim abdelhak

Board of examiners:

Pr. K. RAYANE	Président	UAT Laghouat
Dr. S. BELAID	Examinateur	UAT Laghouat
Dr. A.D. HAMMOU	Encadreur	UAT Laghouat

College year 2023 / 2024

Thanking

We praise and thank Allah above all.

We would like to warmly thank our supervisor, Mr. Hammou Abdelkader Djilali, Lecturer at the Department of Mechanical Engineering, AMARE TLIDJE LAGHOUT UNIVERSITY and our master thesis supervisor for his help, availability and advice throughout this work.

We thank Mr. Rayane for agreeing to chair the jury.

We would also like to thank Mr. Belaid, who agreed to be an examiner for this memory.

We sincerely thank our parents and families for their understanding, support, and encouragement that helped us complete this memory. Many thanks to all the teachers of the Mechanical Engineering Department, my colleagues and all my friends.

Dedication

We would like to dedicate this project to the people who have been our constant support and inspiration throughout this journey.

To our parents, for their unwavering love, guidance, and encouragement. Your sacrifices and belief in us have been the cornerstone of our success, to our brothers and sisters, for their endless support, patience, and understanding. Your faith in us has been a source of strength, to our teachers who must see in this work the pride of a well-acquired knowledge, to our friends, for their companionship, motivation, and cheer. Your encouragement and support have kept us going.

Thank you all for being our pillars of strength. This project would not have been possible without your unwavering support and belief in us.

Abstract

In this study we used a fault simulator and MATLAB to compare Daubechies db4 wavelet analysis and FFT spectrum analysis for diagnosing unbalance faults under stationary and non-stationary speed conditions. FFT-based spectrum analysis excelled at identifying mass imbalance and misalignment faults during stationary operation, but struggled with resonance frequency detection. Conversely, the db4 wavelet analysis proved superior at detecting resonance frequencies and was more effective under non-stationary speeds. The complementary strengths suggest a combined approach could provide a more comprehensive mechanical fault diagnostic tool.

ملخص

في هذه الدراسة استخدمنا جهاز محاكاة الأخطاء و MATLAB لمقارنة تحليل المويجات Daubechies db4 وتحليل طيف FFTلتشخيص أخطاء عدم التوازن في ظل ظروف السرعة الثابتة وغير الثابتة. برع تحليل الطيف المعتمد على تحويل فوربيه السريع (FFT) في تحديد أخطاء عدم التوازن الشامل واختلال المحاذاة أثناء التشغيل الثابت، لكنه واجه صعوبات في اكتشاف التردد الرنيني. وعلى العكس من ذلك، أثبت تحليل المويجات db4 تفوقه في اكتشاف الترددات الرنينية وكان أكثر فعالية في ظل السرعات غير الثابتة. تشير نقاط القوة التكميلية إلى أن النهج المشترك يمكن أن يوفر أداة أكثر شمولاً لتشخيص الأعطال الميكانيكية.

Résumé

Dans cette étude, nous avons utilisé un simulateur de défauts et MATLAB pour comparer l'analyse par ondelettes db4 de Daubechies et l'analyse du spectre FFT pour diagnostiquer les défauts de déséquilibre dans des conditions de vitesse stationnaires et non stationnaires. L'analyse spectrale basée sur la FFT a excellé dans l'identification des déséquilibres de masse et des défauts d'alignement lors d'un fonctionnement stationnaire, mais a eu du mal à détecter la fréquence de résonance. À l'inverse, l'analyse par ondelettes db4 s'est avérée supérieure dans la détection des fréquences de résonance et plus efficace à des vitesses non stationnaires. Les atouts complémentaires suggèrent qu'une approche combinée pourrait fournir un outil de diagnostic des défauts mécaniques plus complet.

Table of content

LIST OF TABLE

List of Figures

Symbols

$\otimes$	The Kronecker (tensor) product
$\boldsymbol{H(n)}$	matrix of the discrete Haar functions
$\boldsymbol{\varphi(x)}$	the scaling function
$\boldsymbol{N}$	number of vanishing moments
$\boldsymbol{g_k}$	wavelet filter coefficients
$\boldsymbol{\psi_{m,n}}$	the wavelet function
$\boldsymbol{a_0}$	fixed dilation parameter
$\boldsymbol{b_0}$	location parameter
$\boldsymbol{T_n^m}$	discrete wavelet transform values
$\boldsymbol{d_m}$	The signal detail
$\boldsymbol{m_0(\omega)}$	the scaling filter in the frequency domain.
$\boldsymbol{z}$	complex number
$\boldsymbol{W(z)}$	function derived from $\lvert m_0(\omega)\rvert^2$
$\boldsymbol{U(z)}$	filter function
$\boldsymbol{\psi(t)}$	the mother wavelet
$\boldsymbol{\sigma}$	standard deviation
$\boldsymbol{\psi}$	wavelet function
$\boldsymbol{\Gamma}$	Gamma function

General Introduction

The diagnosis of faults in rotary machinery is a critical task for ensuring reliable and efficient operation. Many analysis techniques for detecting faults in rotating machines, by analyzing the vibrations induced by these faults in the machine, are used. Among these techniques are spectral analysis (Fast Fourier Transform), which is widely used, and wavelet analysis.

Often, we use the fast Fourier transform of the vibration signal generated by the machine for an initial analysis of defects. But this technique, which is well mastered, is effective in permanent regimes and for defects where their vibration signature is known such as unbalance defects and shaft misalignment defects.

Wavelet analysis is known to be effective in detecting faults in transient conditions. But it is not used much in the maintenance of rotating machines in Algeria. This is why we tried to begin an approach to a wavelet analysis of unbalance defects on a simulator with different unbalance configurations and to compare it with spectral analysis.

There are several types of wavelet analysis which are very complex to treat them all in a single study. In our work, we opted to treat the Daubechies wavelet analysis which proves effective in the detection of faults in transient regimes.

This study explores the comparative effectiveness of db4 wavelet analysis and FFT spectrum analysis for mechanical fault diagnosis in a rotary machine fault simulator.

The work is divided into three key chapters:

Chapter 1 - Literature Review: This chapter examines previous research in the field, summarizing the strengths and limitations of wavelet and FFT techniques as applied to vibration-based fault detection.

Chapter 2 – Wavelet analysis: In this chapter we reviewed the different types of wavelets with their mathematical expressions. The theory behind the db4 wavelet and its implementation in MATLAB is discussed, providing the technical background for the analysis methods used in the study.

Chapter 3 - Experimental analysis: This final chapter presents the findings from testing the two signal processing approaches under both stationary and non-stationary speed conditions. The results highlight the complementary nature of wavelet and FFT analysis for comprehensive mechanical fault diagnosis.

Finally, this work ends with a general conclusion.

CHAPTER 1

LITERATURE REVIEW

LITERATURE REVIEW

The wavelet transform, a time-frequency analysis technique, offers distinct advantages over conventional approaches. Wavelet analysis can effectively capture both the temporal and spectral characteristics of vibration signals, enabling the identification and localization of fault signatures, even in the presence of non-stationary behavior.

The origins of wavelet-based techniques for vibration analysis can be traced back to the early 1980s, when researchers began exploring the limitations of traditional Fourier-based signal processing methods. Fourier analysis, while effective for stationary signals, struggled to capture the non-stationary and transient characteristics often present in vibration data from rotating machinery.

In 1984, Grossmann and Morlet [1] published a seminal paper in the SIAM Journal on Mathematical Analysis, titled "Decomposition of Hardy Functions into Square Integrable Wavelets of Constant Shape." This work introduced the concept of the continuous wavelet transform (CWT) and laid the mathematical foundation for the use of wavelet analysis in various signal processing applications.

Grossmann and Morlet demonstrated that any "Hardy function" (a class of well-behaved, square-integrable functions) could be decomposed into a superposition of wavelet functions with constant shape. This breakthrough allowed for the representation of non-stationary signals, such as those encountered in vibration monitoring, in a more comprehensive and informative manner compared to traditional Fourier-based approaches.

The introduction of the CWT by Grossmann and Morlet paved the way for the subsequent development and widespread adoption of wavelet-based techniques in the field of vibration analysis and condition monitoring of rotating machinery. Their pioneering work laid the foundation for numerous advancements in this area.

Building on the groundbreaking work of Grossmann and Morlet, the mathematician Ingrid Daubechies [2] made significant contributions to the development of wavelet theory in the late 1980s and early 1990s.

Daubechies' pivotal 1988 paper, "Orthonormal Bases of Compactly Supported Wavelets," introduced a family of wavelet functions that were orthonormal and had compact support. This was a significant advancement, as it allowed for the efficient representation and computation of wavelet-based signal processing algorithms.

Daubechies' work focused on constructing wavelet bases with desirable properties, such as smoothness, symmetry, and vanishing moments. These properties were crucial for the effective analysis of various types of signals, including those encountered in vibration monitoring applications.

By developing a systematic approach to the construction of orthonormal wavelet bases, Daubechies enabled the widespread adoption of wavelet-based techniques in a variety of fields, including signal processing, image analysis, and numerical analysis. Her work provided a solid mathematical foundation for the practical implementation of wavelet-based methods.

Daubechies' contributions were instrumental in expanding the application of wavelet analysis beyond the initial work of Grossmann and Morlet. Her introduction of the Daubechies wavelet family, which is widely used in signal processing and data compression, became a cornerstone of wavelet theory and its practical applications.

The impact of Daubechies' research on the field of vibration analysis and condition monitoring cannot be overstated. Her work on compact, orthonormal wavelet bases enabled the development of efficient and robust wavelet-based techniques for the analysis of complex vibration signals, leading to advancements in fault detection, diagnosis, and predictive maintenance strategies.

Soudeh.H.Yaghouti, Sanika.S.Patankar and Jayant.V.Kulkarni [3] published a work in 2012. The aim of this work is to investigates the application of various vibration signal analysis techniques to a mechanical setup consisting of a rotary machine. The experimental setup was designed to introduce a specific fault or uncertainty by using a gear with a broken tooth.

The effects of this uncertainty, introduced into the vibration signal due to the faulty gear, were analyzed using two approaches: Fourier Transform (figure 1.01) and Continuous Wavelet Transform (CWT). For the CWT, the authors employed two different wavelet basis functions

– Daubechies wavelets with three vanishing moments (figure 1.02), and the Mexican Hat wavelet (figure 1.03).

From the experimental results, the paper reports that the uncertainty caused by the broken gear tooth was detected more effectively by the Continuous Wavelet Transform using the Mexican Hat basis function, compared to the Fourier Transform analysis.

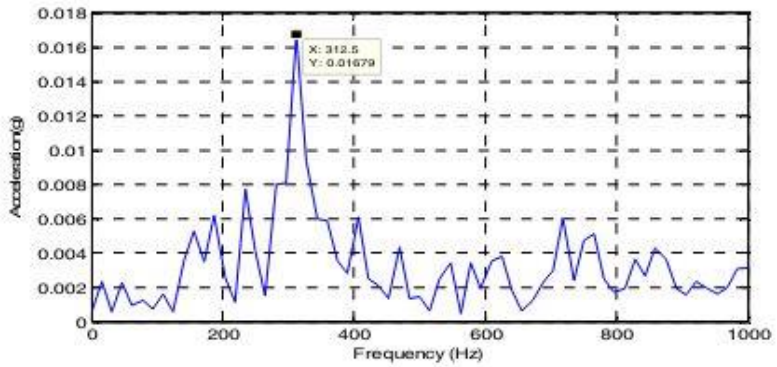

(a)

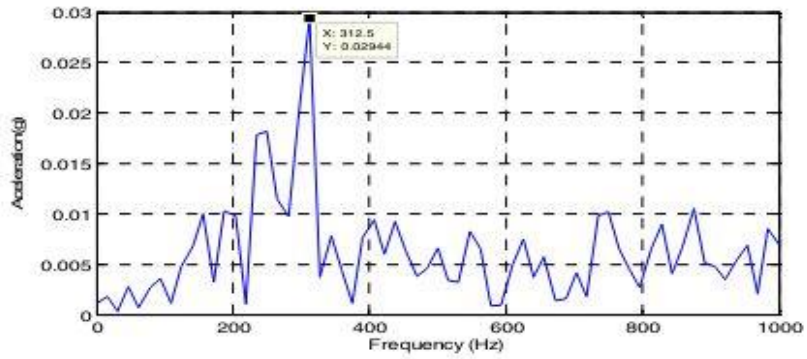

(b)

Figure 1.01. The FFT acceleration spectrums in axial position and 625 RPM. (a)Without any fault, (b) The fault is induced [3].

In 2002, Prabhakar, Mohanty, and Sekhar [4] published a study in the Tribology International journal. This study investigated the application of Discrete Wavelet Transform (DWT) for the detection of bearing race faults. The researchers focused their analysis on vibration signals collected from ball bearings under various fault conditions. These fault conditions included single-point defects as well as multiple-point defects on the inner race, outer race, and a combination of defects across the bearing components.

The key insight gained from the analysis was that the impulses present in the vibration signals, which are indicative of the bearing faults, were prominently featured in the wavelet decompositions (figures 1.04-1.07). This is an important observation, as it demonstrates the ability of the DWT technique to effectively capture and characterize the fault-induced vibration patterns.

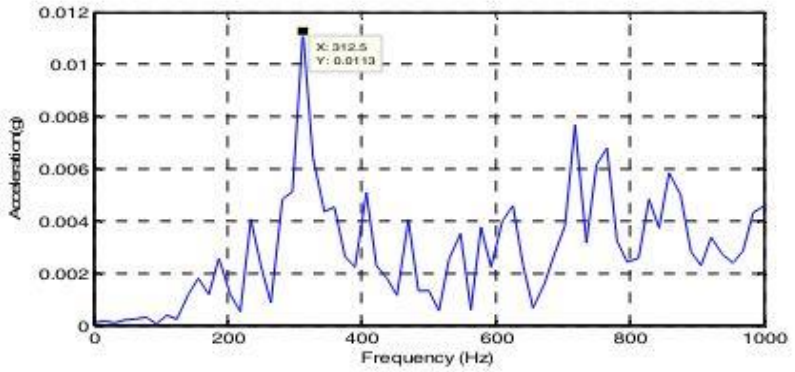

(a)

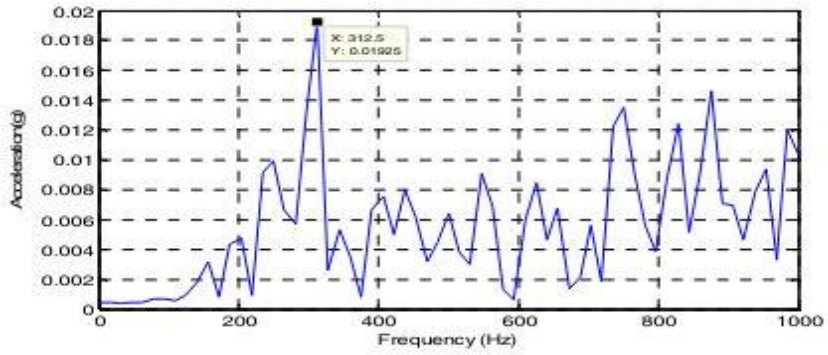

(b)

Figure 1.02. The Daubechies Wavelet Transform acceleration spectrums in axial position and 625 RPM. (a) Without any fault, (b) The fault is induced [3].

Furthermore, the researchers noted that these impulses appeared periodically in the wavelet domain, with the time period of the impulse occurrences corresponding to the characteristic defect frequencies of the bearings. This periodic behavior provides valuable information about the nature and location of the faults within the bearing system.

By closely examining the wavelet decompositions, the researchers were able to discern distinct signatures associated with the different fault conditions, including single-point defects

on the inner race, outer race, and the combination of multiple faults. This level of fault identification and characterization is crucial for effective condition monitoring and predictive maintenance of rotating machinery.

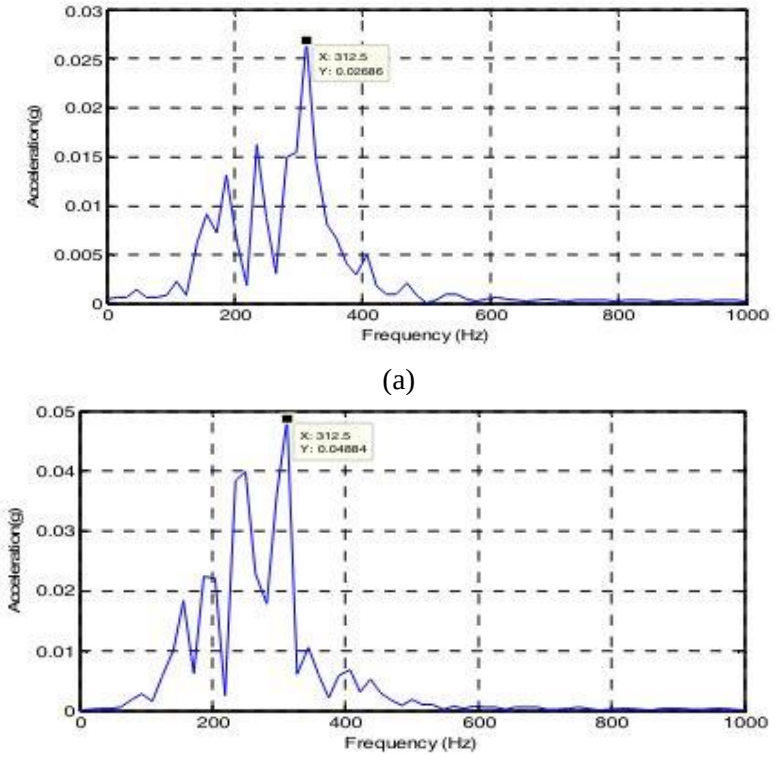

(a)

(b)

Figure 1.03. Mexican Hat Wavelet Transform acceleration spectrums in axial position and 625 RPM. (a) Without any fault, (b) The fault is induced [3].

The ability of DWT to clearly identify and distinguish the fault-induced vibration patterns, as well as the periodic nature of the fault signatures, highlights the potential of this signal processing technique for bearing fault diagnosis. The researchers concluded that the Discrete Wavelet Transform can be considered an effective and reliable tool for the detection of both single and multiple faults in ball bearings, contributing to improved reliability and performance of rotating machinery.

The findings of this study demonstrate the value of advanced signal processing methods, such as DWT, in the field of condition monitoring and fault diagnosis. By leveraging the capabilities of these techniques, researchers and engineers can develop more robust and

accurate approaches for the early detection and identification of bearing faults, ultimately leading to enhanced maintenance strategies and more reliable machinery operations.

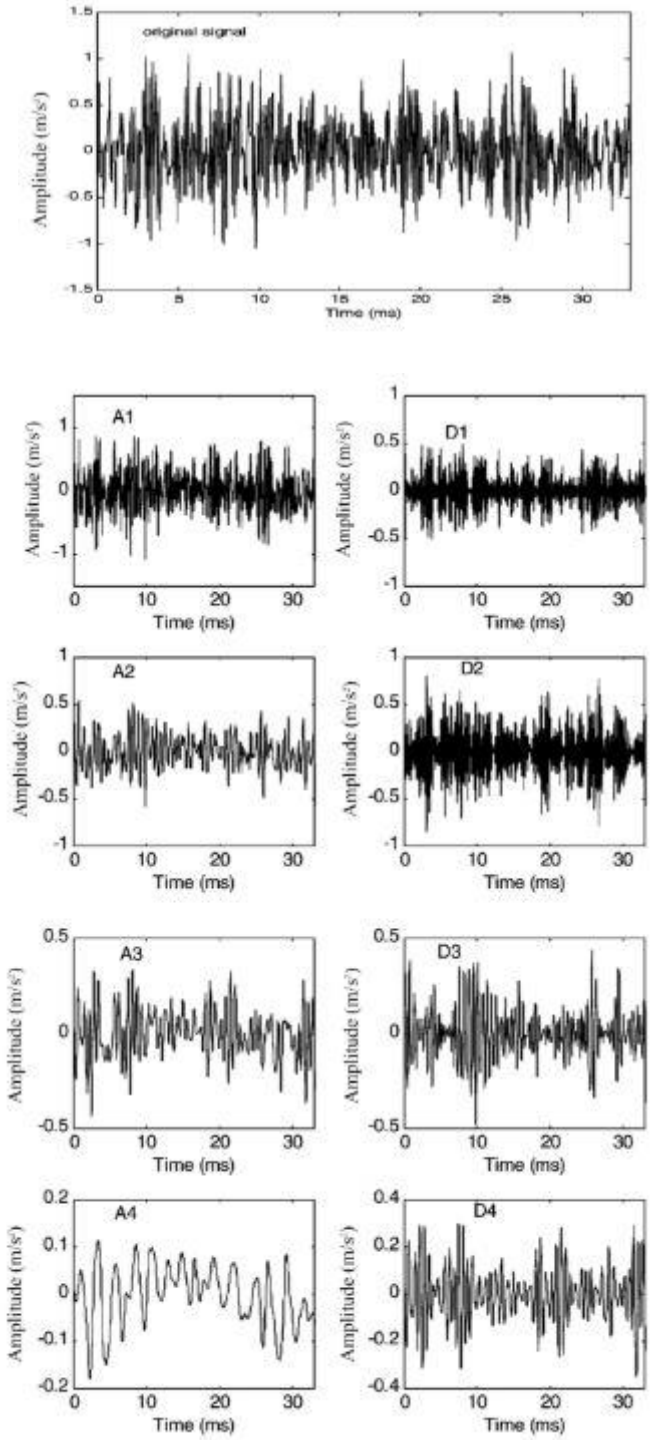

Figure 1.04. Original time signal and the wavelet decompositions for one revolution of the good bearing [4].

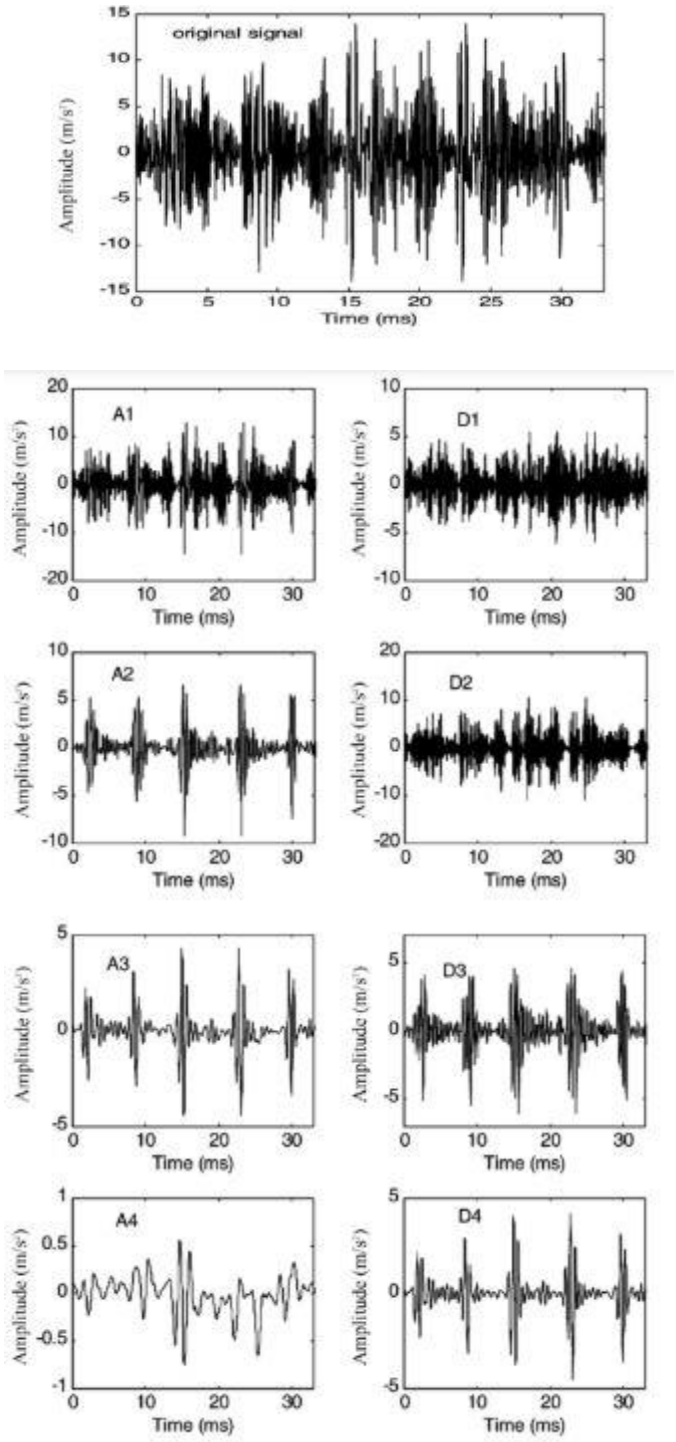

Figure 1.05. Original time signal and the wavelet decompositions for one revolution of the inner race defect bearing [4].

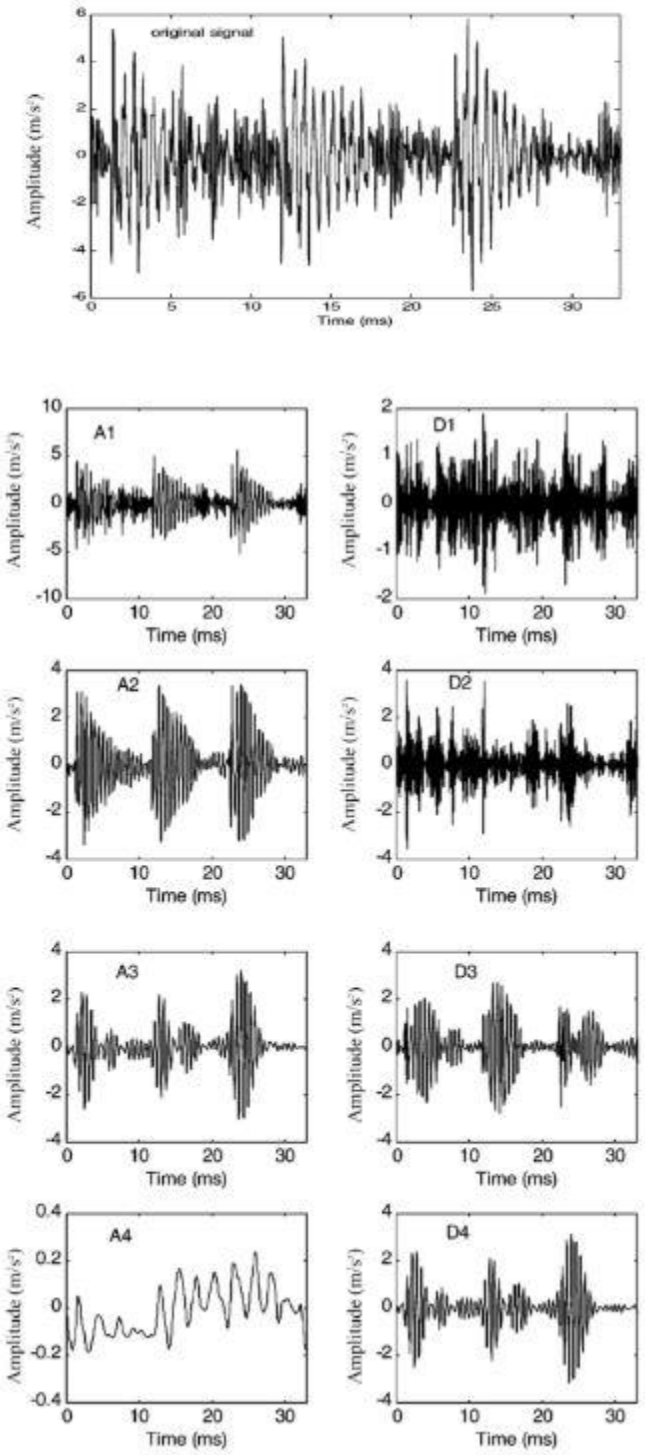

Figure 1.06. Original time signal and the wavelet decompositions for one revolution of the outer race defect bearing [4].

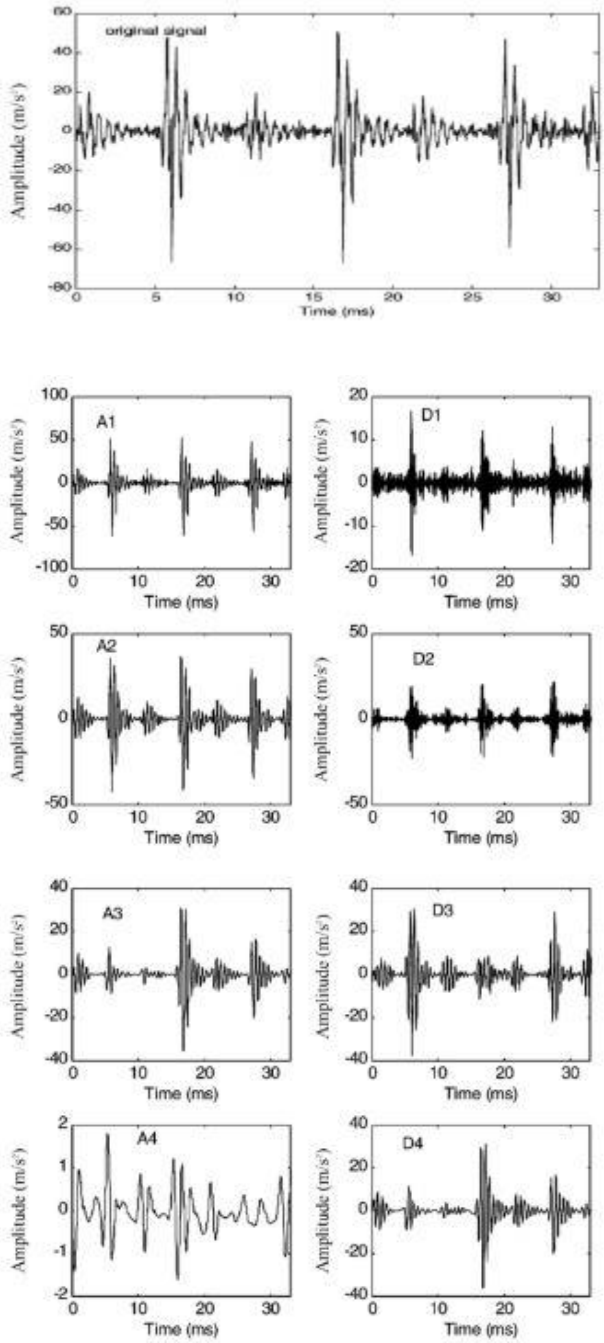

Figure 1.07. Original time signal and wavelet decompositions for one revolution of the bearing with two defects on outer race [4].

In 2012 Hocine Salah and Mohamed [5] published a work in International Journal of Machine Learning and Computing and they found that the analysis of vibration data is crucial for effective condition monitoring and fault diagnosis of rotating machinery. Many signal processing methods have been employed to extract meaningful information from vibration measurements.

Traditionally, spectral analysis techniques based on Fourier Transform (FT) (figure 1.08) have been widely used for this purpose. However, FT-based methods have limitations when dealing with non-stationary vibration signals.

In this work, the authors propose the use of Wavelet Transform (WT) for vibration signal analysis (figures 1.09 and 1.10). Wavelet Transform is a powerful tool for processing non-stationary signals, which is often the case with vibration data obtained from accelerometer sensors. The results demonstrate that the Wavelet Transform approach can effectively identify abnormal changes in the measured vibration data, making it a promising technique for condition monitoring and fault diagnostics of rotating machinery.

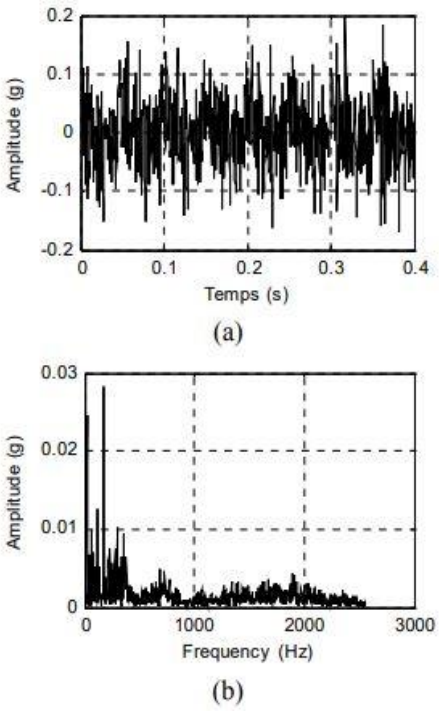

\

Figure 1.08. Vibration signal of mass unbalance and its spectrum [5].

Overall, the study highlights the advantages of employing WT over conventional FT-based methods for vibration analysis, especially in the context of non-stationary signals that are commonly encountered in rotating machinery applications.

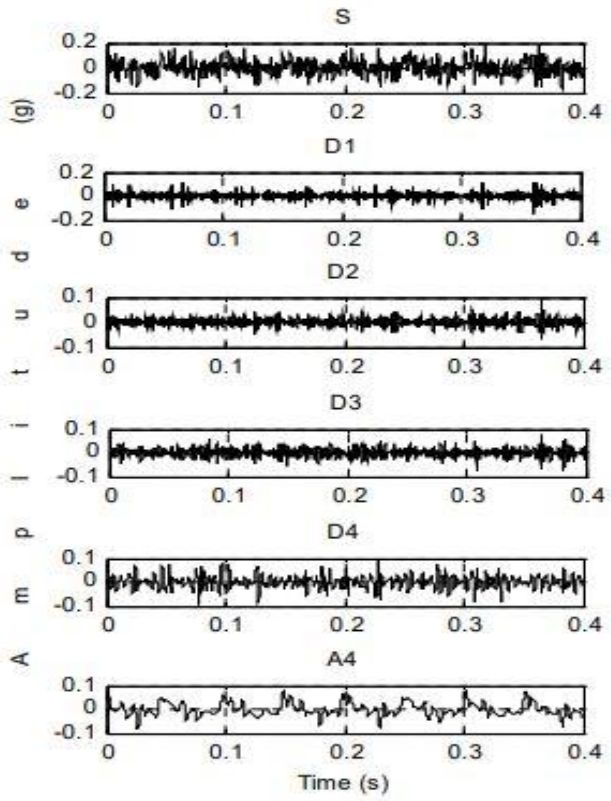

Figure 1.09. Decomposition of vibration signal of mass unbalance at a speed of 1200 rpm with db4 wavelet [5].

In 2010 Ahamed, S. K., Karmakar, S., Mitra, M. & Sengupta, S. [6] published a paper in International Conference on Electrical & Computer Engineering and the goal of this paper was to presents an improved technique for detecting mass imbalance in the rotor of an induction motor. The proposed method analyzes the transient stator current during the motor starting period using continuous wavelet transform (CWT) (figures 1.12-1.14).

Mass imbalance in the rotor generates an unbalanced magnetic pull due to centrifugal forces. This produces excessive vibrations in both the rotor and stator, leading to changes in

the air gap flux distribution. These changes induce voltages in the rotor and stator, and generate a unique signature pattern in the stator current.

During motor starting, the unbalanced magnetic pull is very high, causing the rotor to be pulled across the entire air gap. This increases the amplitudes of existing harmonics and generates new harmonics in the stator current, which can be used to diagnose the fault.

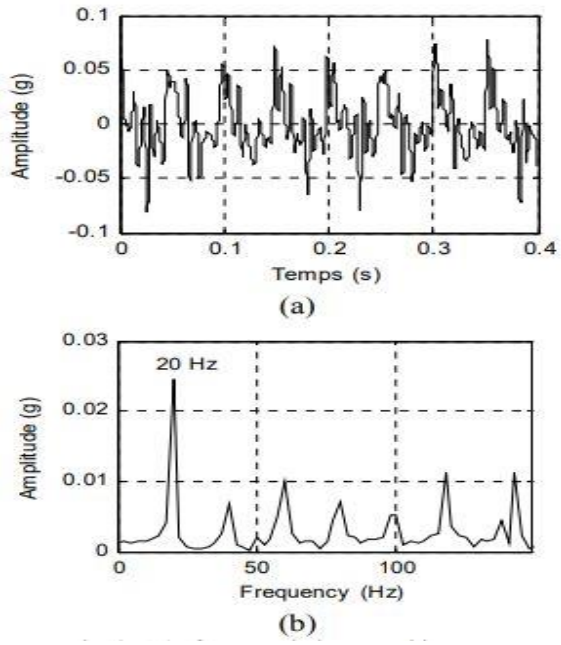

Figure 1.10. Db4 of mass unbalance and its spectrum [5].

The authors propose using the starting current at no-load for fault detection. This approach overcomes the limitations of motor current signature (MCS) analysis during steady-state operation, as the MCS is heavily dependent on the motor's loading conditions. In contrast, the starting current is high even at no-load and does not depend on the load, making it more suitable for fault diagnosis.

The proposed improved technique has been developed and implemented in a laboratory setting using a machine fault simulator (figure 1.11).

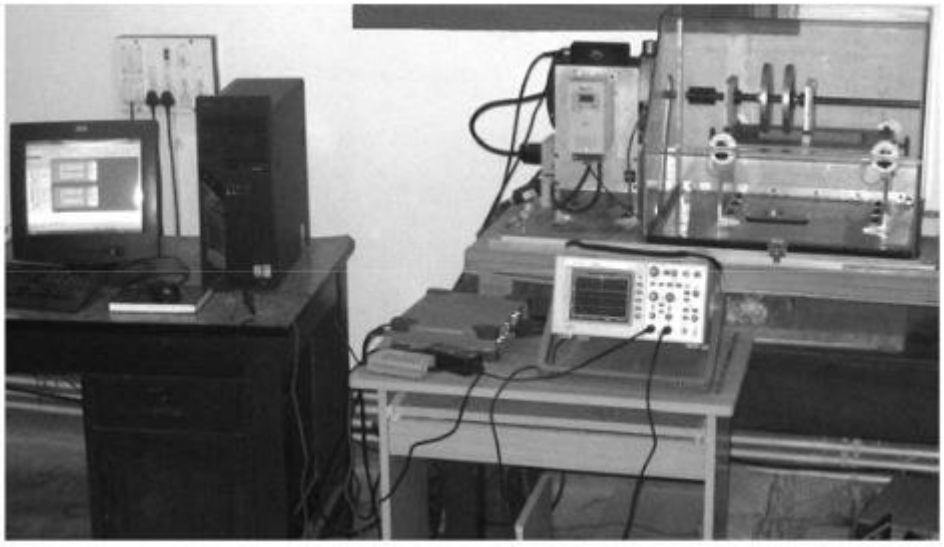

Figure 1.11. Experimental Setup [6].

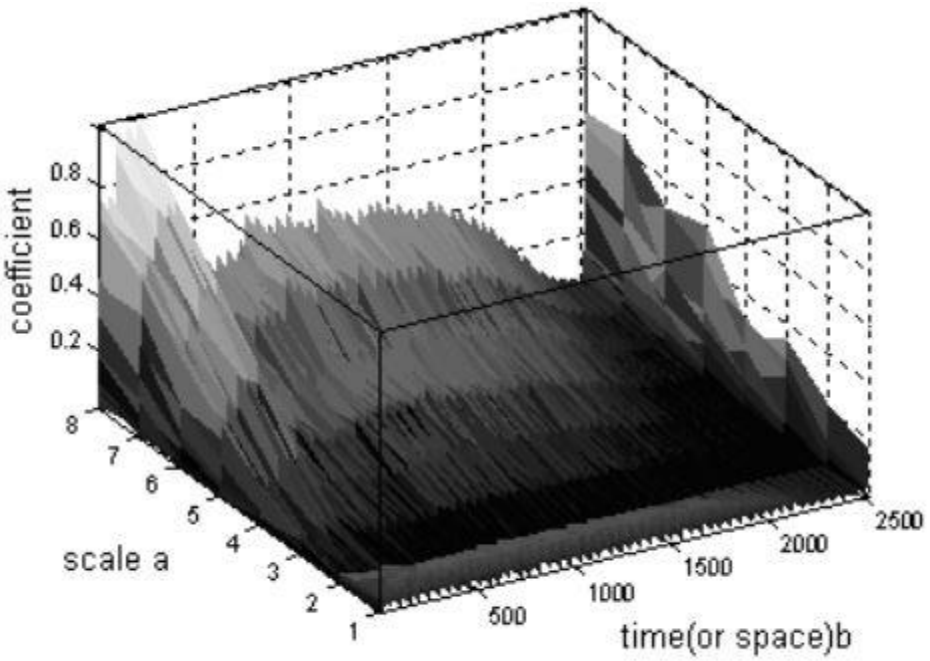

Figure 1.12. CWT of healthy motor [6].

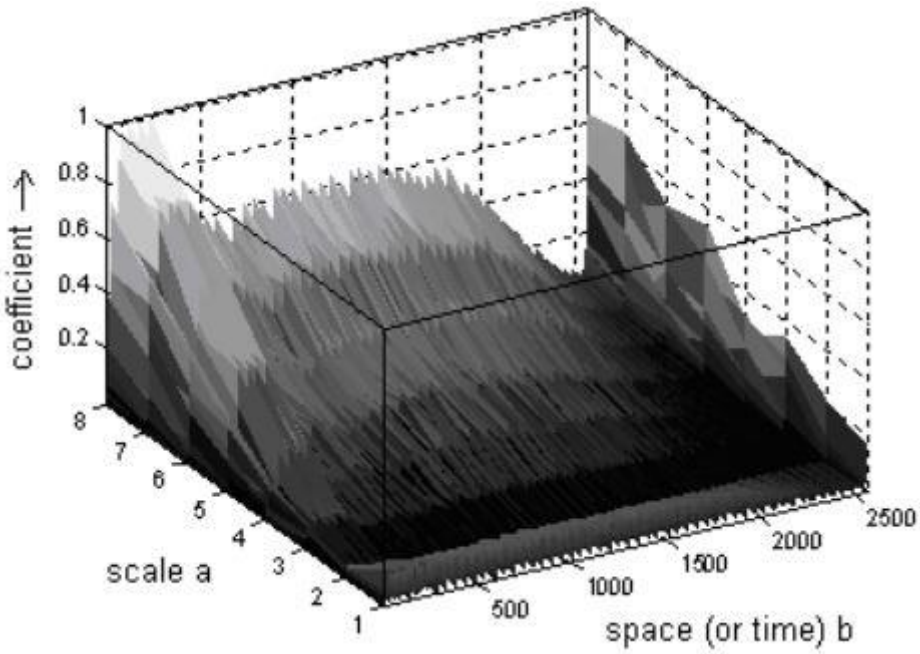

Figure 1.13. CWT of mass unbalance in rotor motor [6].

Scale	Mean Value of CWT coefficients at Motor condition	
	Healthy	Mass unbalance in rotor
1	1.666×10^{-5}	2.2662×10^{-5}
2	0.0024	0.0017
3	0.0808	0.075
4	0.5682	0.6387
5	4.0205	5.6568
6	1.3193×10^{3}	1.4449×10^{3}
7	178.95	107.5351
8	3.6935	11.7653

Table 1.01. comparison of mean value CWT coefficients [6].

CHAPTER 2

Wavelet Analysis

Wavelet Analysis

2.1. The Wavelet Transform:

A wave is typically described as a fluctuating pattern over time or space, often resembling a sinusoidal function. Fourier analysis, which is a form of wave analysis, decomposes signals or functions into sinusoids (or equivalently, complex exponentials), a technique widely employed in mathematics, science, and engineering, particularly for phenomena that are periodic, time-invariant, or stationary.

In contrast, a wavelet, termed as a "small wave," concentrates its energy within a specific time frame, providing a tool for analyzing transient, nonstationary, or time-varying phenomena. While retaining wave-like oscillating characteristics, wavelets offer simultaneous time and frequency analysis with a versatile mathematical framework. This concept is depicted in Figure (2.01), where the sinusoidal wave oscillates infinitely with uniform amplitude over $-\infty < t < \infty$, resulting in infinite energy, while the wavelet exhibits finite energy concentrated around a point.

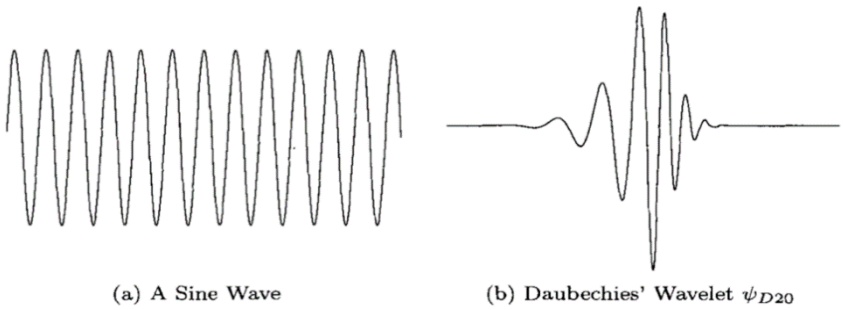

(a) A Sine Wave (b) Daubechies' Wavelet ψ_{D20}

Figure 2.01. A Wave and a Wavelet [7].

Figure (2.01) illustrates a fundamental distinction between a sine wave and a wavelet. Unlike a sine wave, which extends infinitely in time, a wavelet is localized both in time and frequency. This localization property enables the Wavelet Transform to capture time-domain information along with frequency-domain information. As a result, wavelets offer enhanced capabilities for analyzing signals with transient or localized features, making them invaluable in various signal processing applications.

2.2. Discrete wavelet transform (DWT):

In the Discrete Wavelet Transform (DWT), a signal is split into two parts: a rough estimate and detailed information. Discrete Wavelet Transform uses two types of functions: scaling functions and wavelet functions. Scaling functions are like low-pass filters, while wavelet functions are like high-pass filters. By passing the original signal through these filters one after another, we break it down into different frequency bands. First, it goes through a high-pass filter, then through a low-pass filter.

The signal is then down sampled by 2, simply by ignoring every other sample. This constitutes one level of decomposition and this process can be further repeated for both high pass and low pass filter in order to get in depth transformation.

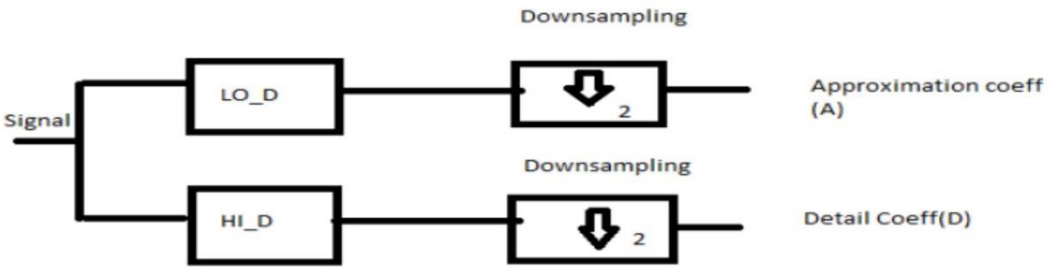

Figure 2.02. 1-D level of Discrete wavelet transforms [8]

2.2.1. The Haar wavelet transform:

Alfred Haar has defined a complete orthogonal system of functions in $L^p([0,1])$, $p\epsilon[1,\infty]$ [9]. In simple terms, the Haar functions are mathematical functions that help us understand and analyze patterns in data. These functions are named after mathematician Alfred Haar.

Nowadays, in literature, there are some different ways people define these Haar functions.

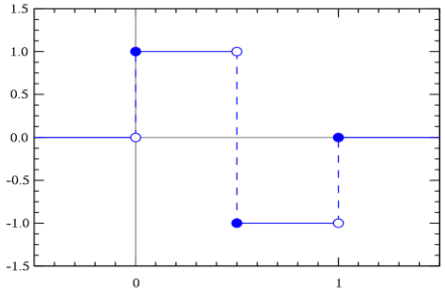

Figure 2.03. The Haar wavelet [10]

These new definitions might give us different perspectives or insights into how we can use them to understand data better. It's like looking at something from different angles to get a clearer picture.

Discrete Haar functions can be defined as functions determined by sampling the Haar functions at 2^n points [8]. These functions can be conveniently represented by means of matrix form. Each row of the matrix $H(n)$ includes the discrete Haar sequence $haar(w,t)$ w: the number of the Haar function، discrete point of the function determination interval).

The Haar matrix of any dimension can be obtained by the following recurrence relation

$$H(n)\begin{bmatrix} H(n-1) & \otimes [1 \quad 1] \\ 2^{\frac{n-1}{2}}\mathrm{I}(n-1) & \otimes [1 \ -1] \end{bmatrix} \tag{2.01}$$

$H(0) = 1$

2.2.2. Daubechies wavelets:

In 1988, Ingrid Daubechies made a big breakthrough by creating a way to build discrete orthonormal basis functions, which we will explain now [11].

Sinusoidal functions are perfectly localized in the frequency domain, but global in the spatial coordinate (position or time) [11]. It is hard to represent a time-limited or spatially limited function using a Fourier basis. However, a wavelet basis is approximately localized in both the frequency domain and the spatial domain. Besides being localized in both conjugate variables, we need all basis functions to be mutually orthogonal and normalized. This puts strict limits on the functions we can use.

In the Daubechies formulation, these properties are achieved through a process called recursion. The scaling functions and wavelets are defined recursively using dilation equations. [12].

The basic dilation equation is a two-scale or dyadic difference equation:

$$\psi(t) = \sqrt{2}\sum_{k=0}^{N-1} g_k \phi(2t-k) \tag{2.02}$$

$\varphi(x)$ is known as the scaling function

N: is the number of vanishing moments, which corresponds to the Daubechies wavelet order.
For example, N=2 for Daubechies 2 (db2), N=4 for Daubechies 4 (db4), and so on.

Daubechies wavelets are orthogonal, biorthogonal, but they are not symmetrical. The compact support, that is the range over which they are non-zero is Daubechies wavelet are widely used in the DWT but also in the CWT. (figure 2.04) shows the Daubechies wavelets db2, 4, 8, and 16

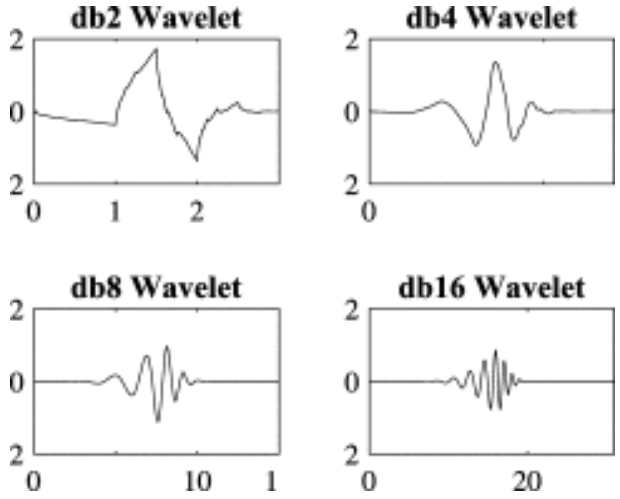

Figure 2.04. Daubechies wavelet [13]

2.2.3. The Coiflet wavelet:

Coiflet wavelets are a family of wavelets designed by Ronald Coifman. They are characterized by their vanishing moments for both the wavelet function and the scaling function, which makes them particularly suitable for representing polynomial functions accurately. Coiflets have the property of having more vanishing moments in the wavelet function than in the scaling function, and they exhibit near symmetry.

The Coiflet wavelet system is an orthogonal multiresolution wavelet system. The wavelet function (equation 2.7) can be defined at scale m and location n as [14]:

$$\psi_{m,n}(t) = \frac{1}{\sqrt{a_0^m}}\psi\left(\frac{t - nb_0a_0}{a_0^m}\right) \tag{2.03}$$

a_0 : fixed dilation parameter

b_0 : location parameter

The discrete wavelet transform values $T_n^m$of a continuous signal $x(t)$ can be expressed as inner product between the signal and the wavelet function $\psi_{m,n}$ **:**

$$T_n^m = \langle x, \psi_{m,n} \rangle \quad (2.04)$$

The signal detail corresponding to scale index m is defined for a finite length signal as

$$d_m(t) = \sum_{n=0}^{2^{M-m}-1} T_n^m \psi_{m,n}(t) \quad (2.05)$$

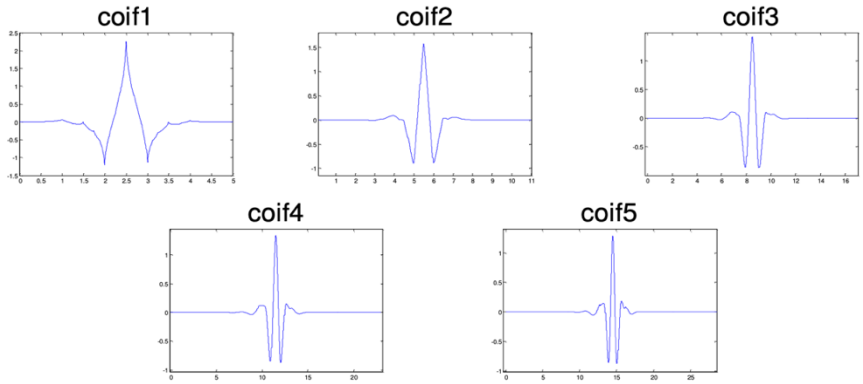

Figure 2.05. The Coiflet wavelet [15]

The choice of the wavelet function depends on the application. The Haar wavelet algorithm has the advantage of being simple to compute and easy to understand. The Coiflet algorithm is conceptually more complex and has a slightly higher computational overhead. But, the Coiflet algorithm picks up details which are missed by the Haar wavelet algorithm [14].

2.2.4. The Symlets wavelet:

Symlets (Symmetric wavelets) are a family of orthogonal wavelets similar to Daubechies wavelets but with improved symmetry properties. Developed by Ingrid Daubechies, Symlets are designed to achieve nearly linear phase characteristics while retaining compact support and a specified number of vanishing moments. [16]

In symN, N is the order. Some authors use 2N instead of N. Symlets are only near symmetric; consequently, some authors do not call them Symlets.

Daubechies proposes modifications of her wavelets that increase their symmetry can be increased while retaining great simplicity. The idea consists of reusing the function m_0 introduced in the dbN, considering the $|m_0(\omega)|^2$ as a function W of $z = e^{i\omega}$ [17]:

$$W(z) = U(z)\overline{U\left(\frac{1}{z}\right)} \quad (2.06)$$

By selecting *U* such that the modulus of all its roots is strictly less than 1, we build Daubechies wavelets *dbN*. The *U* filter is a "minimum phase filter". By making another choice, we obtain more symmetrical filters these are Symlets. [17]

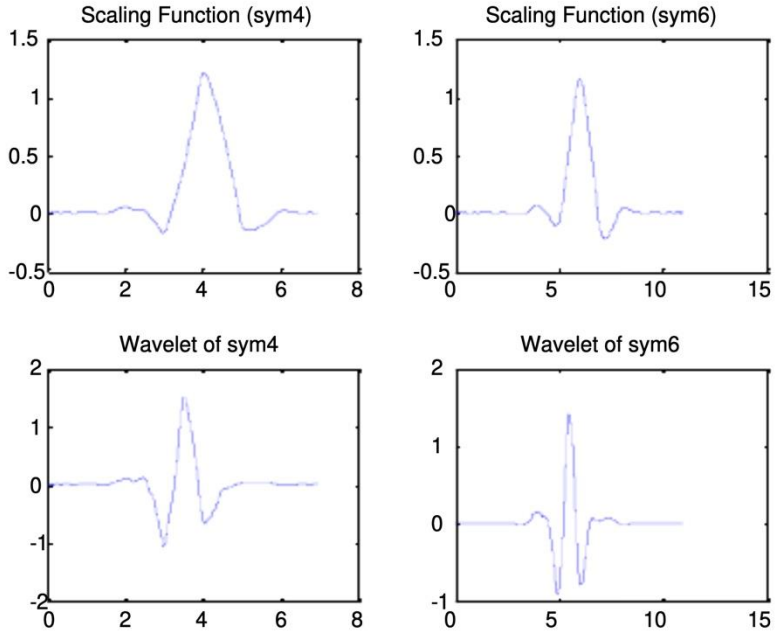

Figure 2.06. The Symlets wavelet [18]

2.3. The Continuous Wavelet Transform:

The wavelet transformation was approached in the 1980s with the work of engineer J. Morlet and his team by defining the Continuous Wavelet Transform (CWT) using a specific wavelet with its name [19].

The CWT is similar to the sliding window Fourier transform and the S transform [20] since it makes it possible to provide a redundant two-dimensional representation to highlight the local oscillatory characteristics of the signal.

A wavelet is a continuous time signal satisfying the following properties:

$$\int_{-\infty}^{\infty} \psi(t)dt = 0 \quad (2.07)$$

$$\int_{-\infty}^{\infty} |\psi(t)|^2 \, dt < \infty \quad (2.08)$$

where $\psi(t)$ is defined as the mother wavelet [20].

The wavelet transform continues:

$$W(a,b) = \int_{-\infty}^{\infty} x(t)\psi^* a,b(t)dt \quad (2.09)$$

where $x(t)$ is any square integrable function, a is the dilation parameter, b is the translation parameter and is the complex conjugate of the mother wavelet defined as [19]:

$$\psi^* a,b(t) = \frac{1}{\sqrt{|a|}}\,\psi\left(\frac{t-b}{a}\right) \quad (2.10)$$

The signal $x(t)$ can be reconstructed from the transformation into continuous wavelet provided that the parent wavelet satisfies the admissibility condition:

$$C = \int_{-\infty}^{\infty} \frac{|\psi(\omega)|^2}{|\omega|}\,d\omega < \infty \quad (2.11)$$

where $\psi(\omega)$ is the Fourier Transform of $\psi(t)$

At a small scale (high frequency), CWT provides high temporal resolution and at a larger scale (lower frequency) CWT provides high frequency resolution [21].

2.3.1. The Mexican hat wavelet:

The Mexican hat wavelet (Figure 2.07), also known as the Ricker wavelet, is indeed proportional to the negative value of the second derivative of a Gaussian function. Its functional form can be expressed as [18]:

$$\psi(t) = \frac{2}{\sqrt{3\alpha}\pi^{\frac{1}{4}}}\left(1-\left(\frac{t}{\sigma}\right)^2\right)e^{-\frac{t^2}{2\sigma^2}} \quad (2.12)$$

where t is the time variable, σ the standard deviation that controls the width.

We mentioned that most of its energy is within the interval (−5,5), which is the typical range where it is often used. However, for more accurate results, a larger interval, such as (−8,8), is sometimes chosen to capture a wider range of frequencies or features in the signal.

Unlike some other wavelets, the Mexican hat wavelet doesn't have a scaling function associated with it. This means that it doesn't have a corresponding scaling equation that can generate a multi-resolution [21].

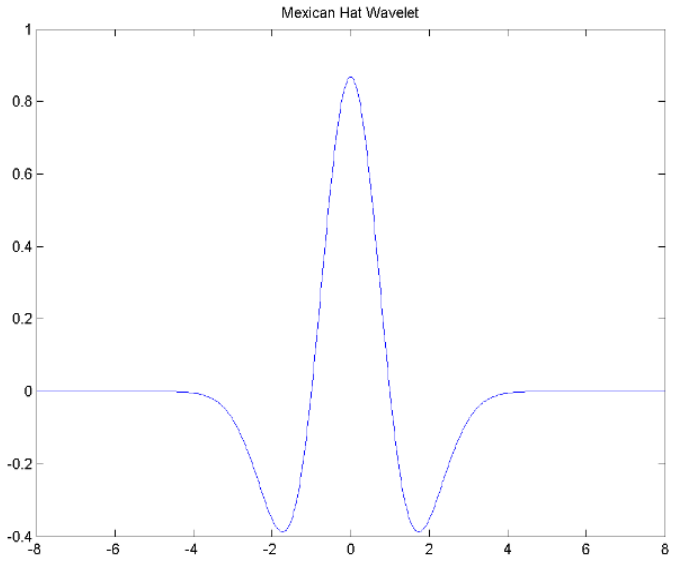

Figure 2.07. The Mexican hat [22]

2.3.2. The Gaussian wavelet:

The Gaussian wavelet is a type of wavelet that belongs to the family of non-orthogonal wavelets. Unlike orthogonal wavelets, which have orthogonality properties that simplify signal analysis, non-orthogonal wavelets do not necessarily possess such properties.

The Gaussian wavelet is derived from the Gaussian function, also known as the bell curve or normal distribution. It's characterized by its bell-shaped curve, which is similar to the shape of the Gaussian function. The Gaussian wavelet is used in various signal processing applications, particularly in cases where the properties of the Gaussian function are desirable for analysis.

Non-orthogonal wavelets like the Gaussian wavelet offer flexibility in signal representation and analysis but may require different techniques for processing compared to orthogonal wavelets. They can be useful in scenarios where the signal characteristics are better suited to non-orthogonal decomposition or when specific properties of the wavelet function are desired for the analysis.

The Gaussian wavelet can indeed be used with functions like the Continuous Wavelet Transform (CWT) for signal analysis.

In the context of the Continuous Wavelet Transform, the Gaussian wavelet serves as the basis function for decomposing signals into time-frequency components. The CWT essentially involves convolving the signal with scaled and translated versions of the wavelet function

across different scales and time points, allowing for the analysis of both frequency and time localization of the signal [23].

The wavelet function ψ is [23]:

$$\psi = \frac{(-1)^{n+1}}{\sqrt{\Gamma\left(n+\frac{1}{2}\right)}} \frac{\partial^n}{\partial x^n} e^{\left(\frac{-x^2}{2}\right)} \quad (2.13)$$

2.4. comparative analysis of continuous wavelet and discrete wavelet:

Continuous Wavelet Transform (CWT) and Discrete Wavelet Transform (DWT) are two methods used for signal processing and analysis, particularly in the domain of time-frequency representation. Here's a comparative analysis of both:

2.4.1. Time-Frequency Resolution:

- **CWT**: Provides a continuous representation of both time and frequency domains, allowing for precise localization in both domains. It offers excellent resolution in time and frequency, which is particularly useful for analyzing signals with non-stationary characteristics [24].
- **DWT**: Provides a multi-resolution analysis, decomposing the signal into different frequency bands at different resolutions. While it offers good frequency resolution, its time resolution varies depending on the scale of analysis [25]

2.4.2. Orthogonality:

- **CWT**: Typically uses non-orthogonal wavelets, meaning the wavelets are not orthogonal to each other. This allows for flexibility but may complicate certain aspects of analysis [26].
- **DWT**: Uses orthogonal wavelets, meaning the wavelets are orthogonal to each other. This simplifies the analysis and reconstruction process, making it more computationally efficient [25].
-

2.4.3. Computational Complexity:

- **CWT**: Can be computationally intensive, especially for fine-scale analysis, due to its continuous nature.

- **DWT**: Generally, more computationally efficient compared to CWT, especially for real-time or large-scale applications, due to its discrete nature and the availability of fast algorithms like the Fast Wavelet Transform (FWT).

2.4.4. Boundary Effects:

- **CWT**: Handles boundary effects better due to its continuous nature, but may require careful consideration of boundary conditions in certain applications.
- **DWT**: Can suffer from boundary effects, particularly at the edges of the signal, which may require additional processing techniques such as boundary extension or wavelet packet decomposition to mitigate.

2.4.5. Applications:

- **CWT**: The CWT is used for mapping the changing properties of non-stationary [27]. signals, such as seismic signals, biomedical signals, and speech signals.
- **DWT**: Widely used in image compression, denoising, and feature extraction applications, as well as in various other signal processing tasks where multi-resolution analysis is beneficial.

In summary, the choice between CWT and DWT depends on the specific requirements of the application, including considerations such as time-frequency resolution, computational complexity, and the nature of the signal being analyzed.

2.5. Properties of Daubechies wavelets properties in mass unbalance:

Daubechies wavelets are particularly well-suited for diagnosing mass unbalance faults in machinery due to their distinct and advantageous properties. Their compact support ensures that they are non-zero only over a finite interval, allowing them to effectively capture and analyze localized, sharp changes in vibration signals caused by mass unbalance. Orthogonality of Daubechies wavelets allows for a precise decomposition and reconstruction of signals without information loss, which is crucial for accurately identifying faults. The multiple vanishing moments of Daubechies wavelets enable them to filter out smooth, polynomial trends in the signal and focus on the abrupt changes and irregularities that are indicative of faults. This property is particularly useful in distinguishing the specific vibrations caused by mass unbalance from other operational noises or vibrations. Moreover, their excellent frequency resolution allows for the effective differentiation of various frequency components within the

vibration signal, enabling the pinpointing of specific frequencies related to the rotational speed of the machinery and thus to the mass unbalance fault. Additionally, the adaptability of Daubechies wavelets, available in various forms such as db2, db4, and db6, allows engineers to select the wavelet type that best matches the characteristics of the vibration signal being analyzed. This adaptability ensures that higher-order Daubechies wavelets can be used for more complex signals requiring finer resolution. These combined properties make Daubechies wavelets exceptionally effective for isolating and identifying the transient, localized changes in vibration signals that indicate the presence of mass unbalance in rotating machinery, leading to more accurate and reliable fault diagnosis and maintenance decisions.

In our case we tried db2, db4, and db6, we found that db4 effective in terms of extracting information from the original signal without losing important information while neglecting external factors.

2.6. Simulation with MATLAB

MATLAB stands for matrix laboratory, is a high-level programming language and interactive environment developed by MathWorks, extensively used for numerical computation, data analysis, algorithm development, and visualization. It is optimized for matrix and array operations, providing built-in functions and specialized toolboxes for applications such as signal processing, control systems, image processing, and machine learning. MATLAB's interactive environment supports iterative analysis, rapid prototyping, and data visualization with advanced graphics capabilities. It integrates with other programming languages and supports hardware integration, parallel computing, and scalability for handling large datasets and complex computations. Widely used in engineering, scientific research, data analysis, and modeling, MATLAB offers comprehensive documentation and community support, making it a vital tool in both academia and industry [28].

In order to analyze the signals while using wavelet method first we need to make sure that MATLAB recognized them by using a specific reading function just as shown in the script under, then we can see that the signals are in the work space and the software divide the data file into data sets and each data set represent a column from the QUICK DAQ extracted .txt files, the first column represent the time and the second column represent the first sensor on bearing 1 and the third column represent the second sensor of the second bearing ,then we can

start the wavelet processing by analyzing each sensor vibration signal Using the MATLAB program, the program divides the mother signal into several signals (figure 2.08) according to the level of division by using Daubechies db4 equation by setting N=4 (2.02)throughout the toolbox of wavelet script just as the given example code [28], approximation A4 (blue plot) represent the important signal sins it's have all important information from the mother wave. the rest of decompositions represent unnecessary information (green plots).

sins we have A4 in time domain we have to transfer it to frequency domain by using spectrum (figure 2.09) to have better reading.

The reading script:

```
%original file to read
filename = 'C:\Users\InfoTEC\Downloads\wavelet\H1 with1and2.txt';
% temporary file for replacing  comma with dot
NewFileName= 'C:\Users\InfoTEC\Downloads\wavelet\tempread.txt';
Data = fileread(filename);
% replace comma with dot in file
Data = strrep(Data, ',', '.');
FID = fopen(NewFileName, 'w');
% save to temporary file
fwrite(FID, Data, 'char');
fclose(FID);



% Open the text file
fileID = fopen(NewFileName, 'rt');
% Skip the first 9 lines
for i = 1:9
   fgetl(fileID);
end

% Read the data into variables
data = textscan(fileID, '%f%f%f%f', 'Delimiter', '\t');

% Close the file
fclose(fileID);

% Extract the columns into vectors
column1 = data{1};
column2 = data{2};
column3 = data{3};
column4 = data{4};
```

Example of Performing a 3-level wavelet decomposition of the signal using the order 2 Daubechies wavelet and Extracting the coarse scale approximation coefficients and the detail coefficients from the decomposition :

```
[c,l] = wavedec(sumsin,3,"db2");
approx = appcoef(c,l,"db2");
[cd1,cd2,cd3] = detcoef(c,l,[1 2 3]);
```

Fot plotting the coefficients:

```
tiledlayout(4,1)
nexttile
plot(approx)
title("Approximation Coefficients")
nexttile
plot(cd3)
title("Level 3 Detail Coefficients")
nexttile
plot(cd2)
title("Level 2 Detail Coefficients")
nexttile
plot(cd1)
title("Level 1 Detail Coefficients")
```

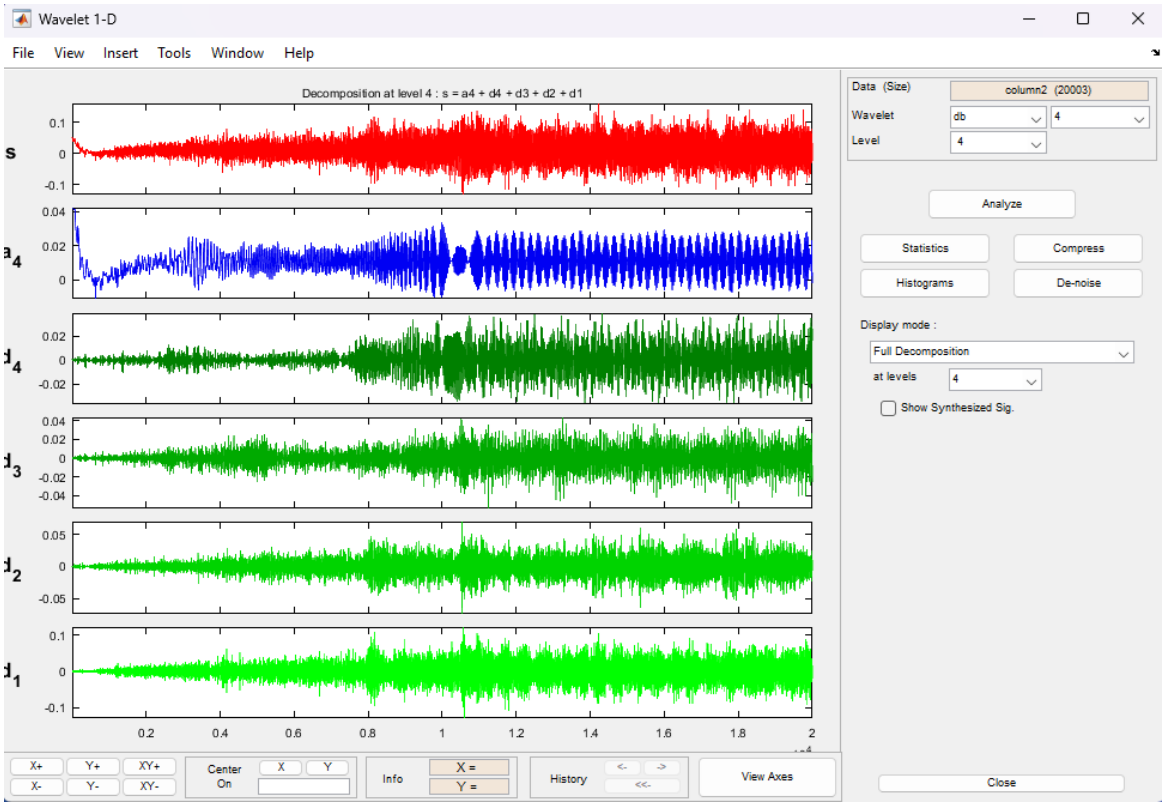

Figure 2.08. Discret Daubechies decomposition at level 4.

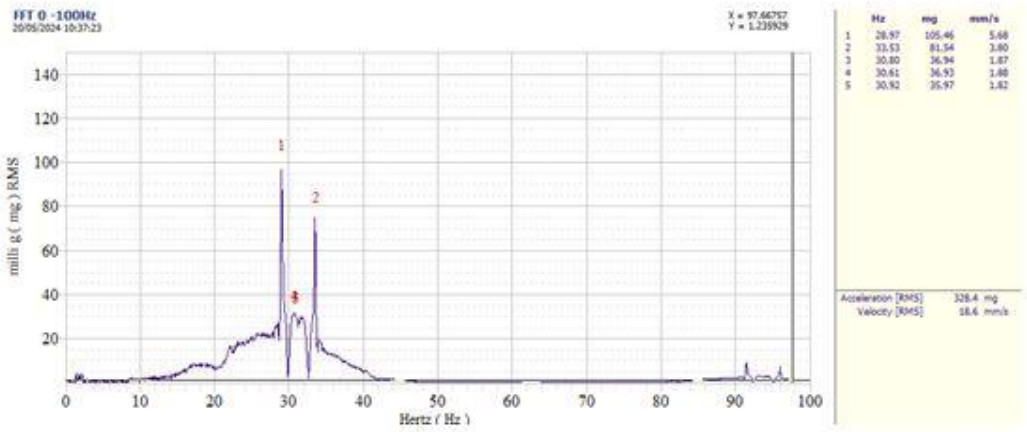

Figure 2.09. Spectrum of approximation A4

CHAPTER 3

Experimental study

Experimental study

3.1. Introduction:

In this chapter, we examine the use of the wavelet transform in vibration diagnosis using specialized equipment to simulate a mass imbalance scenario. We aim to extract vibration signals from the simulator during operation and subsequently process the extracted data using software tools.

The essential methodology of this experiment involves extracting signals from two sensor positions set up on the simulator (bearings 1 and 2) on vertically and horizontally directions. We initiate recording with accelerometer sensors and transferring the data to a computer via the Quick DAQ software. The data is then processed in MATLAB using the wavelet transform, specifically employing the Discrete Daubechies wavelet db4. Following this, the Fast Fourier Transform (FFT) is applied to convert the signal of approximation a4 from the time domain to the frequency domain, thereby facilitating improved data analysis and interpretation. To compare the wavelet transform results with the classical spectrum analysis we use for the latter the Vib360 software. The tests were carried out with a speed varying from stopping up to a speed of 34 Hz for a total duration of 20 seconds. Almost 8.5 seconds at variable speed and the rest at constant speed.

3.2. The experiment setup:

We did our researches using Machinery fault simulator Lite (MFS-LT) (figure 3.01) Model from Spectra Quest.inc and it provided tools to create a default scenario in the experiments in order to have a better study.

The simulator is equipped with a three-phase motor rated at 0.5 horsepower, featuring a pre-wired, self-aligning mounting system for straightforward installation and removal (Figure 3.02). It operates at a voltage of 230 VAC, single phase, 60/50 Hz. Additionally, the system includes a variable frequency AC drive with a 1/2 HP rating, and a multi-featured, front-panel programmable controller (Figure 3.03). The motor's RPM range extends from 0 to 6000 RPM (for short durations), allowing for variable speed control. It is equipped with a built-in tachometer featuring an LCD display and provides one pulse per revolution analog TTL output for data acquisition

(Figure 3.04). The system is aligned with two accelerometer sensors for precise measurements (Figure 3.06) and data acquisition purposes (Figure 3.05).

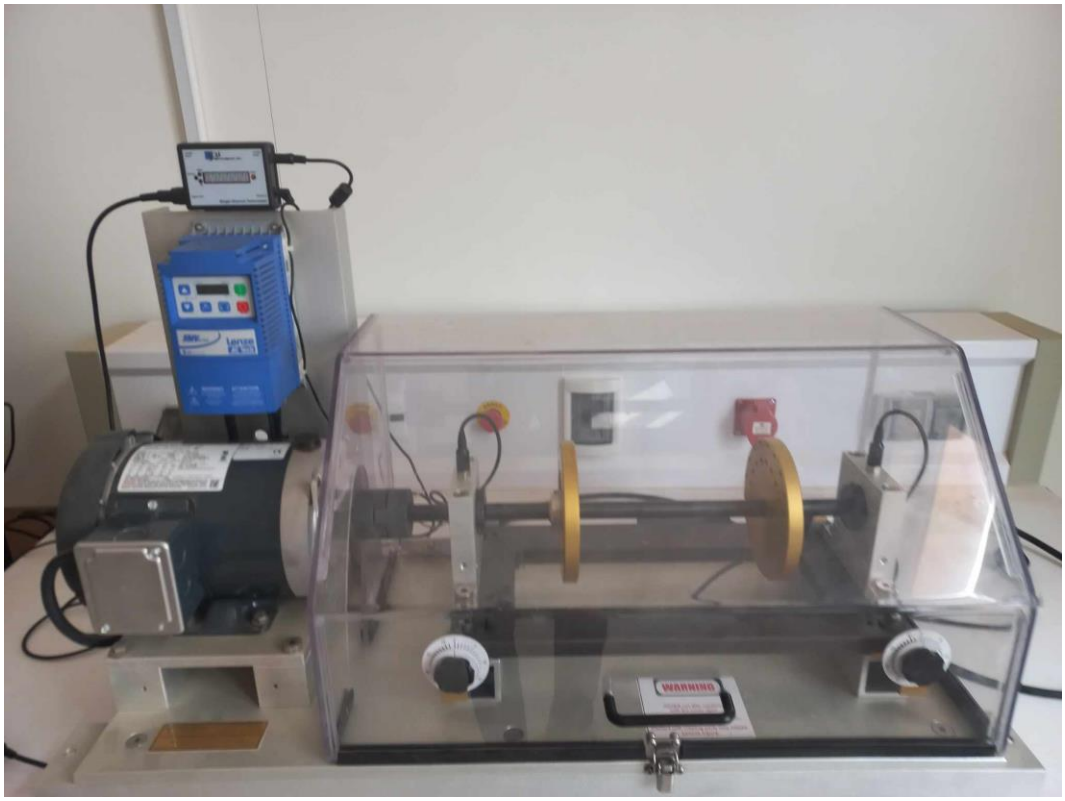

Figure 3.01. Machinery fault simulator Lite (MFS-LT).

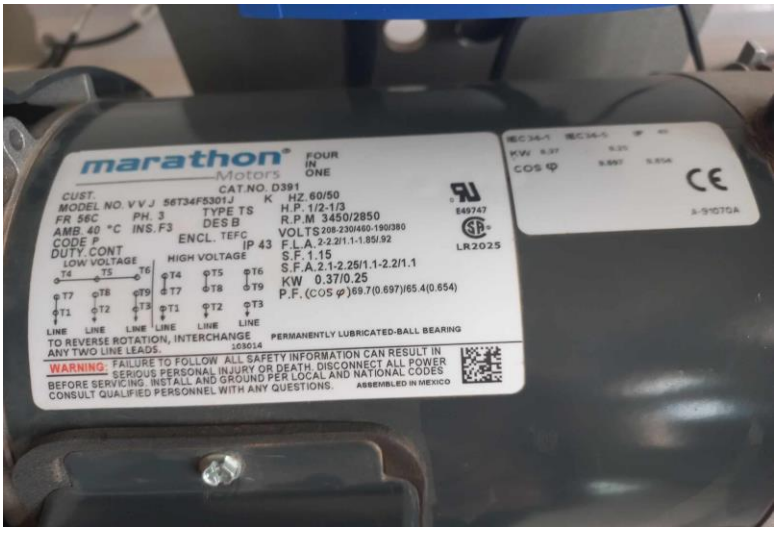

Figure 3.02. 3 phase motor with 0.5 horse power pre-wired.

Figure 3.03. Variable frequency AC drive.

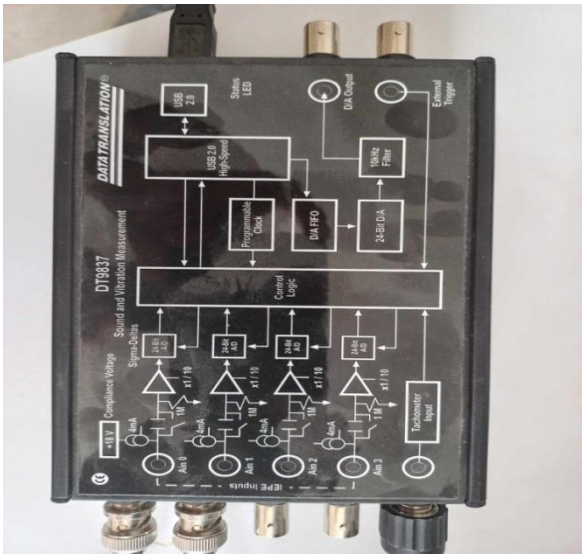

Figure 3.04. Analogue TTL output

Figure 3.05. Built-in tachometer.

For the mechanical side, this simulator contains a Rotor Base with a 381 mm long, completely movable using jack bolts for easy horizontal misalignment and standard shims for vertical misalignment Pinned for easy realignment and a two aluminum discs with 18 threaded holes at 20-degree intervals for introducing unbalance and a two sealed rolling element in aluminum horizontally split bracket housing for easy changes, tapped for transducer mount. Bearing mounts can be mounted in five different positions for variable rotor span and a safety cover Lockable clear, impact resistant hinged plastic cover with motor interlock switch to shut down motor when cover is raised.

Figure 3.06. Accelerometer sensor.

3.3. Results and discussion:

Before carrying out the tests, it is essential to determine the residual imbalances of the discs by creating an unbalance of known mass (5.56g) in all the holes of the discs. Next, we created an unbalance of mass 4.95 g in different positions in the first and the second disk then in the two disks. To viewing the effect of unbalance on the analyses, we carried out fault-free unbalance measurements.

3.3.1. Residual unbalance:

In the domain of mechanical engineering, the term "residual unbalance" refers to the persistent imbalance that remains in a system or mechanism, even after efforts have been made to balance or equalize it. This phenomenon is particularly prevalent in the operation of rotating machinery, where the slightest deviation from perfect mass distribution can have significant consequences.

The causes of residual unbalance in rotating machinery can be traced back to a variety of factors. Imperfections or variations introduced during the manufacturing or assembly process can lead to uneven mass distribution, while the gradual deformation or wear of components over time can exacerbate the issue. Additionally, the accumulation of deposits or uneven attachment of additional components to the rotating shaft can further contribute to the problem.

In order to determine the residual imbalance in our simulator, we measured the vertical acceleration of the residual unbalance at different masses and positions (Figures 3.07-3.10).

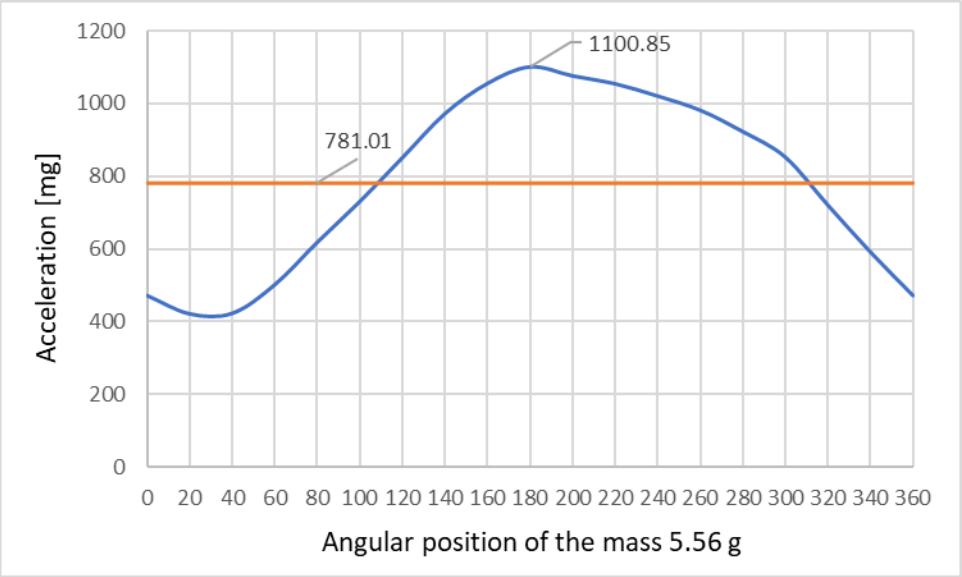

Figure 3.07. Disc 1 bearing 1: residual unbalance 2.28 g, position 180°.

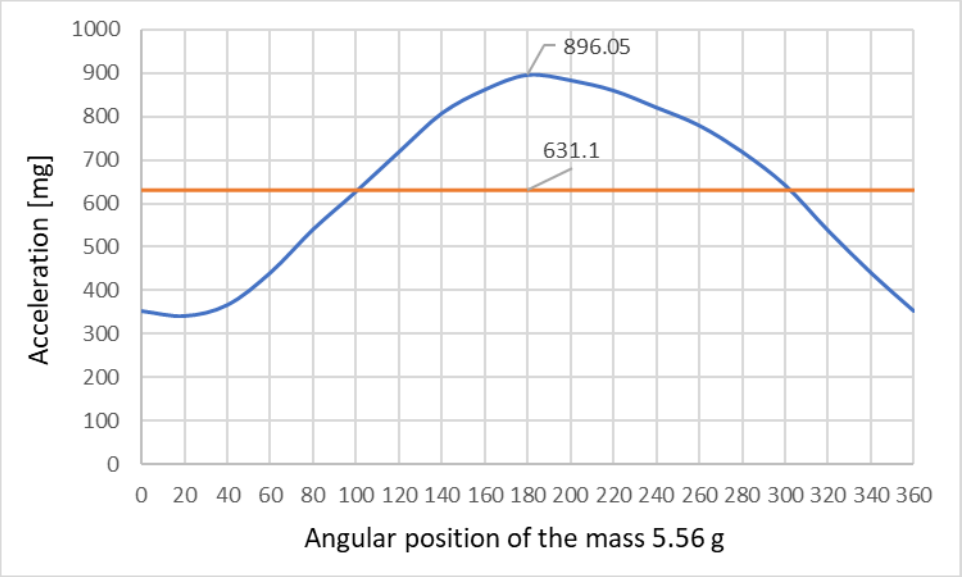

Figure3.08. Disc 1, bearing 2: residual unbalance 2.33 g, position 180°.

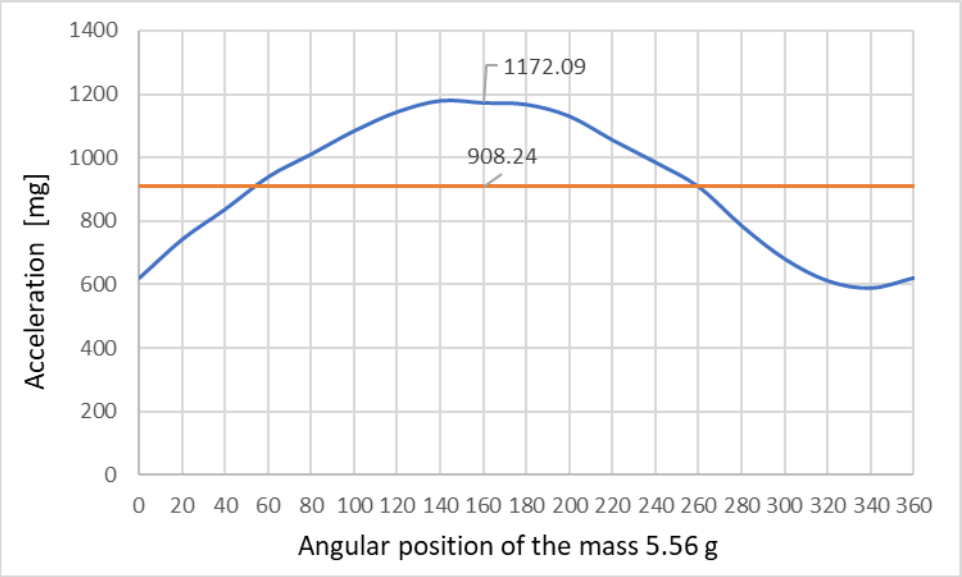

Figure.3.09. Disc 2, bearing 1: residual unbalance 1.66 g, position 160°.

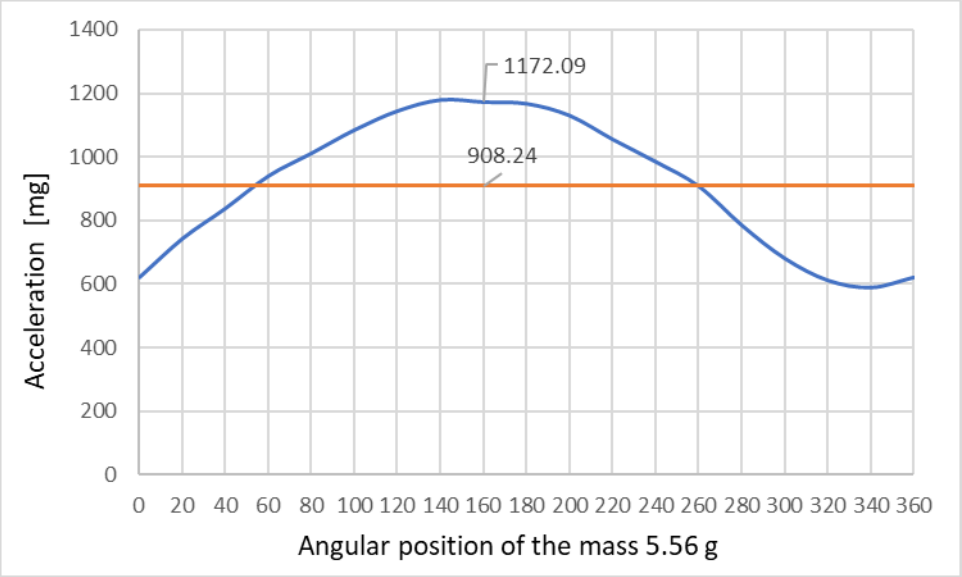

Figure.3.10. Disc 2 bearing 2: residual unbalance 1.81 g, position 180°.

As the results show from the figures, we can see that the value of residual unbalance goes from 600 mg to 900 mg depending on the mass and the position.

3.3.2. Spectrum analysis:

For the spectrum analysis, we did many tests putting the masses at different positions in the simulator and extracted the vibration signals and transform it from time domain to frequency domain. Some tests are analyzed on a non-stationary speed (from the start to 34 Hz) and some on a stationary speed (34 Hz).

3.3.2.1. Stationary speed spectrum analysis:

In figures (3.11 and 3.12), we have presented the frequency spectrum of the vertical measurements on the two bearings with the discs without created unbalance. We note the presence of the residual unbalance previously determined at the speed 33.44 Hz (peak 1) with an acceleration of 183.27 mg at bearing 1 and143.05 mg at bearing 2. As observed from both figures, there is evidence of a minor mass imbalance, as indicated by a significant increase in the peak at 1x. Additionally, the remaining peaks suggest minor frequency misalignment at both figures.

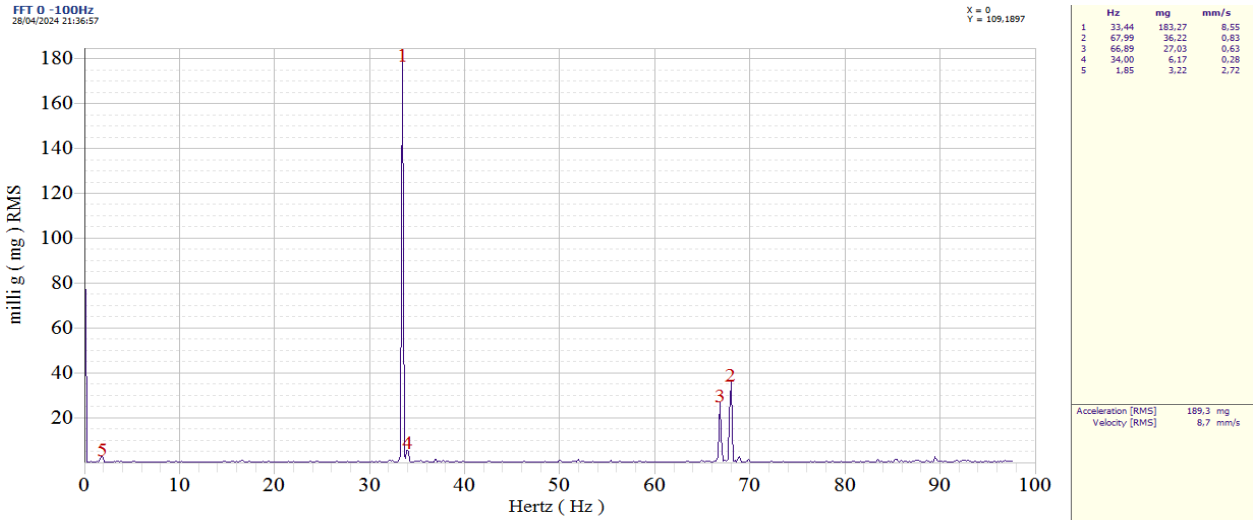

Figure 3.11. Vertical acceleration spectrum on bearing 1 with rotor speed 34 Hz without mass.

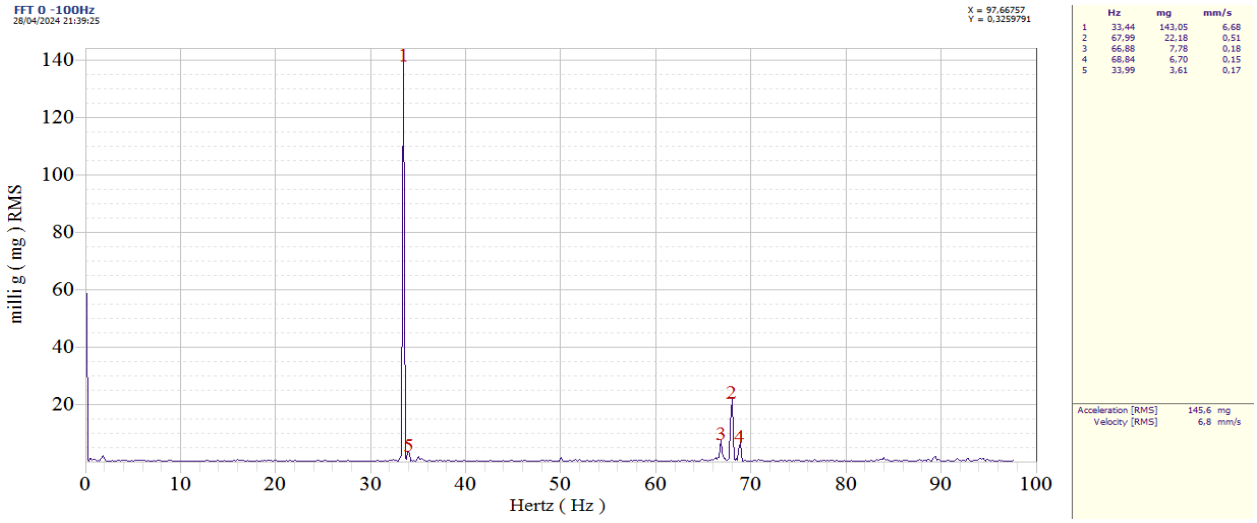

Figure 3.12. Vertical acceleration spectrum on bearing 2 with rotor speed 34 Hz without mass.

The figures (3.13 and 3.14) present the frequency spectrum of the horizontal measurements on the two bearings with the discs without created unbalance. We note the presence of the residual unbalance previously determined at the speed 33.47 Hz (peak 1) with an acceleration of 128.35 mg at bearing 1 and 69.95 at bearing 2. According to these two spectra, we note the presence of second harmonic with the same intensity as the fundamental frequency (127.88 mg) at bearing 1 and with a second harmonic twice then as the fundamental frequency at bearing 2 (133.8 mg).

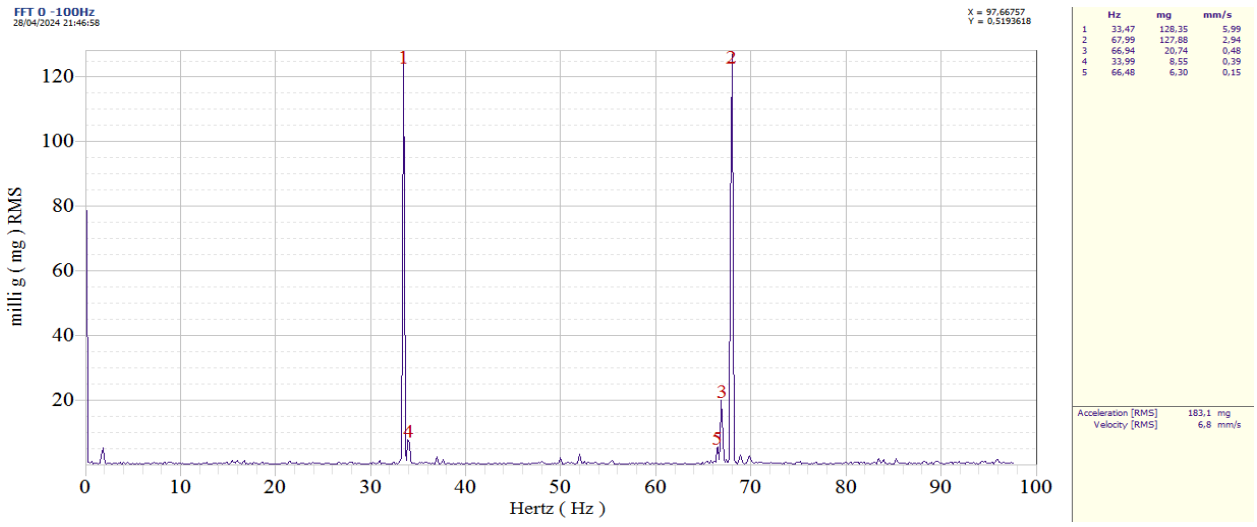

Figure 3.13. Horizontal acceleration spectrum on bearing 1 with rotor speed 34 Hz without mass.

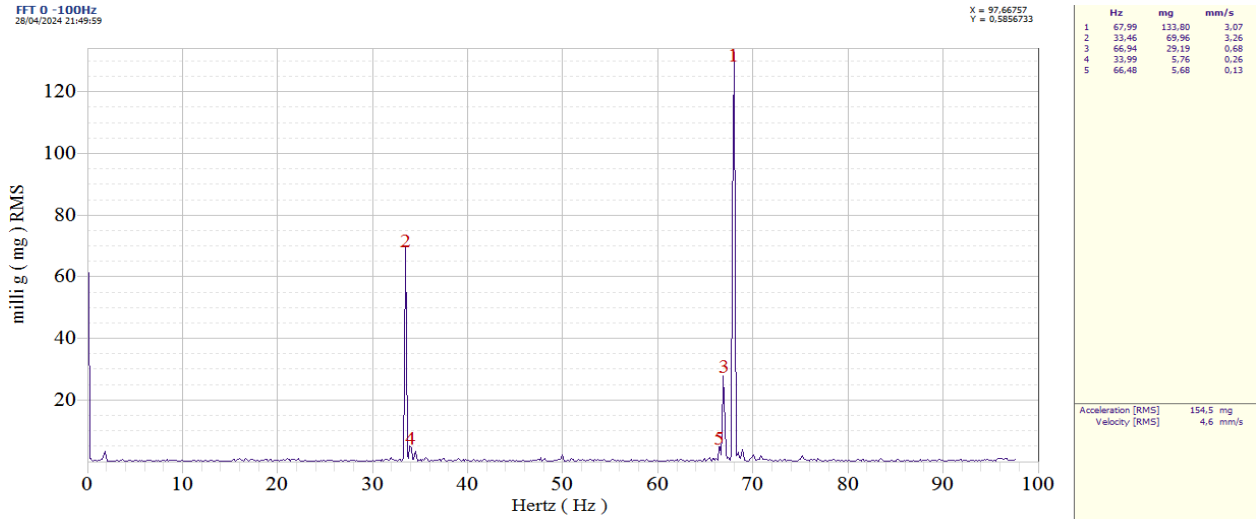

Figure 3.14. Horizontal acceleration spectrum on bearing 2 with rotor speed 34 Hz without mass.

The addition of a mass of 4.95 g at the 0° position of disk 1 manifested by a peak at the fundamental frequency 33.44 Hz with almost no increase in acceleration (127.74 mg) (figure 3.15). This is due to the balancing of this mass added to the mass of the residual unbalance of disk 1. On the other hand, this mass has not balanced the mass of the residual of disk 2 (figure 3.16), this is visible with the increase in the fundamental frequency acceleration (835.49 mg).

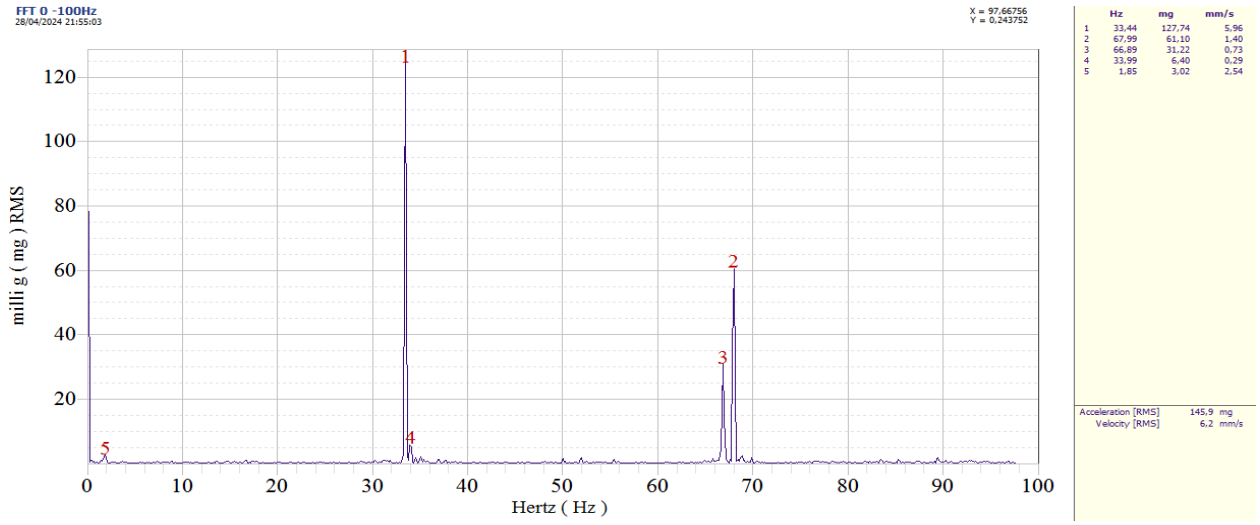

Figure 3.15. Vertical acceleration spectrum on bearing 1 with rotor speed 34 Hz with unbalance mass 4.95 g on disk 1 in position 0°.

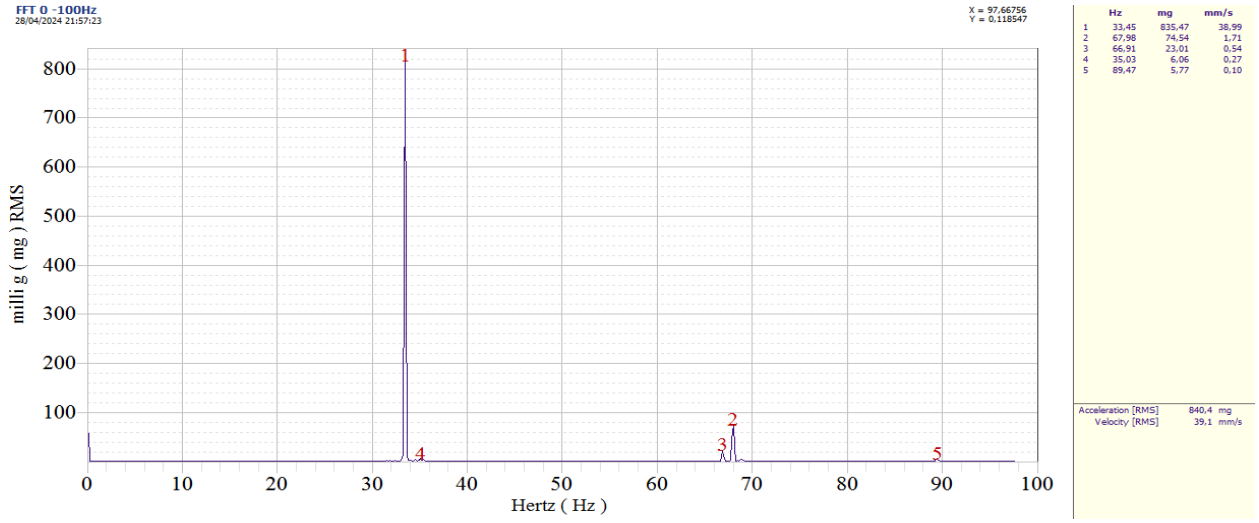

Figure 3.16. Vertical acceleration spectrum on bearing 2 with rotor speed 34 Hz with unbalance mass 4.95 g on disk 1 in position 0°.

In the horizontal direction, we still see the presence of misalignment with an increase in the acceleration of the fundamental frequency 33.48 Hz. This increase is more visible at bearing 2 (777.98 mg) (figure 3.18) than bearing 1(515.07 mg) (figure 3.17). This is due to the same remark cited for the previous vertical accelerations.

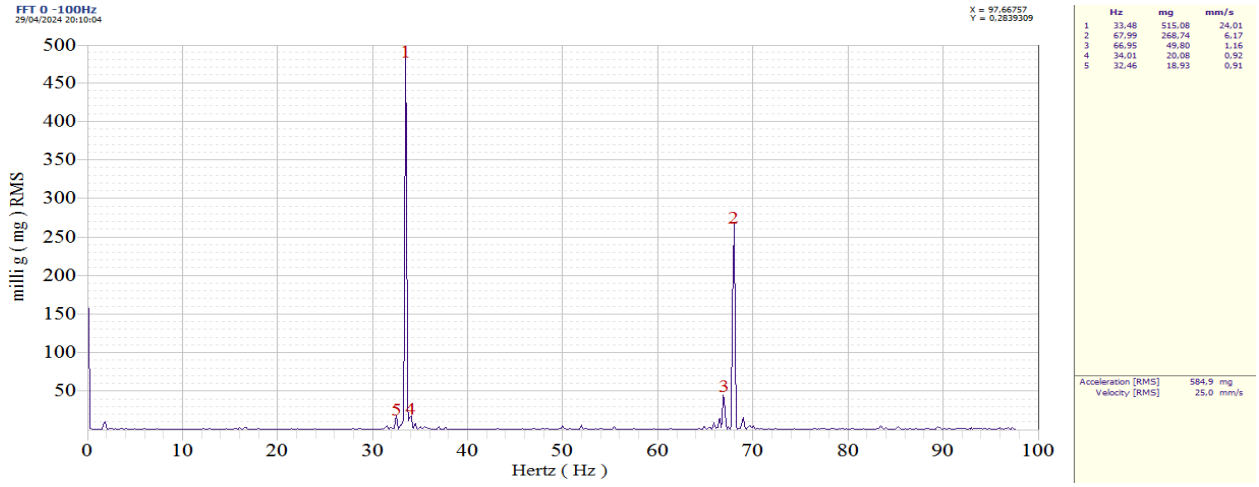

Figure 3.17. Horizontal acceleration spectrum on bearing 1 with rotor speed 34 Hz with unbalance mass 4.95 g on disk 1 in position 0°.

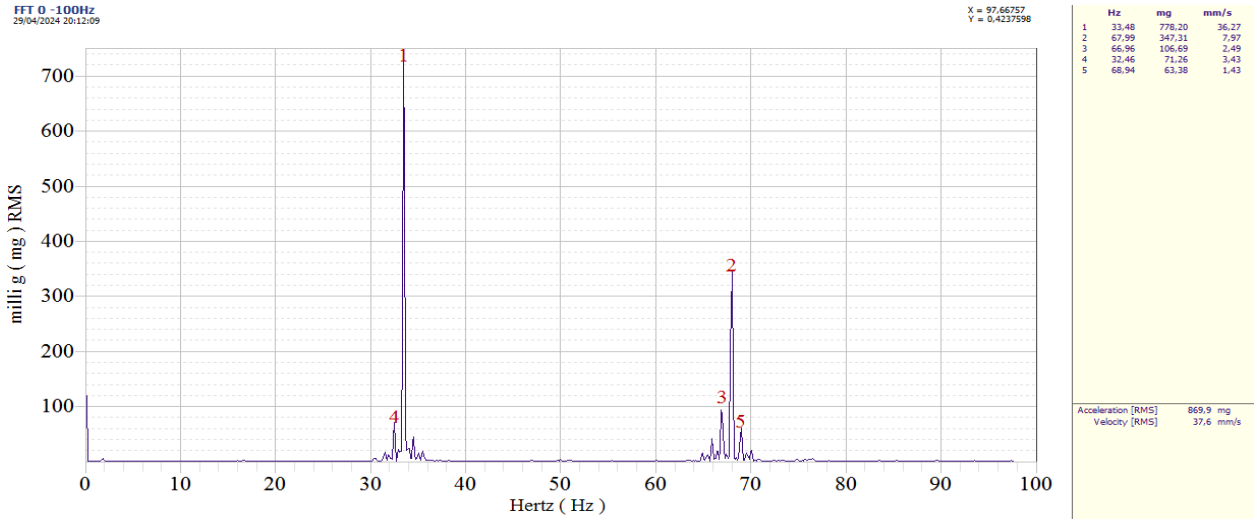

Figure 3.18. Horizontal acceleration spectrum on bearing 2 with rotor speed 34 Hz with unbalance mass 4.95 g on disk 1 in position 0°.

When two masses of 4.95 g each are placed in the two disks at the same angular positions 0°, the vertical acceleration spectrum give peaks at the fundamental frequency (33.45 Hz) with values of 303.14 mg at bearing 1 and 1894.53 mg at bearing 2 (figures 3.19 and 3.20). We can clearly see that the acceleration at bearing 2 is much higher than that of bearing 1. This is due to the second mass of disk 2 which accentuated its unbalance and which created an unbalance of disk 1.

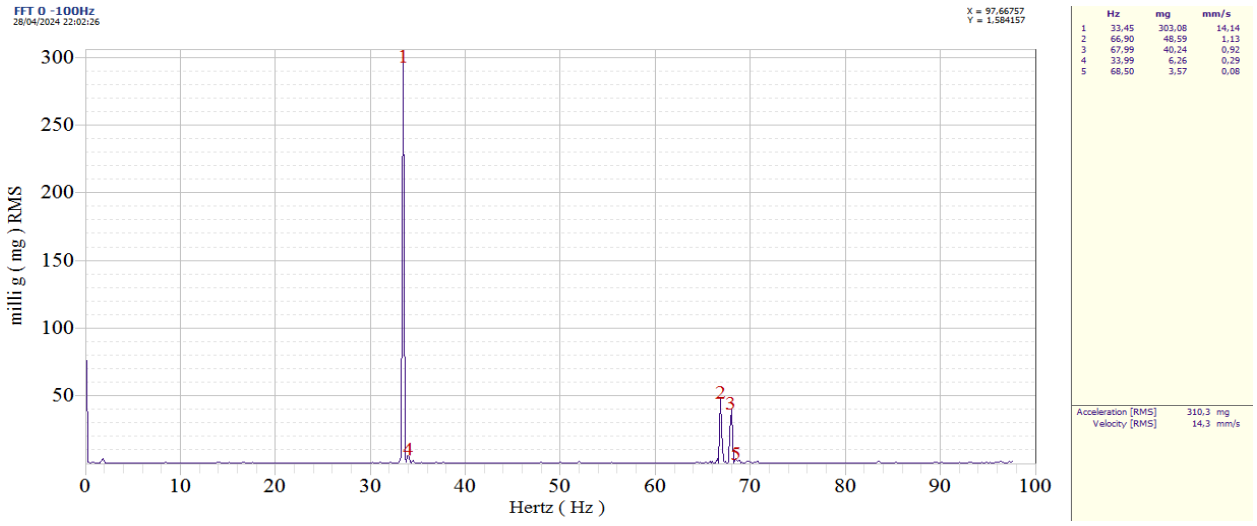

Figure 3.19. Vertical acceleration spectrum on bearing 1 with rotor speed 34 Hz with unbalance masses 4.95 g on disks 1 and 2 in positions 0°.

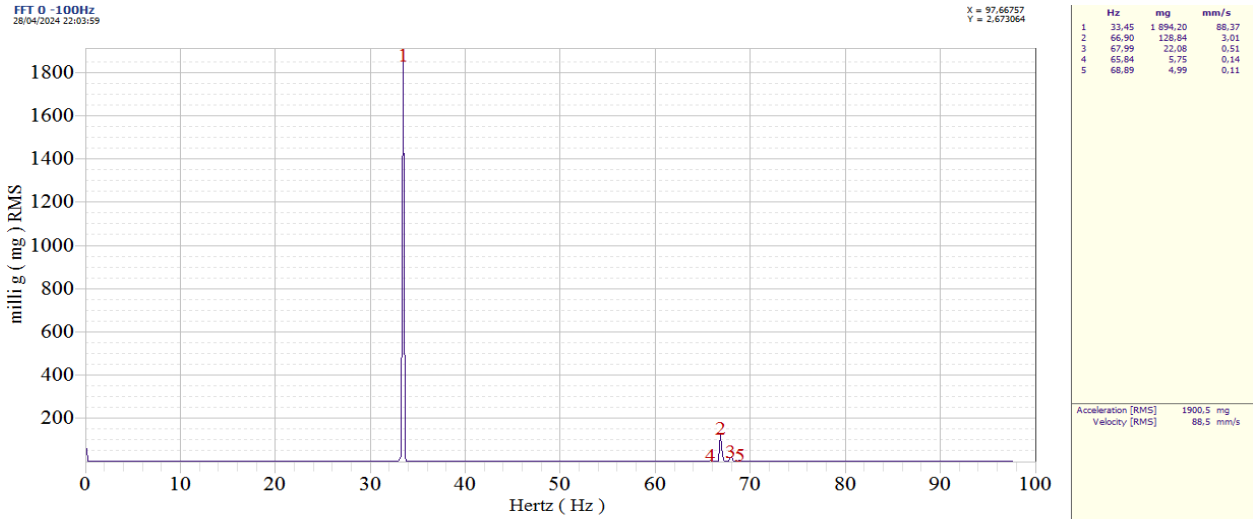

Figure 3.20. Vertical acceleration spectrum on bearing 2 with rotor speed 34 Hz with unbalance masses 4.95 g on disks 1 and 2 in positions 0°.

In figures (3.21 and 3.22), we have presented the frequency spectra of the horizontal acceleration at bearings 1 and 2 respectively. We notice that the masses added to the discs accentuate the unbalance, particularly on bearing 2.

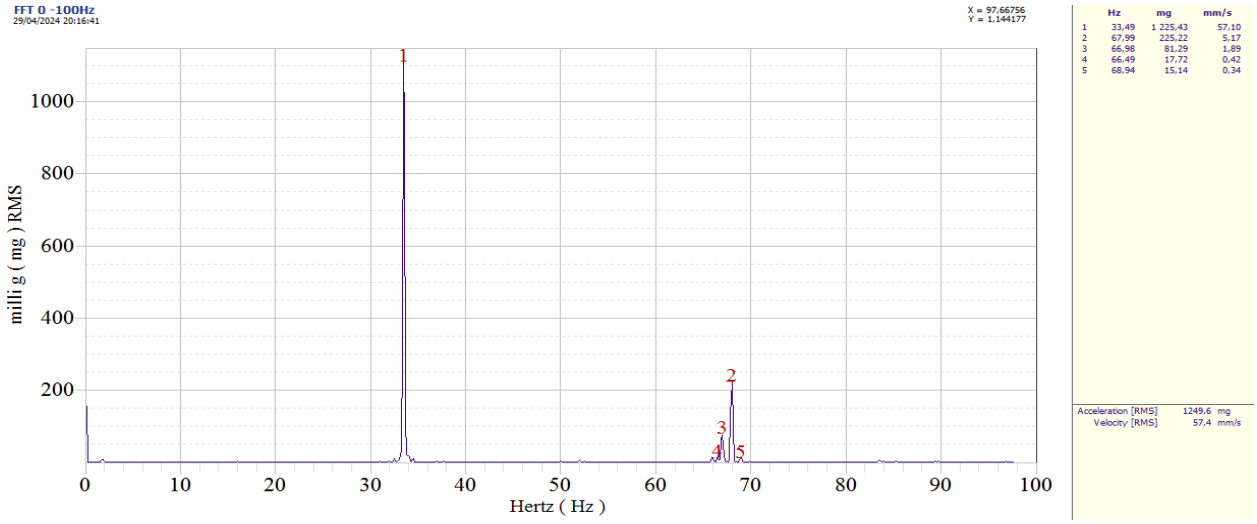

Figure 3.21. Horizontal acceleration spectrum on bearing 1 with rotor speed 34 Hz with unbalance masses 4.95 g on disks 1 and 2 in positions 0°.

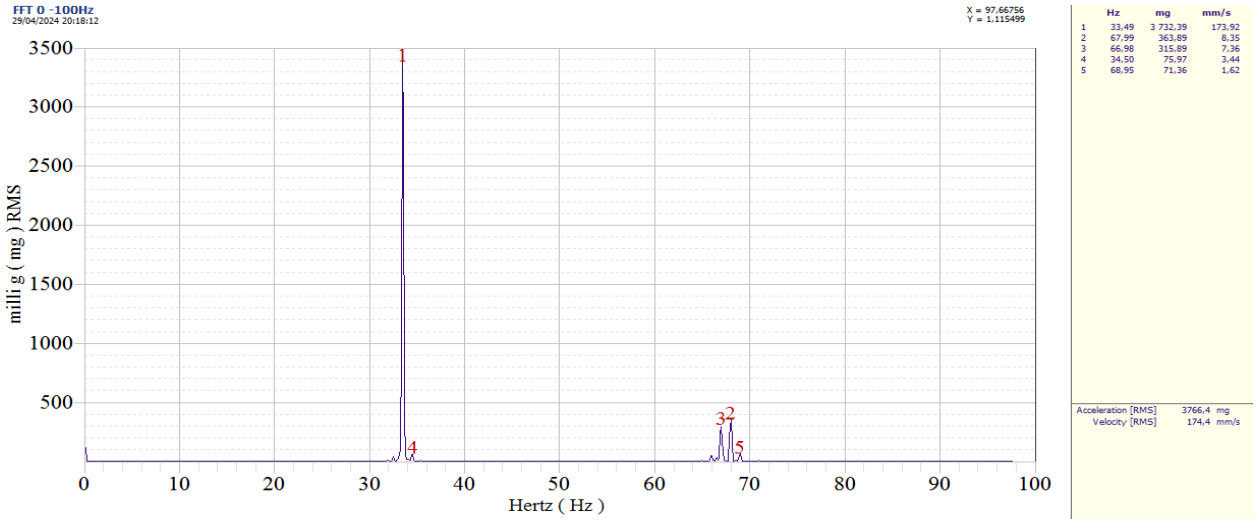

Figure 3.22. Horizontal acceleration spectrum on bearing 2 with rotor speed 34 Hz with unbalance masses 4.95 g on disks 1 and 2 in positions 0°.

3.3.2.2. Non stationary speed spectrum analysis:

In this part of the analysis, we tried to extract the frequency spectrum for the measurements carried out with variable speed from start to stationary speed 34 Hz. The aim of this analysis is to understand the spectral representation of frequencies for variable speeds.

Figures (3.21 and 3.22) represent the frequency spectra of the vertical acceleration recordings with the variable speed from 0 to 34Hz without added masses for bearings 1 and 2 respectively. We notice a visible difference with the spectra with constant speed 34 Hz (figures 3.11 and 3.12) where we see the almost disappearance of harmonics and the appearance of a frequency sweep in the 16-33.42 Hz zone. This in the case of an analysis for a stationary speed is a sign of turbulence in this frequency zone which will mislead us. The intensity of the acceleration is slightly overestimated for the frequency 33.42 Hz.

For horizontal accelerations (figure 3.23 and 3.24), we notice the frequency sweep 20-33.43 Hz which characterizes turbulence in this frequency zone. This analysis confirms the presence of a horizontal misalignment detected in the figures (3.13 and 3.14).

The signature of turbulence in the 16-34 Hz zone appears in all the spectra when we add the mass 4.95 g and in the different configurations treated previously with the confirmation of the

unbalance (figures 3.25-3.32). We also notice the disappearance of harmonics when there is no misalignment fault.

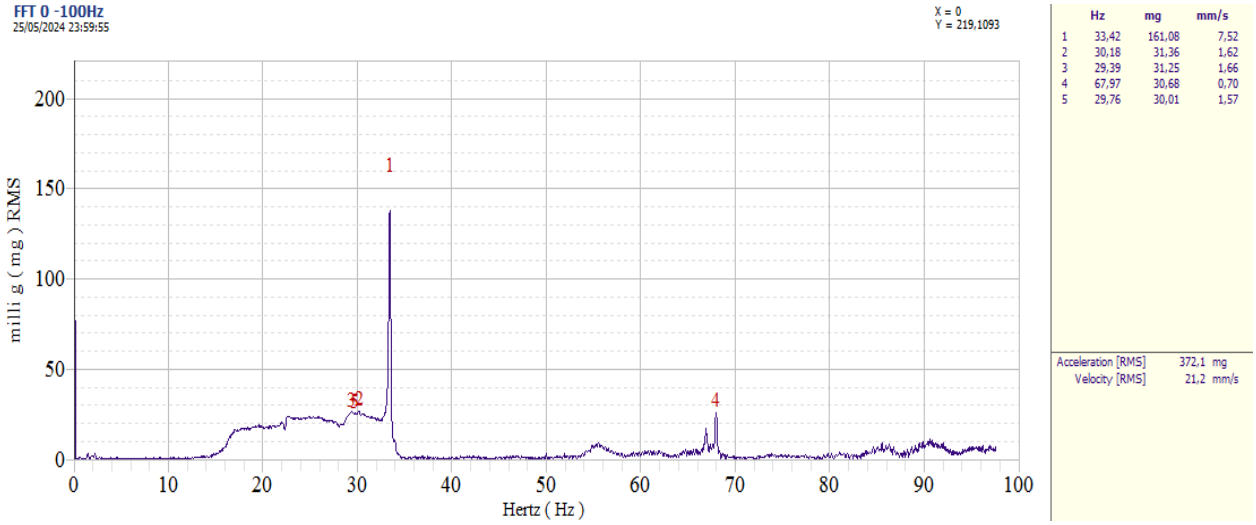

Figure 3.21. Vertical acceleration spectrum on bearing 1 with variable speed 0-34 Hz without mass.

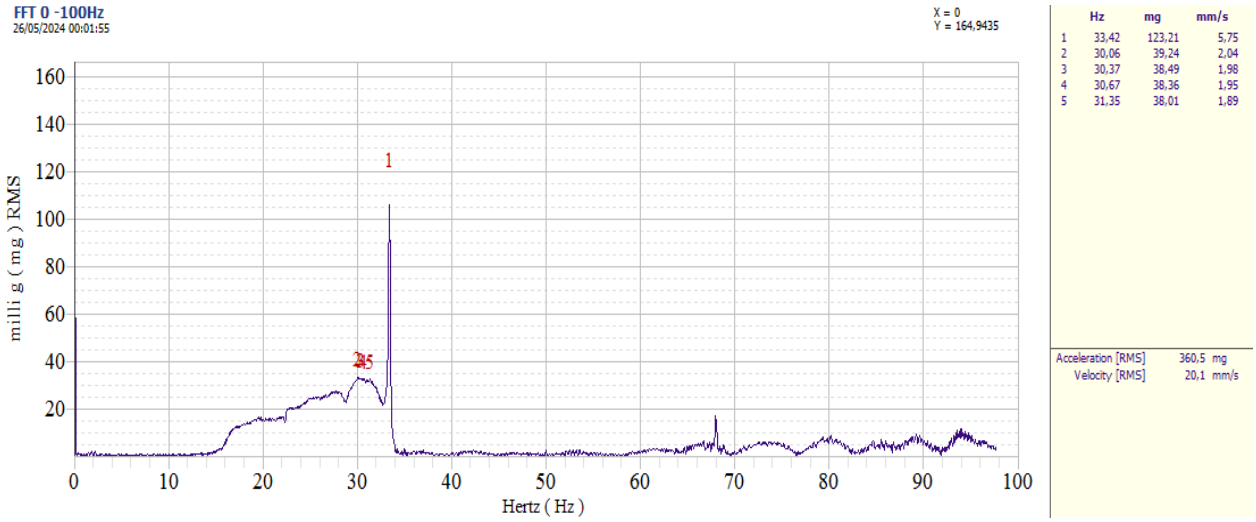

Figure 3.22. Vertical acceleration spectrum on bearing 2 with variable speed 0-34 Hz without mass.

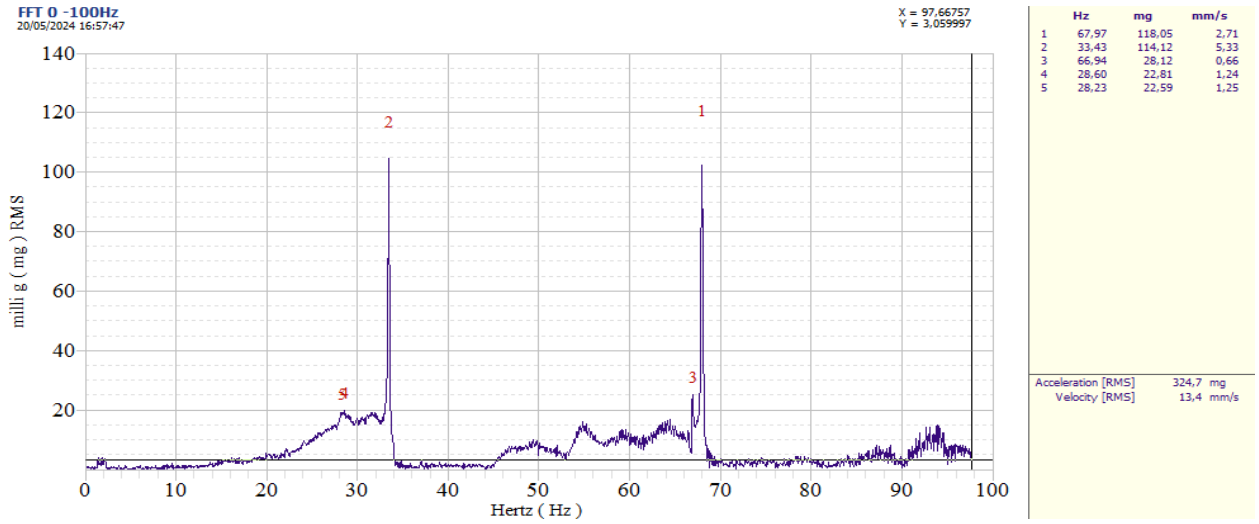

Figure 3.23. Horizontal acceleration spectrum on bearing 1 with variable speed 0-34 Hz without mass.

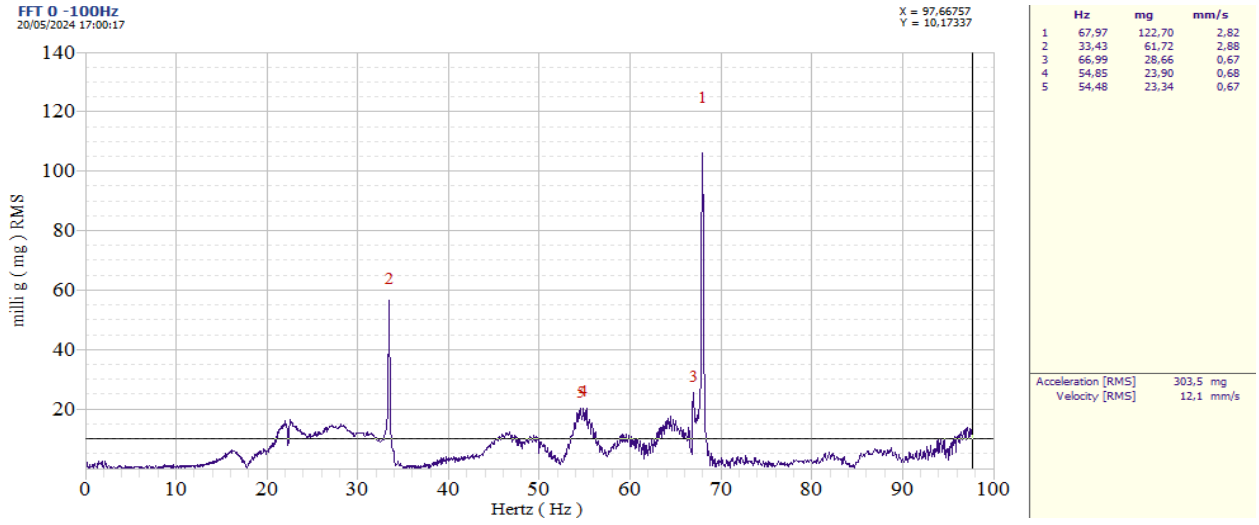

Figure 3.24. Horizontal acceleration spectrum on bearing 2 with variable speed 0-34 Hz without mass.

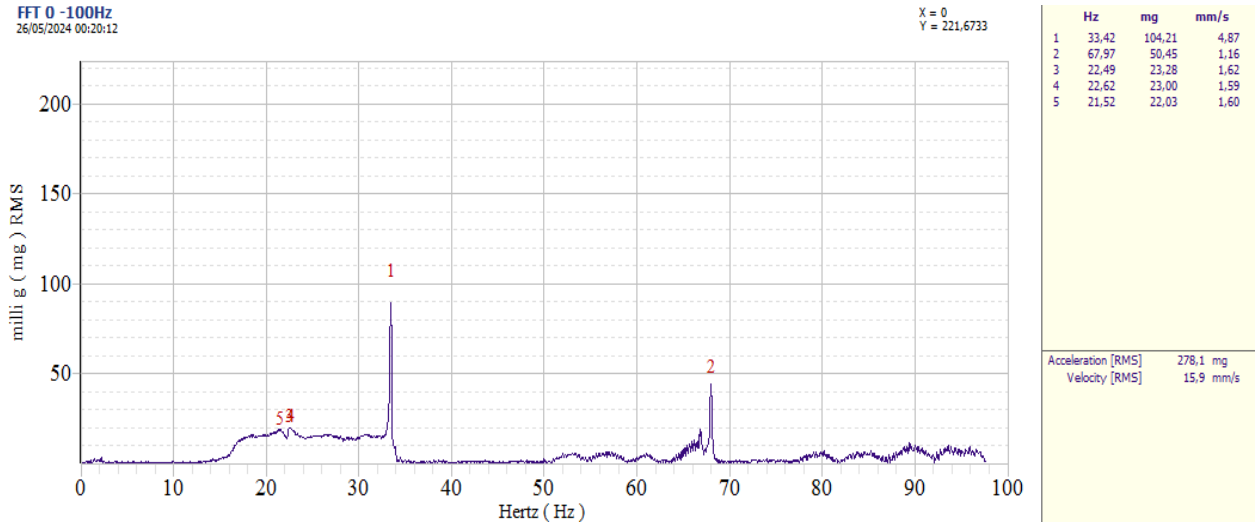

Figure 3.25. Vertical acceleration spectrum on bearing 1 with variable speed 0-34 Hz with unbalance mass 4.95 g on disk 1 in position 0°.

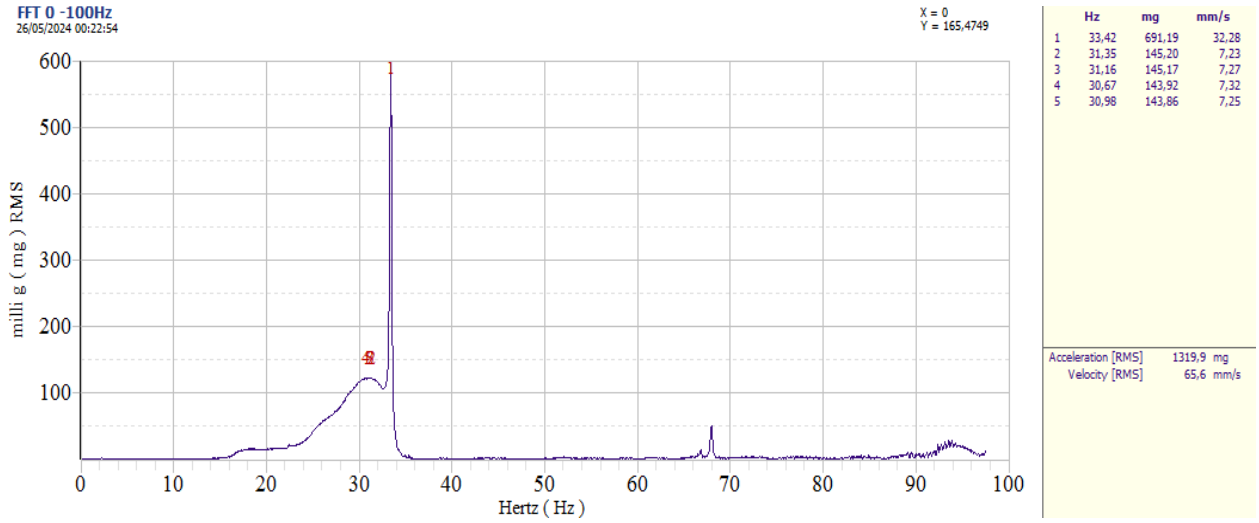

Figure 3.26. Vertical acceleration spectrum on bearing 2 with variable speed 0-34 Hz with unbalance mass 4.95 g on disk 1 in position 0°.

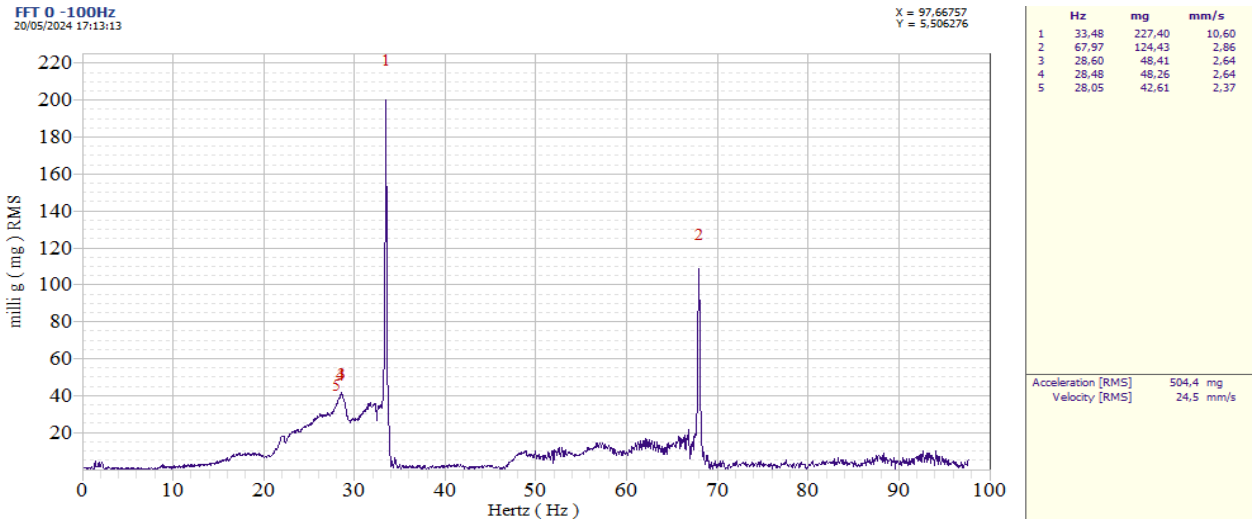

Figure 3.27. Horizontal acceleration spectrum on bearing 1 with variable speed 0-34 Hz with unbalance mass 4.95 g on disk 1 in position 0°.

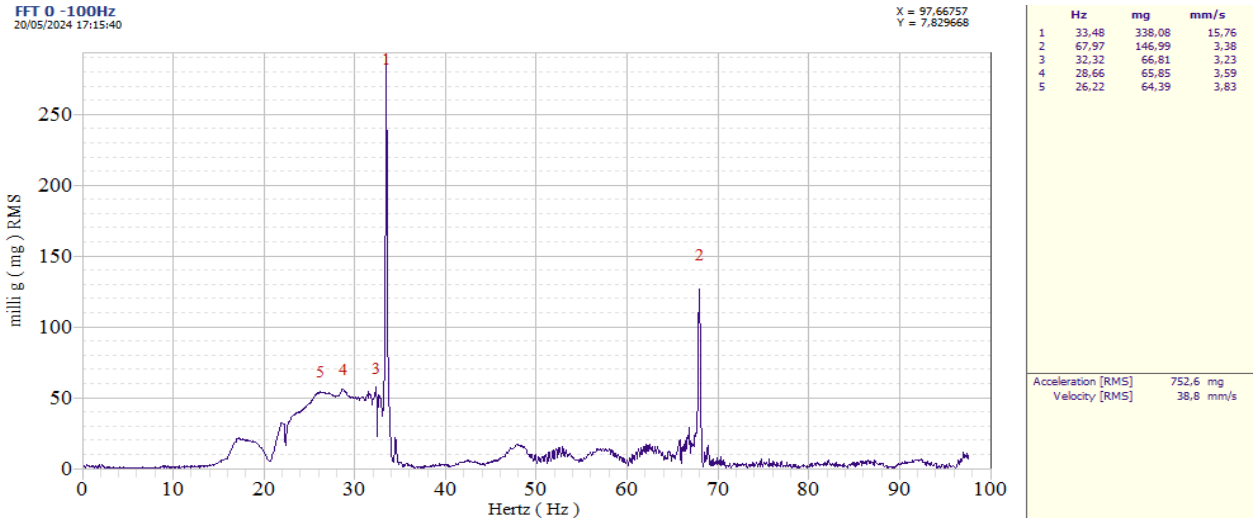

Figure 3.28. Horizontal acceleration spectrum on bearing 2 with variable speed 0-34 Hz with unbalance mass 4.95 g on disk 1 in position 0°.

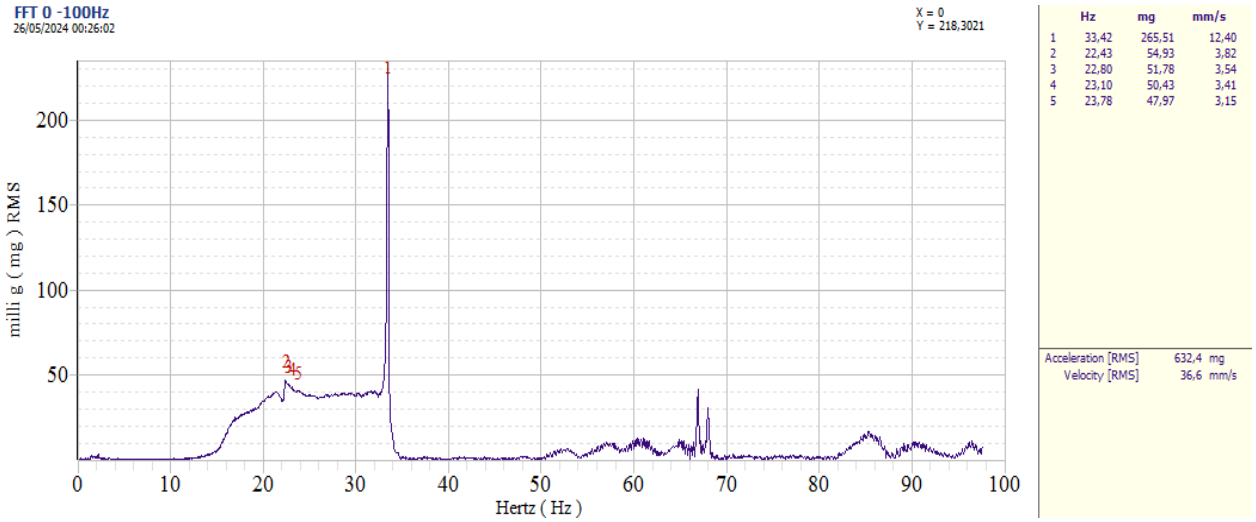

Figure 3.29. Vertical acceleration spectrum on bearing 1 with variable speed 0-34 Hz with unbalance mass 4.95 g on disks 1 and 2 in positions 0°.

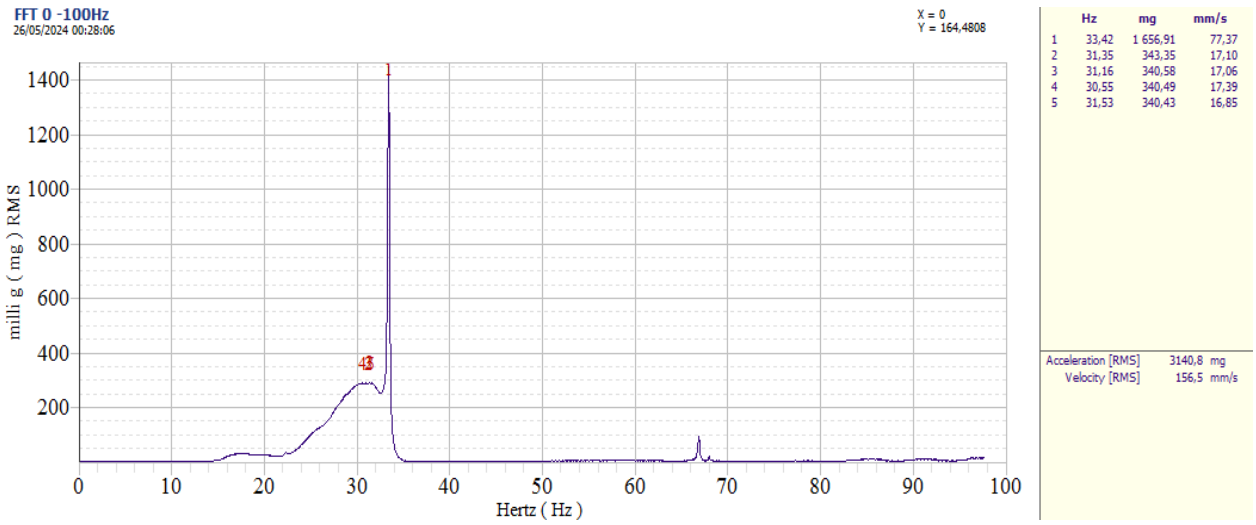

Figure 3.30. Vertical acceleration spectrum on bearing 2 with variable speed 0-34 Hz with unbalance mass 4.95 g on disks 1 and 2 in positions 0°.

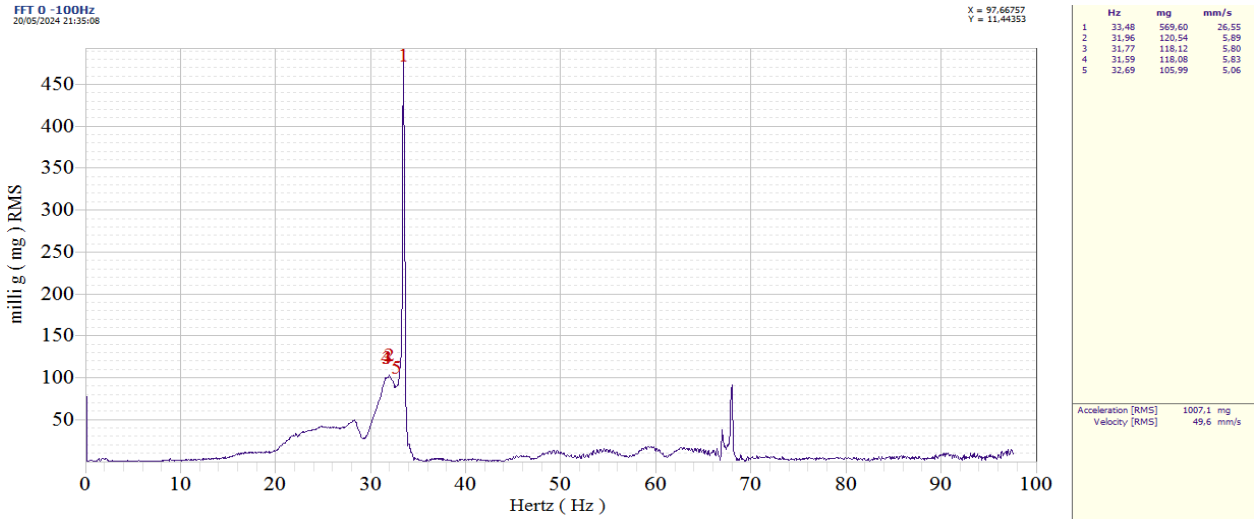

Figure 3.31. Horizontal acceleration spectrum on bearing 1 with variable speed 0-34 Hz with unbalance mass 4.95 g on disks 1 and 2 in positions 0°.

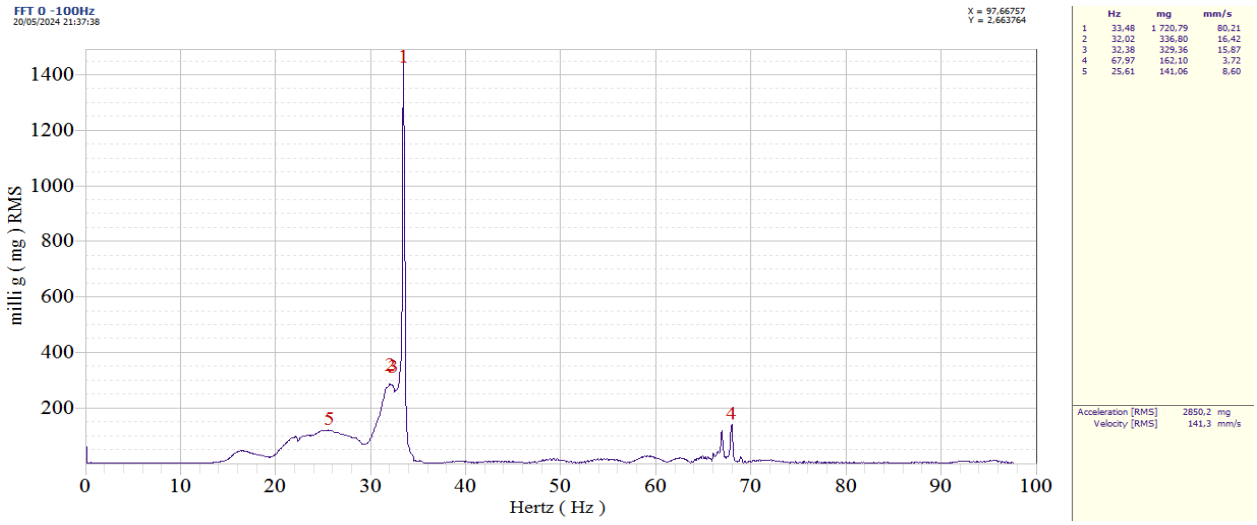

Figure 3.32. Horizontal acceleration spectrum on bearing 2 with variable speed 0-34 Hz with unbalance mass 4.95 g on disks 1 and 2 in positions 0°.

3.3.3. Daubechies wavelet analysis

In this section, we treat the results of the Daubechies wavelet transform of the program carried out on MATLAB on the signals recorded from the different configurations treated in the previous sections with variable speed 0-34 Hz. We have presented in the figures (3.33-3.56), and for all the cases treated previously, the calculation results given by MATLAB of the Daubechies wavelet transform of level 4 in image formats and its frequency spectra corresponding to the 4th level of this wavelet transform.

In all the spectra of the Daubechies wavelet, we notice two distinct peaks, the first around 29 Hz and a second lower peak which corresponds to the rotation frequency of the rotor. The first peak does not appear in the spectra of the previous sections, but it can be noticed in those of the variable speed and in all cases, like mentioned, the noise zone in the area below the fundamental frequency. This directs us towards a rapid passage of a resonance frequency of the rotor since this peak of the same frequency appears in both vertical and horizontal directions and the two bearings.

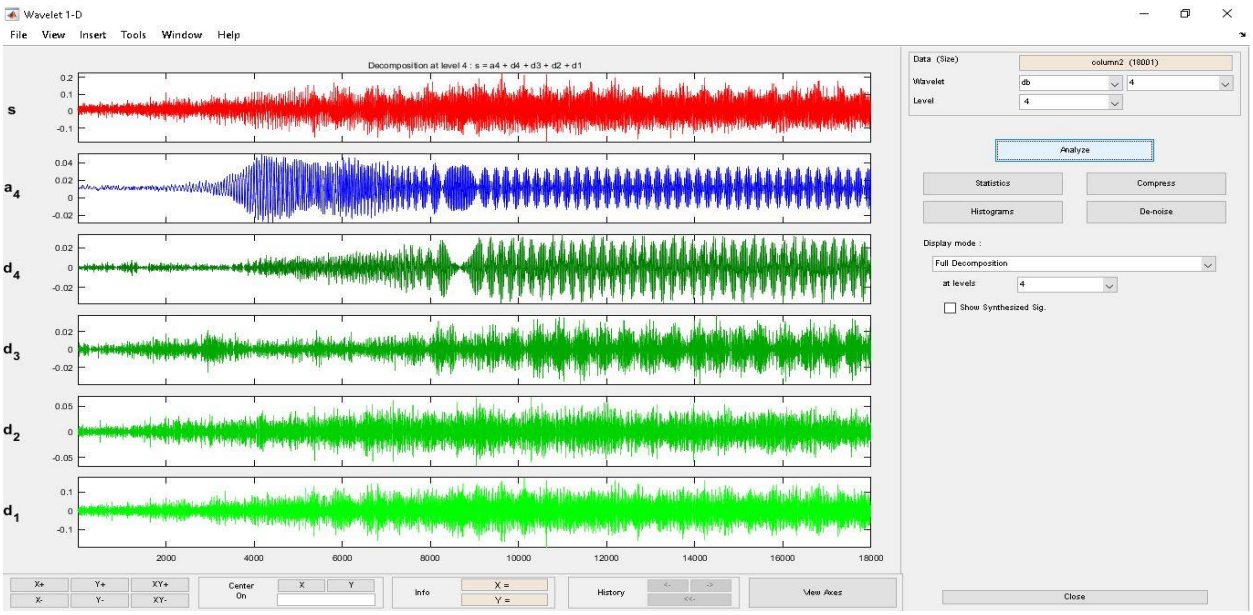

Figure 3.33. Daubechies wavelet calculation of vertical acceleration on bearing 1 with variable speed 0-34 Hz without mass.

This passage can be observed in the calculation images between 8 and 9 seconds from the start of the rotor. This resonance passage is not detected in the spectral analysis and it could only be unraveled by wavelet analysis. It is noted that the unbalance is visible in this analysis but of less importance than in the spectral analysis at stationary speed.

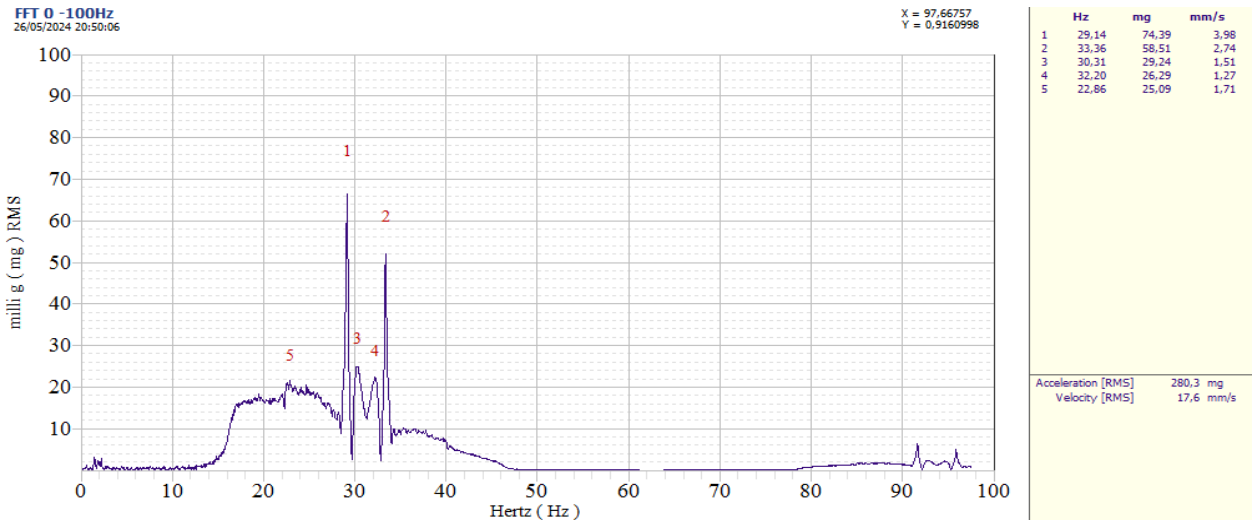

Figure 3.34. Daubechies wavelet spectrum of vertical acceleration on bearing 1 with variable speed 0-34 Hz without mass.

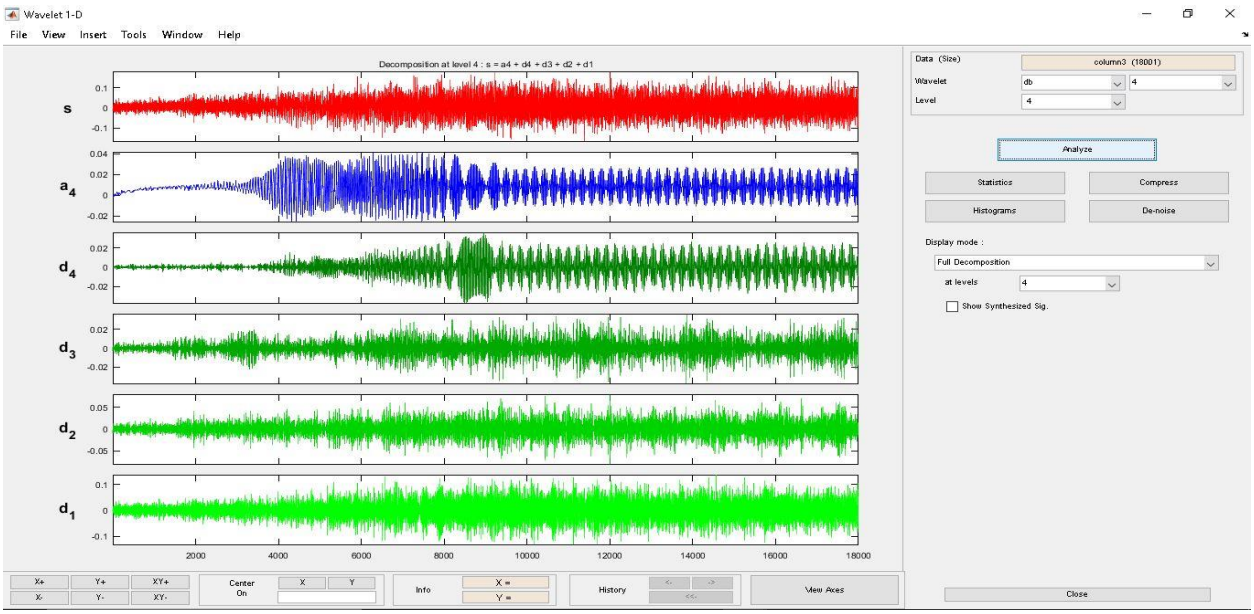

Figure 3.35. Daubechies wavelet calculation of vertical acceleration on bearing 2 with variable speed 0-34 Hz without mass.

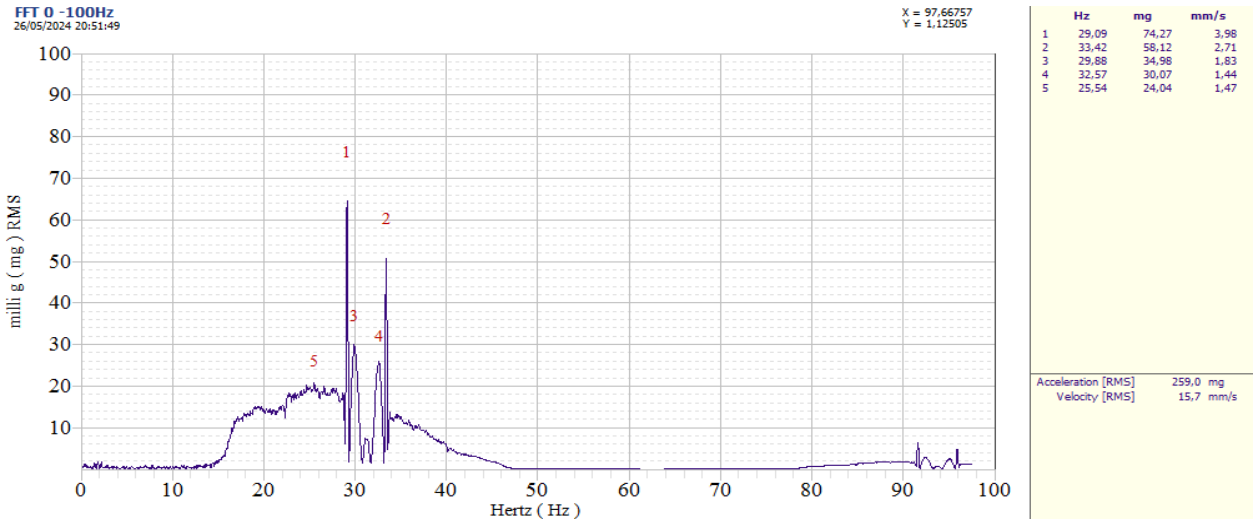

Figure 3.36. Daubechies wavelet spectrum of vertical acceleration on bearing 2 with variable speed 0-34 Hz without mass.

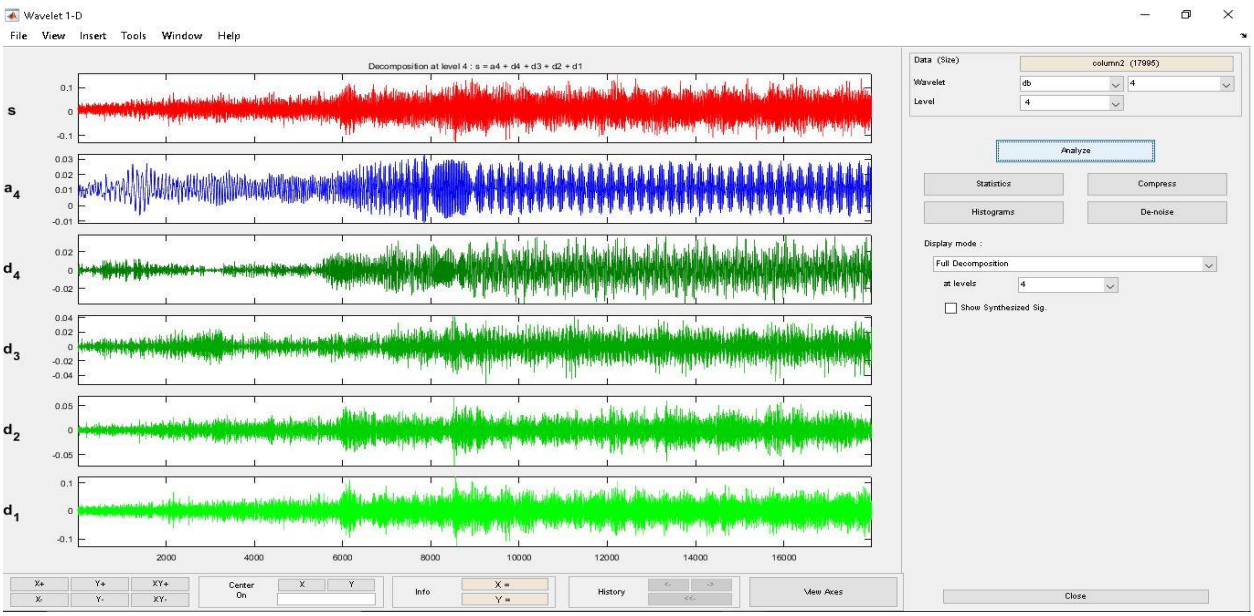

Figure 3.37. Daubechies wavelet calculation of horizontal acceleration on bearing 1 with variable speed 0-34 Hz without mass.

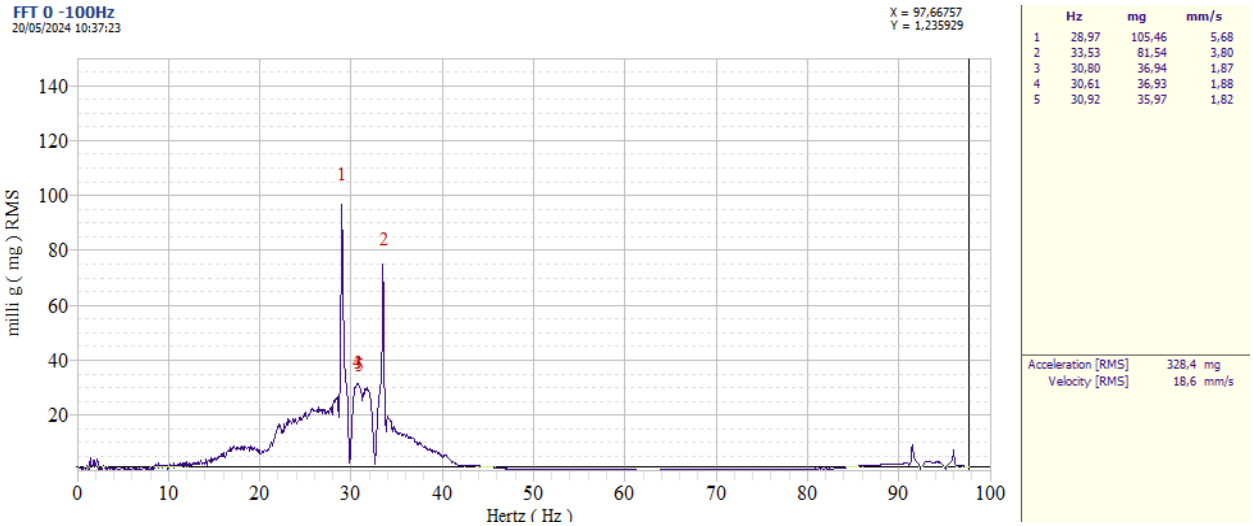

Figure 3.38. Daubechies wavelet spectrum of horizontal acceleration on bearing 1 with variable speed 0-34 Hz without mass.

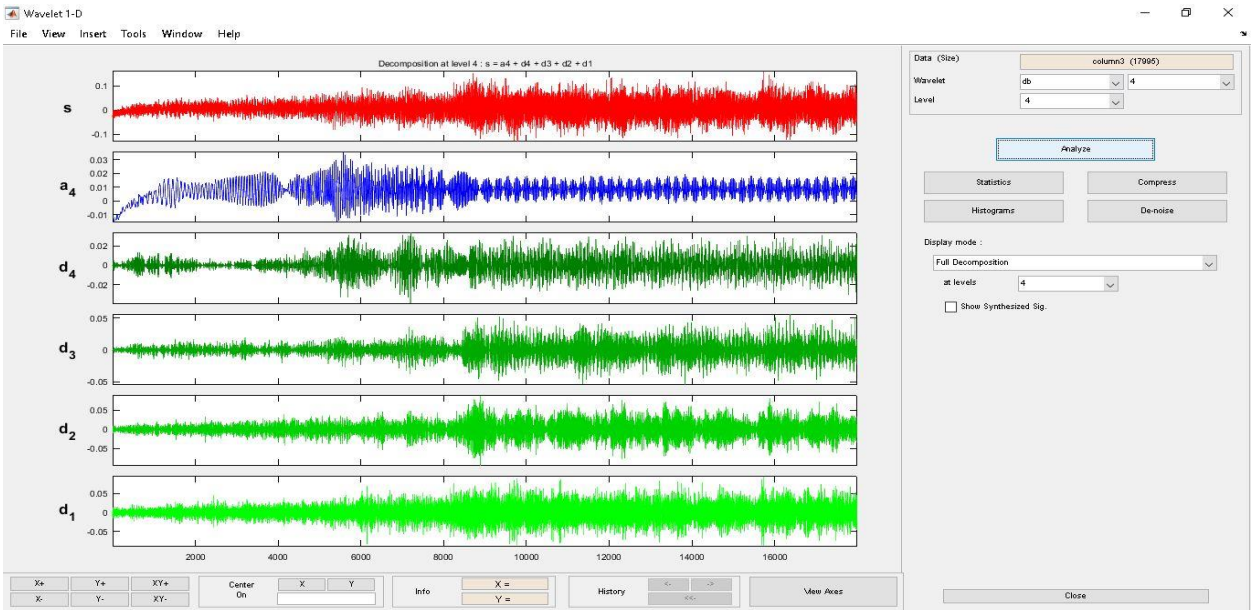

Figure 3.39. Daubechies wavelet calculation of horizontal acceleration on bearing 2 with variable speed 0-34 Hz without mass.

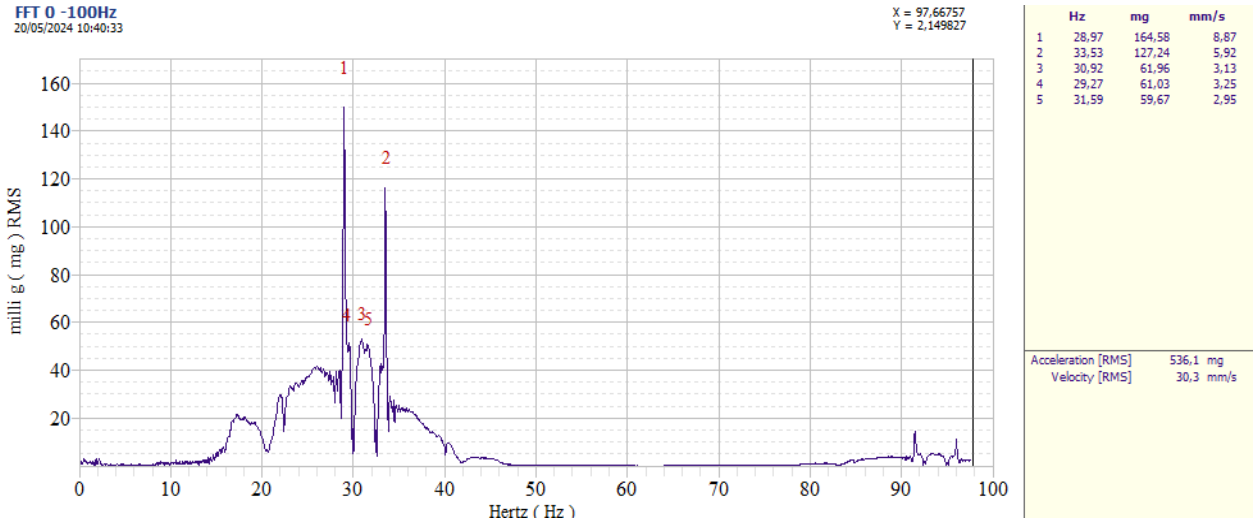

Figure 3.40. Daubechies wavelet spectrum of horizontal acceleration on bearing 1 with variable speed 0-34 Hz without mass.

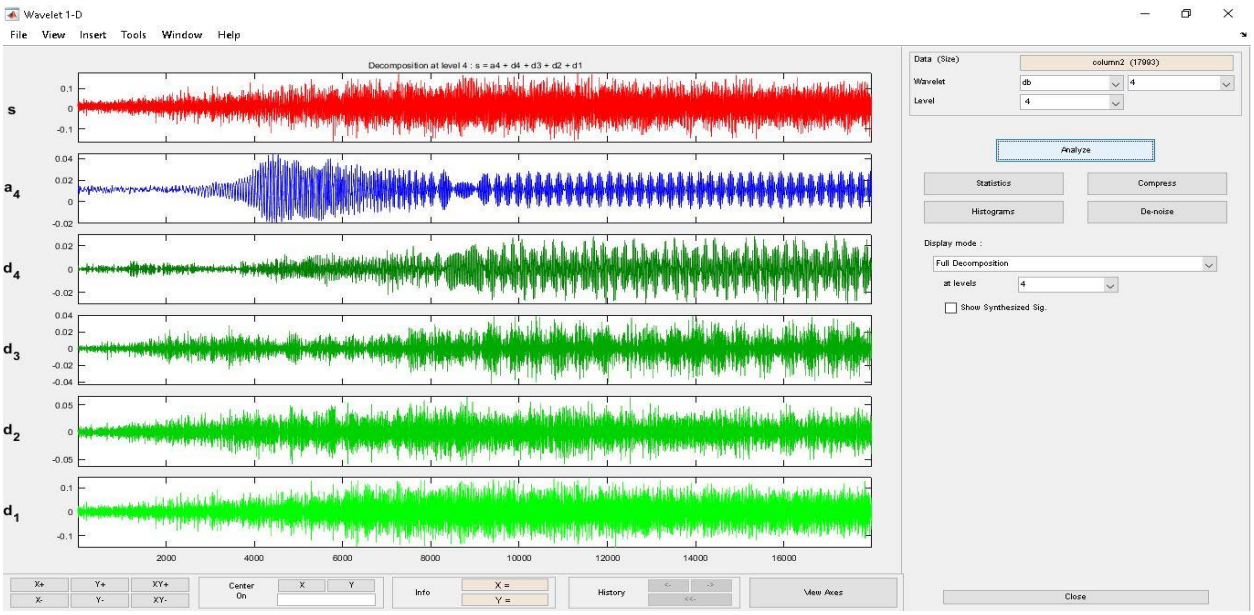

Figure 3.41. Daubechies wavelet calculation of vertical acceleration on bearing 1 with variable speed 0-34 Hz with unbalance mass 4.95 g on disk 1 in position 0°.

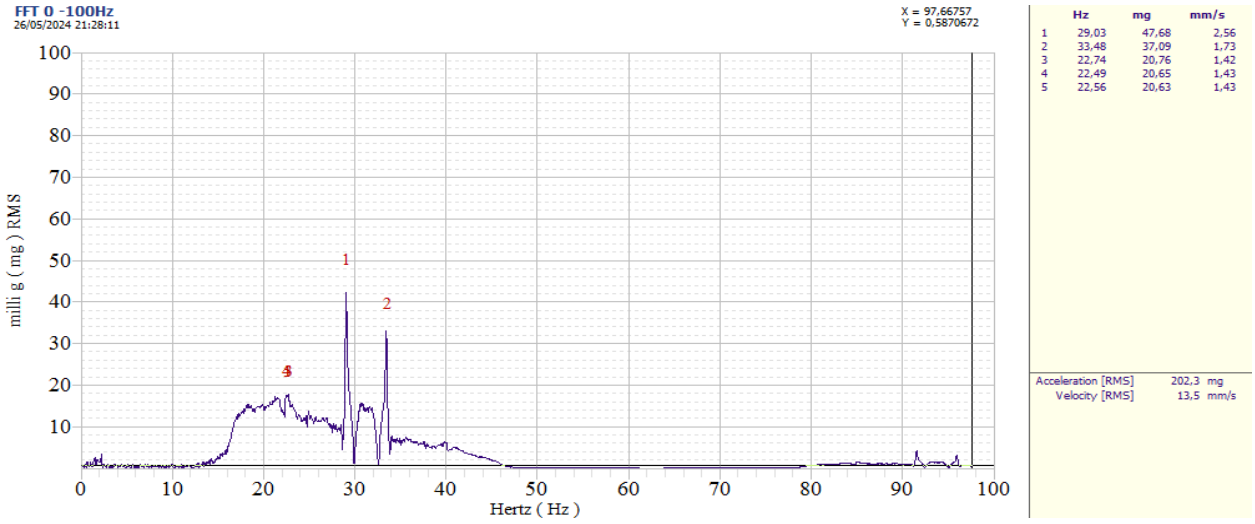

Figure 3.42. Daubechies wavelet spectrum of vertical acceleration on bearing 1 with variable speed 0-34 Hz with unbalance mass 4.95 g on disk 1 in position 0°.

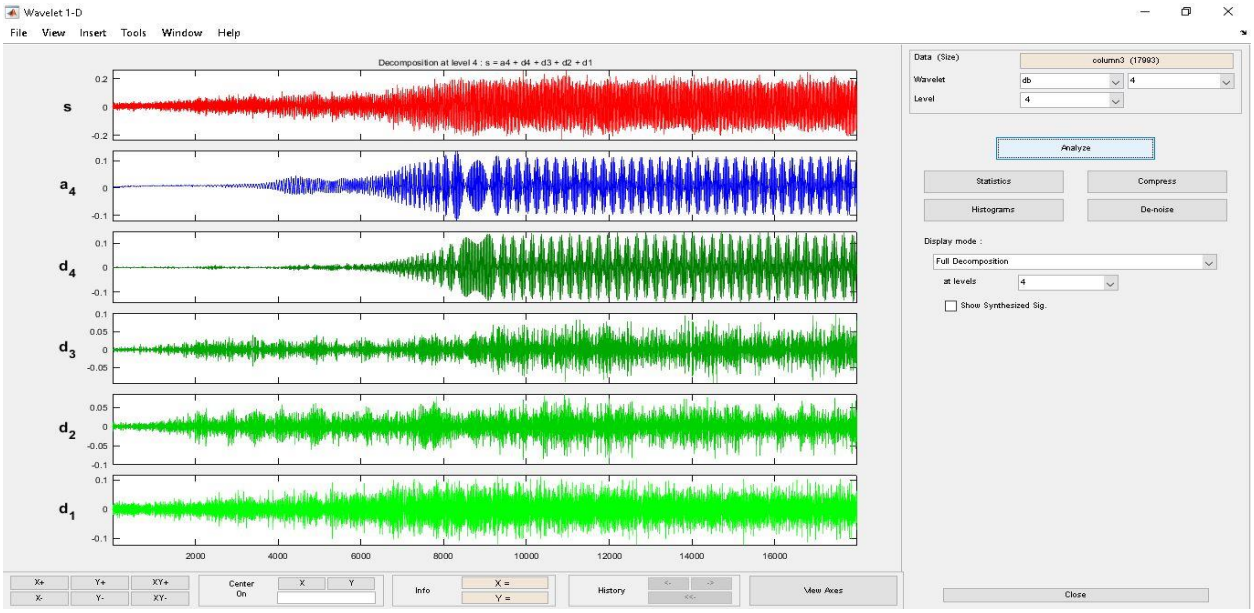

Figure 3.43. Daubechies wavelet calculation of vertical acceleration on bearing 2 with variable speed 0-34 Hz with unbalance mass 4.95 g on disk 1 in position 0°.

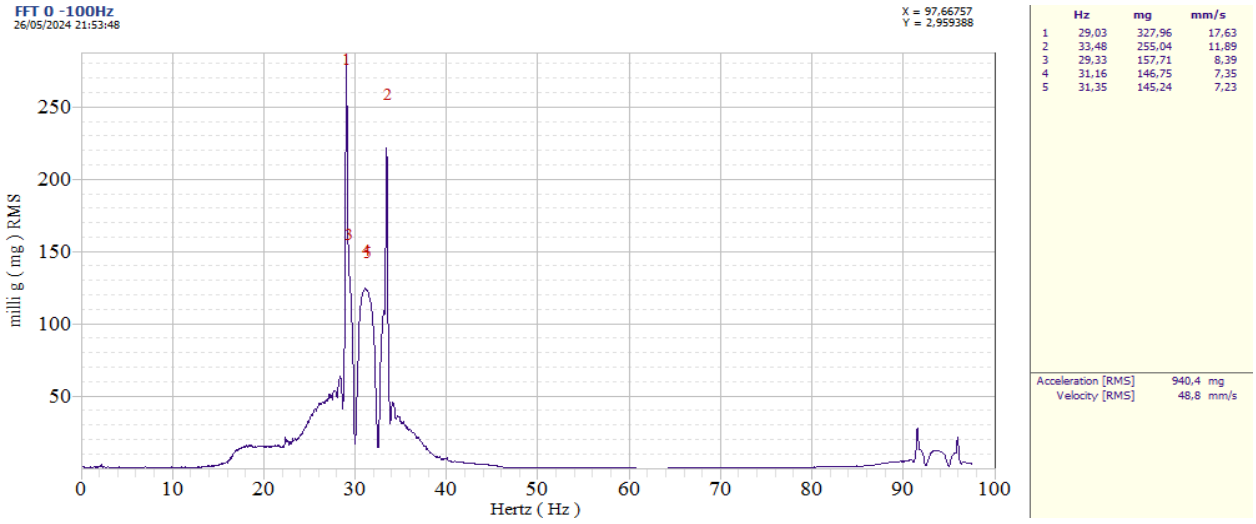

Figure 3.44. Daubechies wavelet spectrum of vertical acceleration on bearing 2 with variable speed 0-34 Hz with unbalance mass 4.95 g on disk 1 in position 0°.

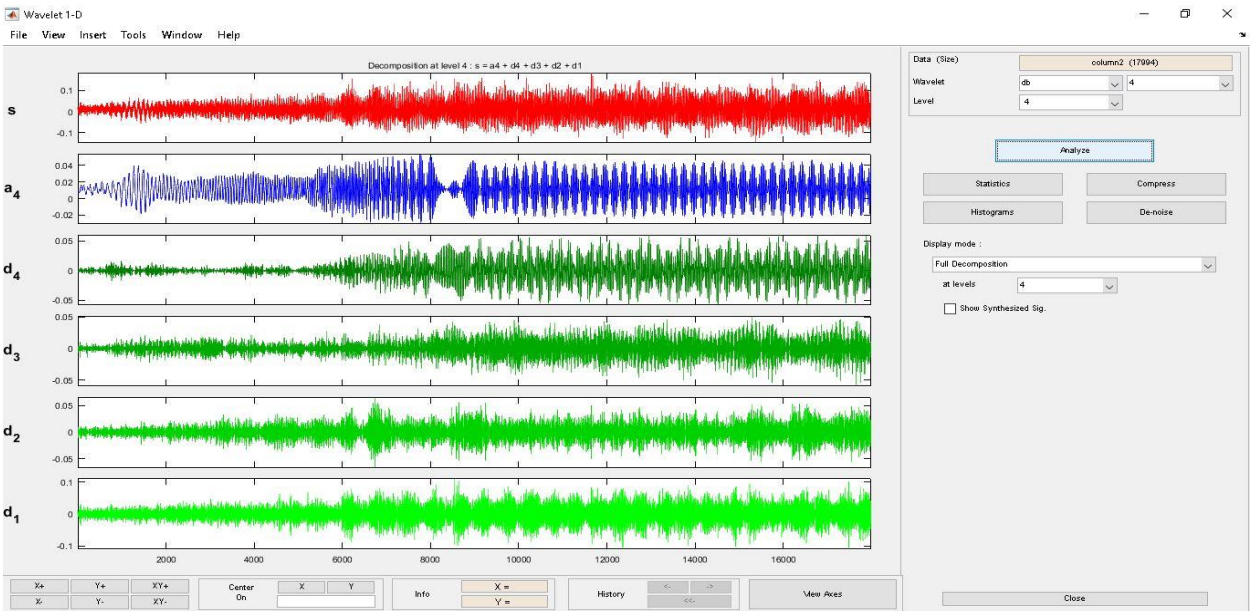

Figure 3.45. Daubechies wavelet calculation of horizontal acceleration on bearing 1 with variable speed 0-34 Hz with unbalance mass 4.95 g on disk 1 in position 0°.

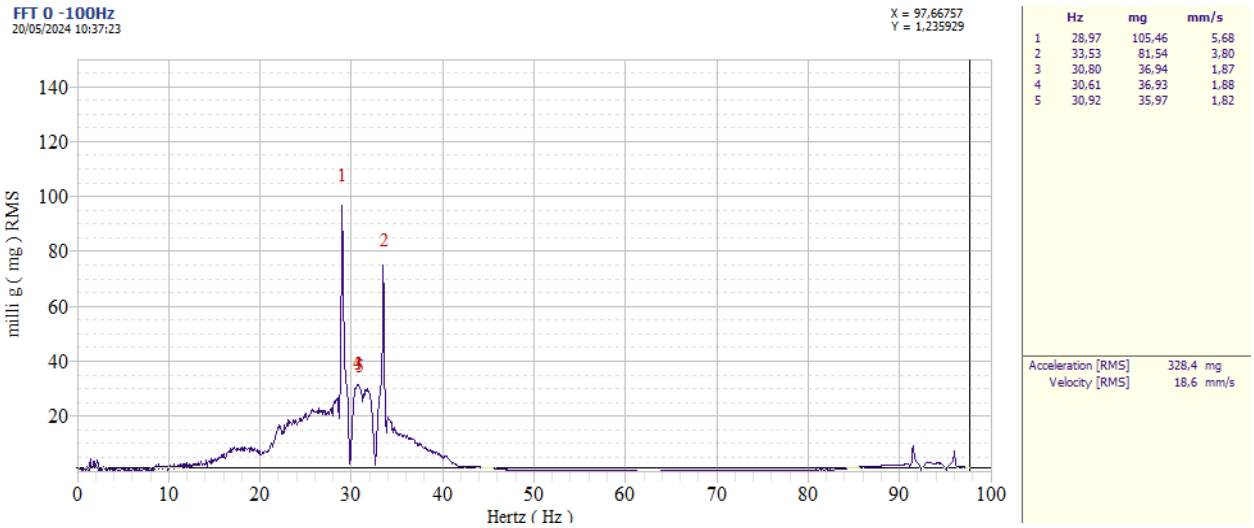

Figure 3.46. Daubechies wavelet spectrum of horizontal acceleration on bearing 1 with variable speed 0-34 Hz with unbalance mass 4.95 g on disk 1 in position 0°.

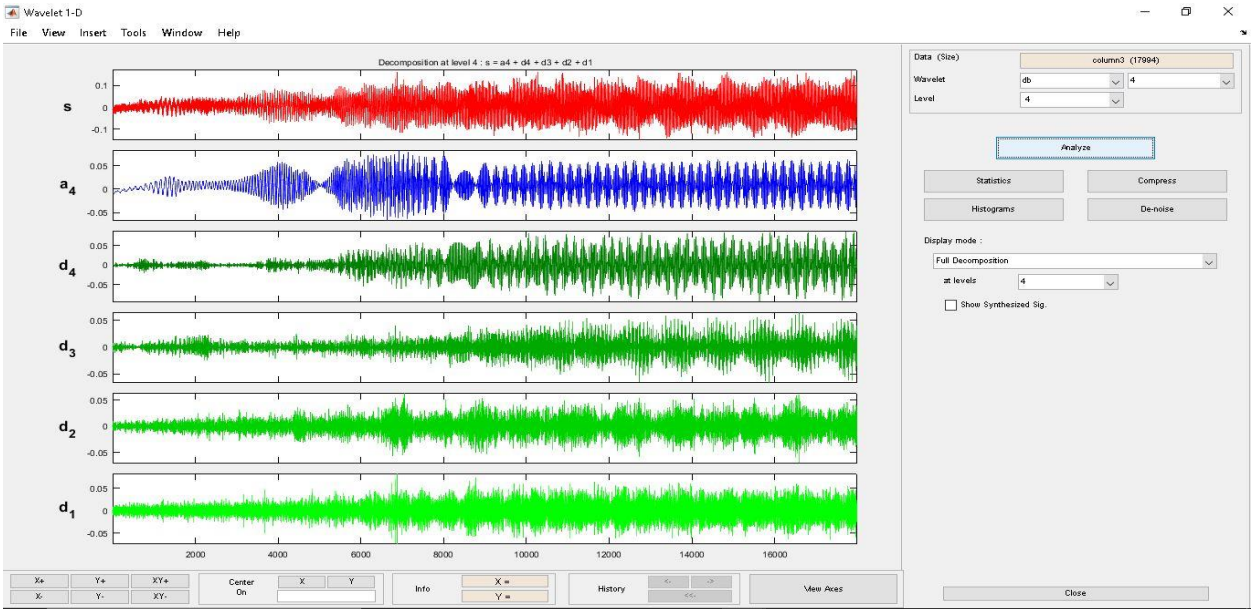

Figure 3.47. Daubechies wavelet calculation of horizontal acceleration on bearing 2 with variable speed 0-34 Hz with unbalance mass 4.95 g on disk 1 in position 0°.

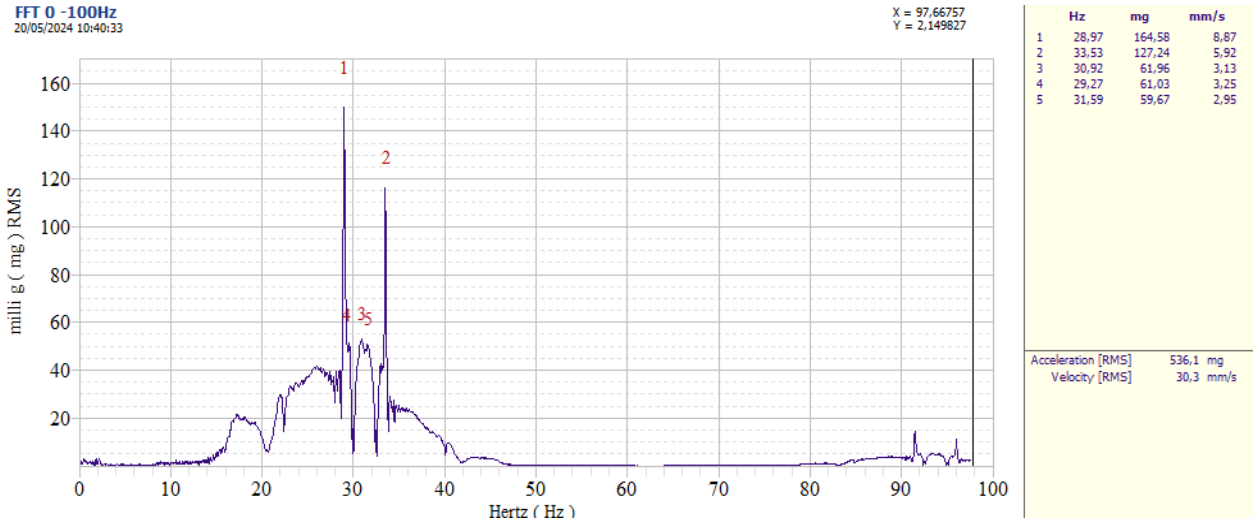

Figure 3.48. Daubechies wavelet spectrum of vertical acceleration on bearing 2 with variable speed 0-34 Hz with unbalance mass 4.95 g on disk 1 in position 0°.

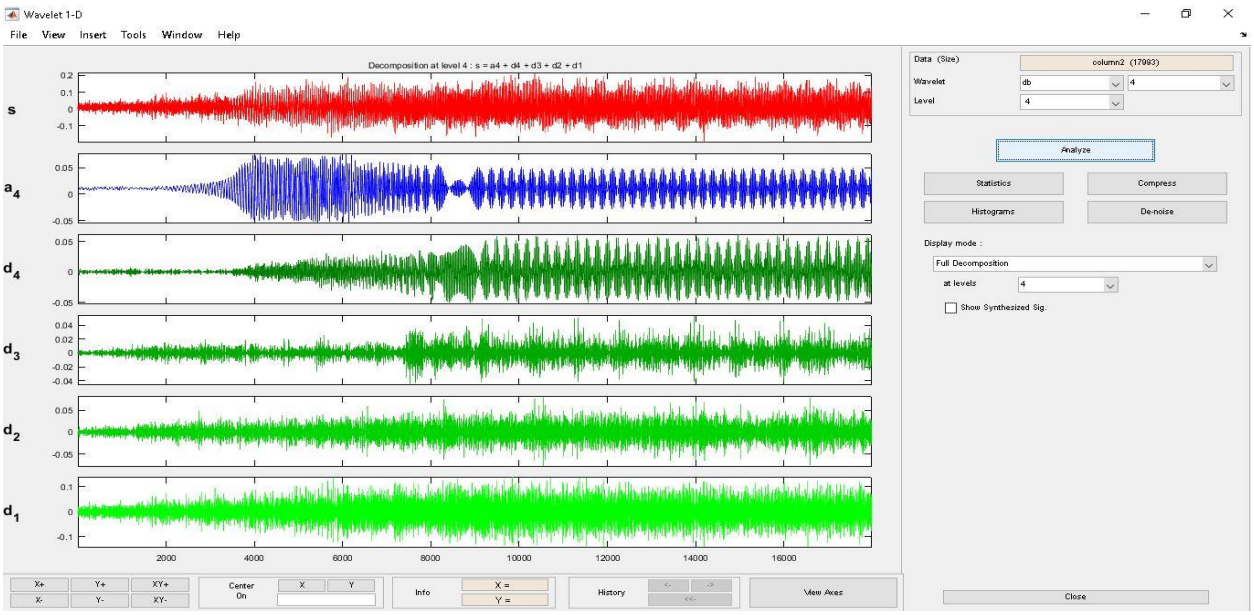

Figure 3.49. Daubechies wavelet calculation of vertical acceleration on bearing 1 with variable speed 0-34 Hz with unbalance mass 4.95 g disks 1 and 2 in position 0°.

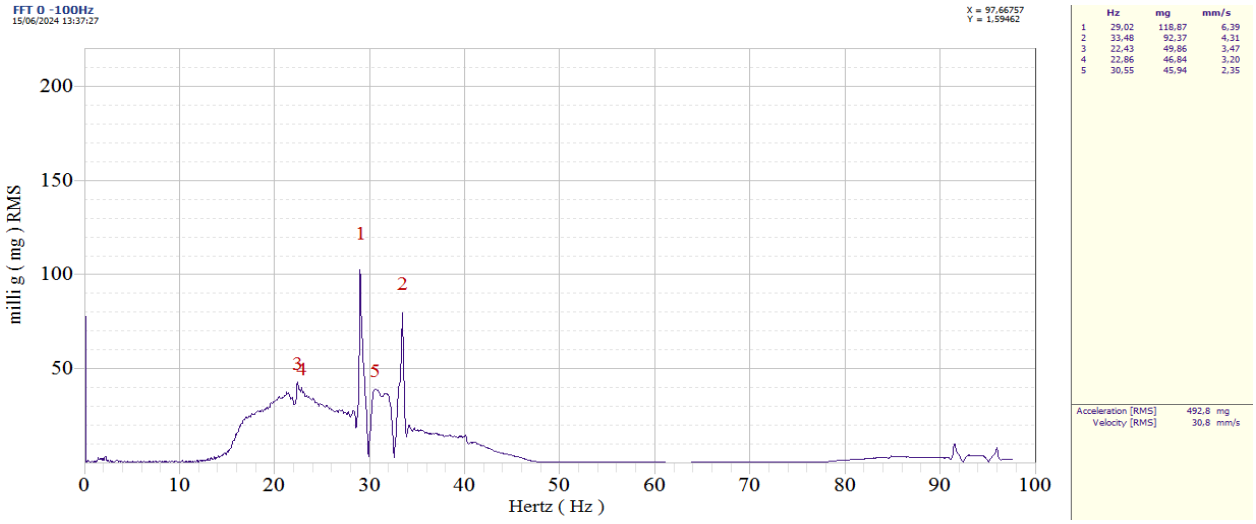

Figure 3.50. Daubechies wavelet spectrum of vertical acceleration on bearing 1 with variable speed 0-34 Hz with unbalance mass 4.95 g on disks 1 and 2 in position 0°.

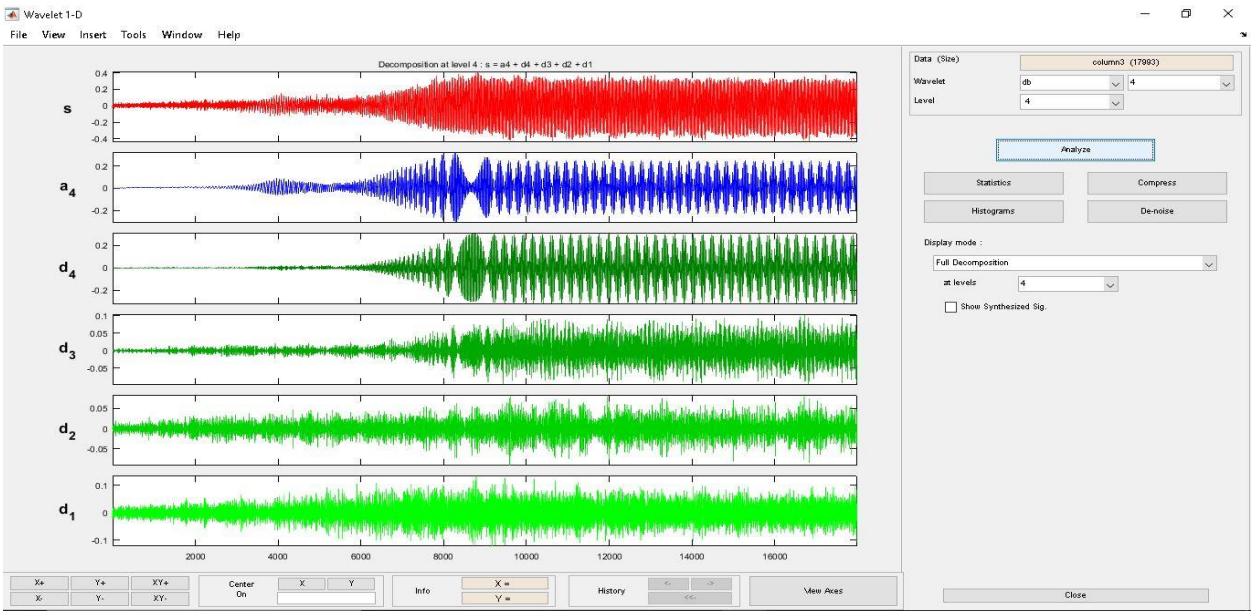

Figure 3.51. Daubechies wavelet calculation of vertical acceleration on bearing 2 with variable speed 0-34 Hz with unbalance mass 4.95 g disks 1 and 2 in position 0°.

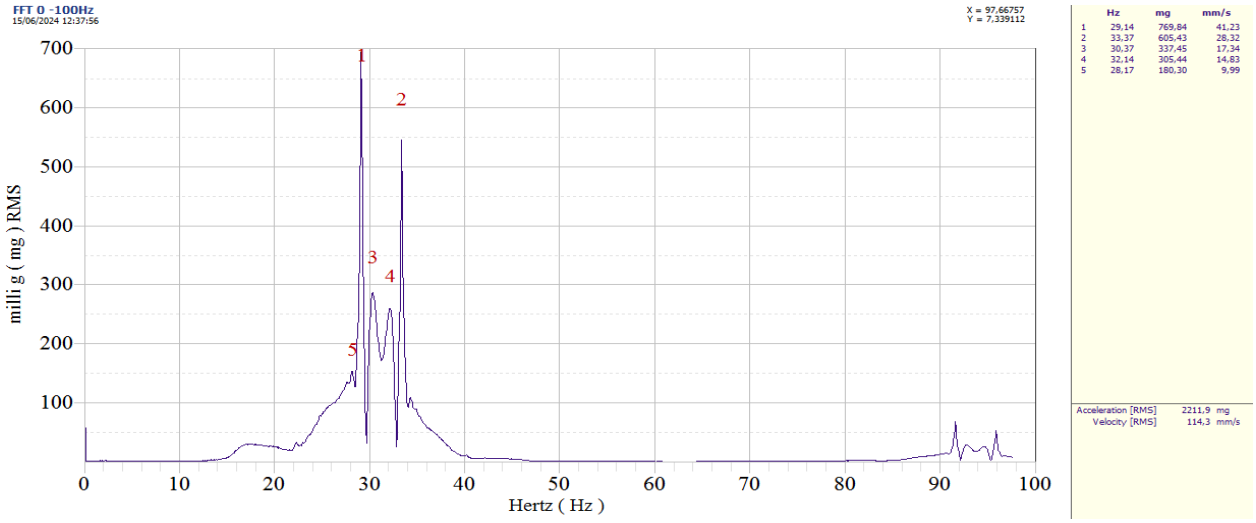

Figure 3.52. Daubechies wavelet spectrum of vertical acceleration on bearing 2 with variable speed 0-34 Hz with unbalance mass 4.95 g on disks 1 and 2 in position 0°.

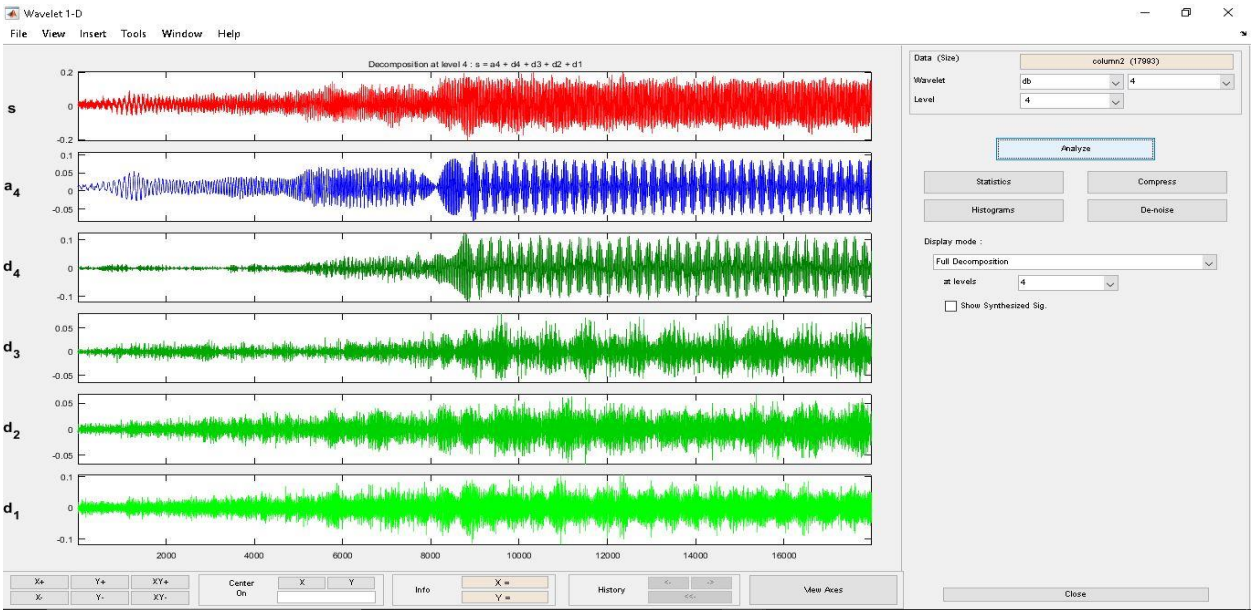

Figure 3.53. Daubechies wavelet calculation of horizontal acceleration on bearing 1 with variable speed 0-34 Hz with unbalance mass 4.95 g disks 1 and 2 in position 0°.

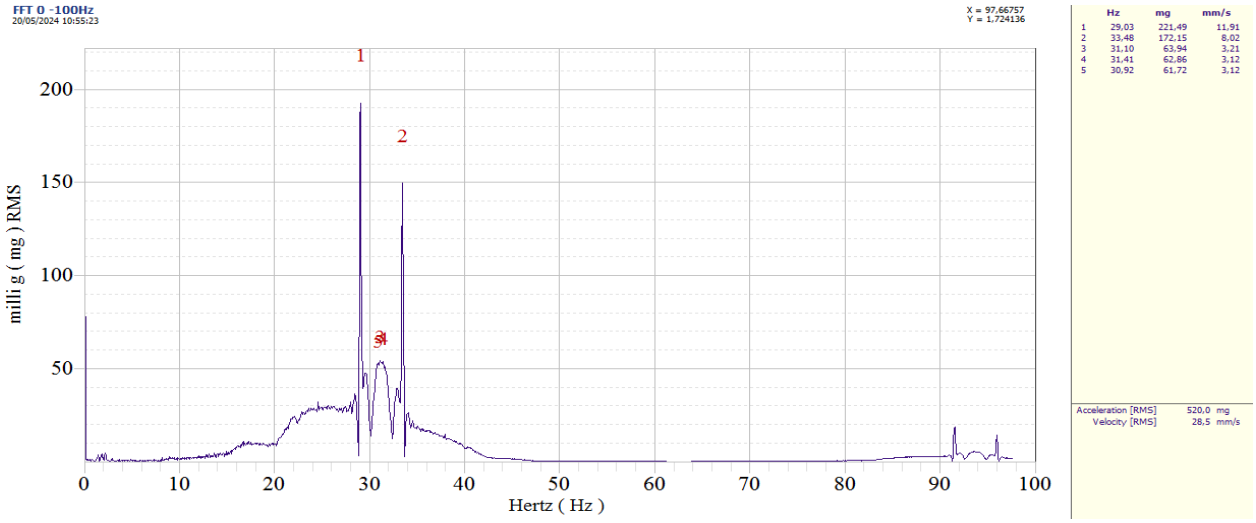

Figure 3.54. Daubechies wavelet spectrum of horizontal acceleration on bearing 1 with variable speed 0-34 Hz with unbalance mass 4.95 g on disks 1 and 2 in position 0°.

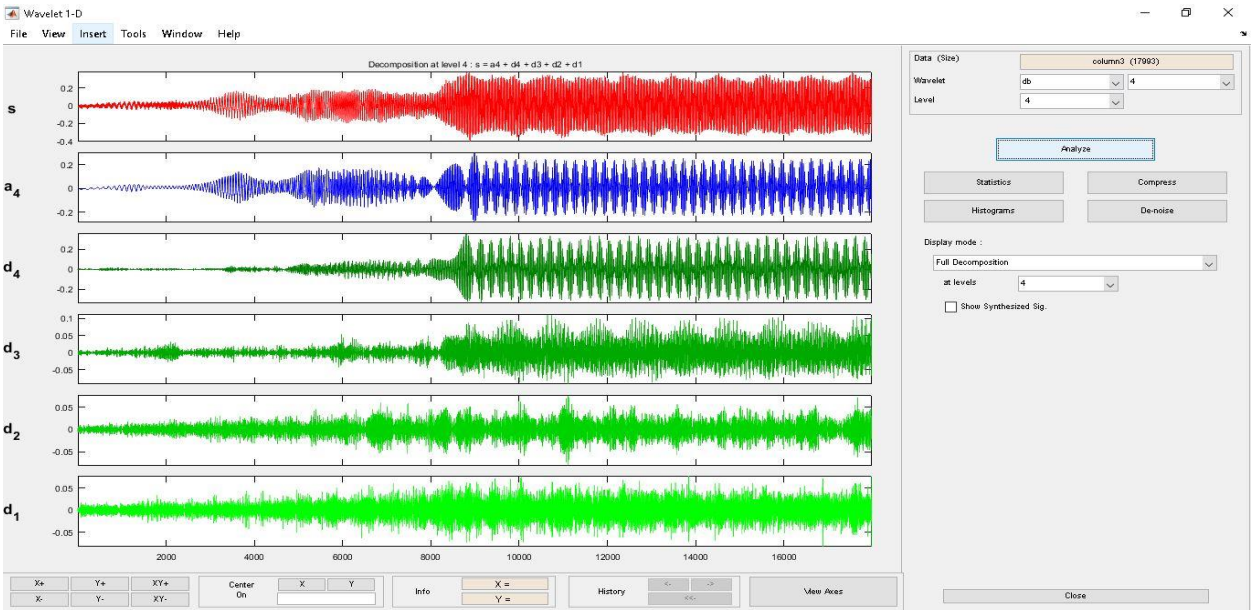

Figure 3.55. Daubechies wavelet calculation of horizontal acceleration on bearing 2 with variable speed 0-34 Hz with unbalance mass 4.95 g disks 1 and 2 in position 0°.

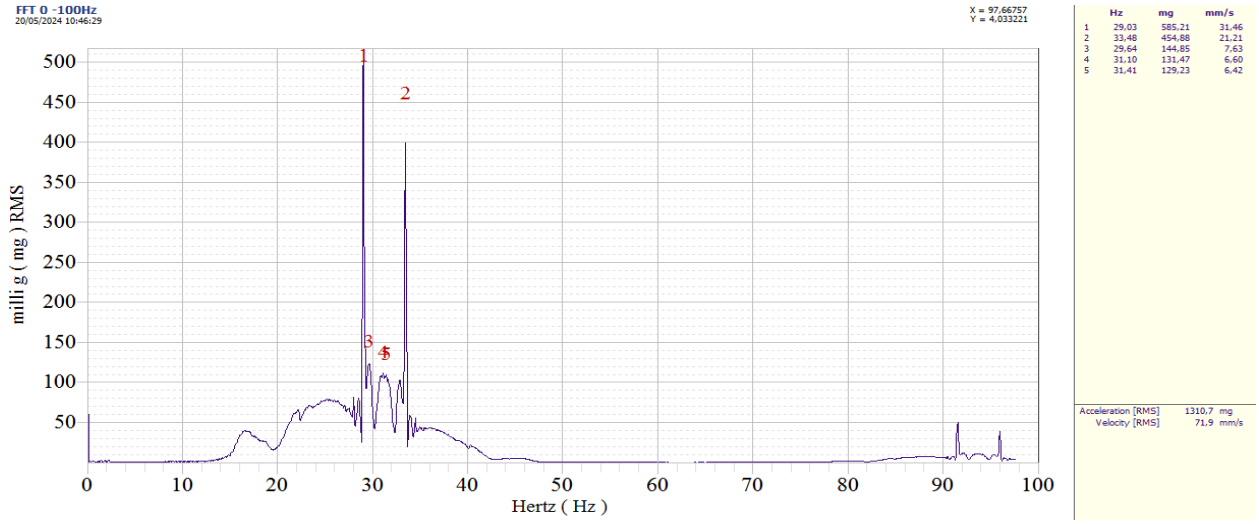

Figure 3.56. Daubechies wavelet spectrum of horizontal acceleration on bearing 2 with variable speed 0-34 Hz with unbalance mass 4.95 g on disks 1 and 2 in position 0°.

3.3.4. Spectra comparison:

In this section, we have superimposed the spectra of the different analyzes to better visualize and make comparison between the different analyzes for the different unbalance fault configurations (figures 3.57-3.68). First of all, note that for all the tests the unbalance is better detected by the spectral analysis in steady state since its intensity is greater than for the other analyses. In the analysis of Daubechies wavelets, the unbalance is less present despite its detection at the stationary frequency of the rotor. But the unbalance has a significant effect at the resonance passing frequency because the intensity of this frequency increases with the increase in unbalance, especially at bearing 2. Then, we notice the disappearance of the misalignment defects in the horizontal direction in the wavelet analysis (figures 3.59-3.61 and 3.63-3.64). This observation can be the subject of additional study.

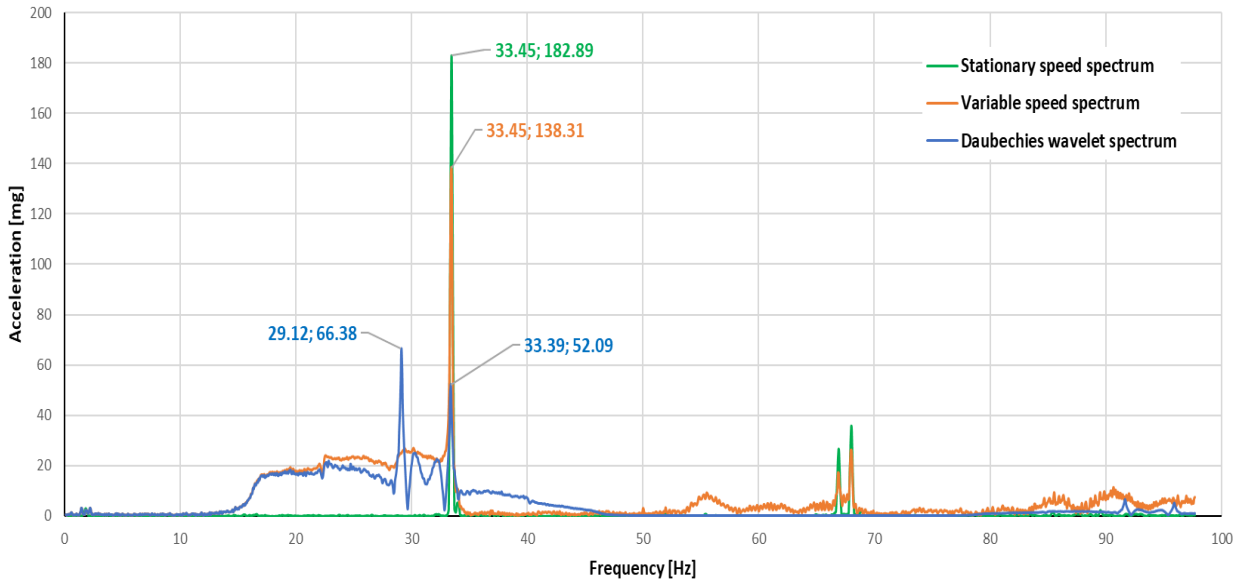

Figure 3.57. Spectra comparison of vertical acceleration on bearing 1 without mass.

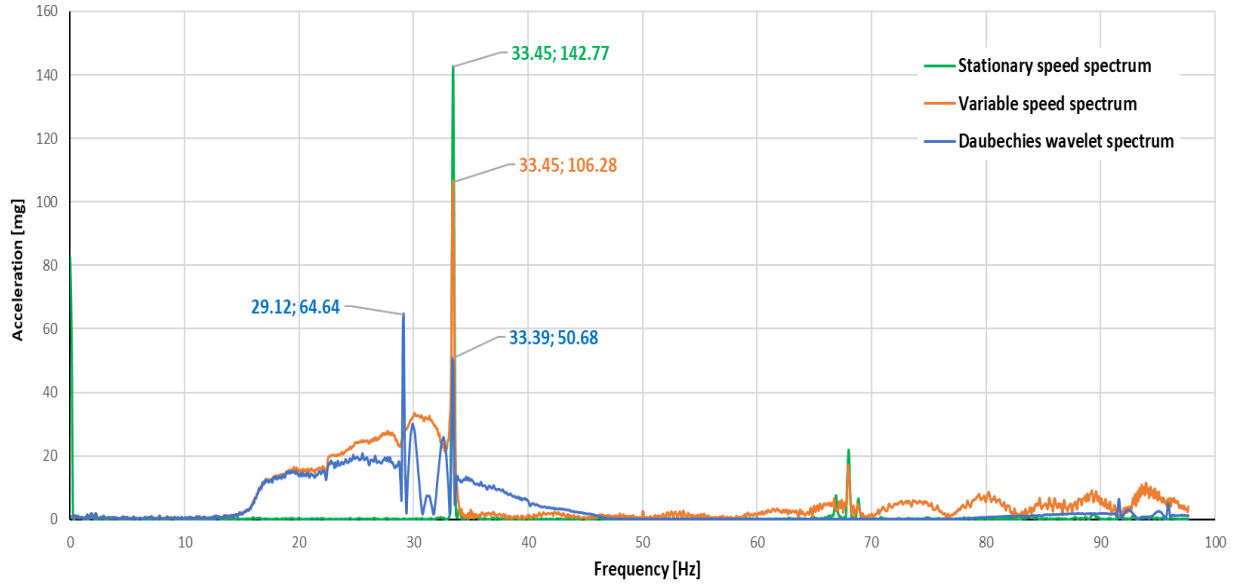

Figure 3.58. Spectra comparison of vertical acceleration on bearing 2 without mass.

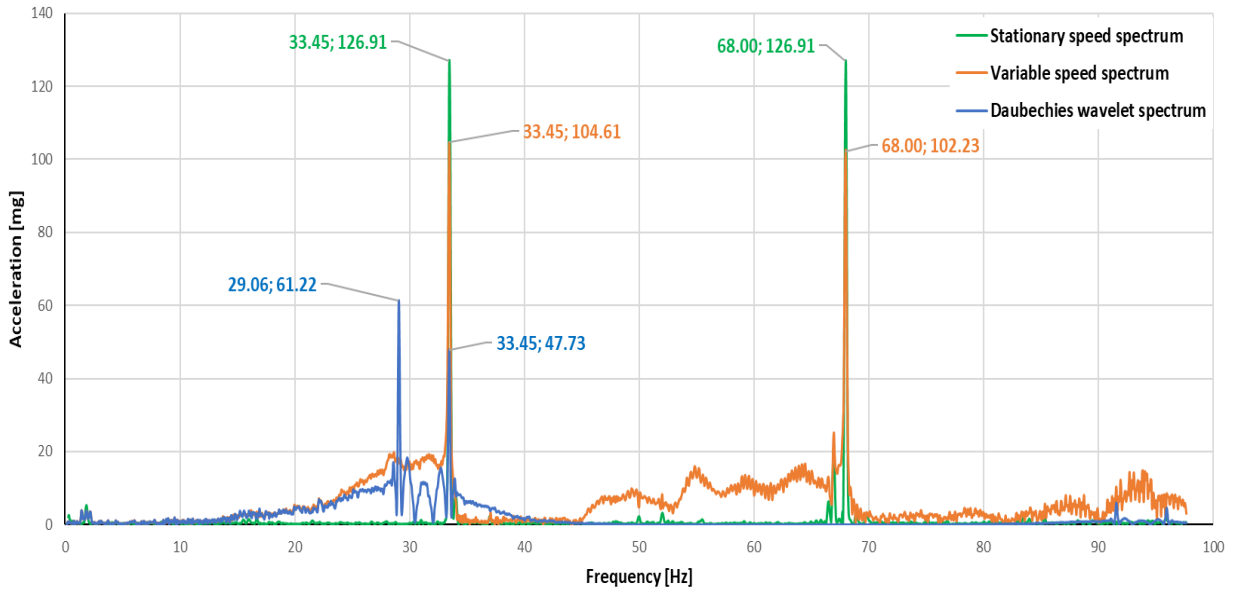

Figure 3.59. Spectra comparison of horizontal acceleration on bearing 1 without mass.

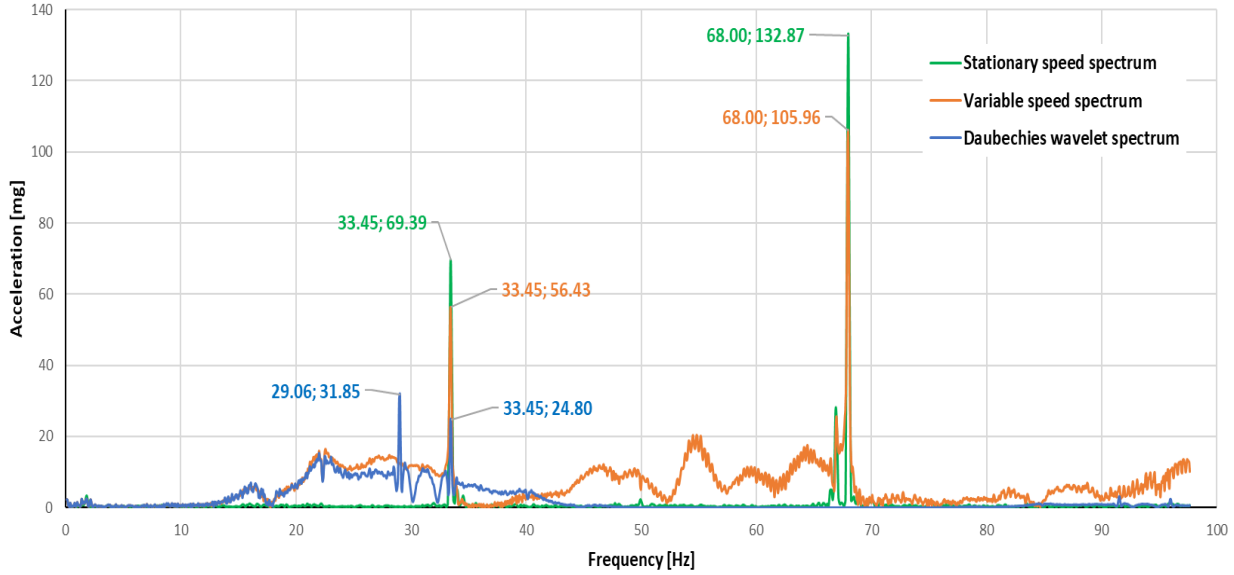

Figure 3.60. Spectra comparison of horizontal acceleration on bearing 2 without mass.

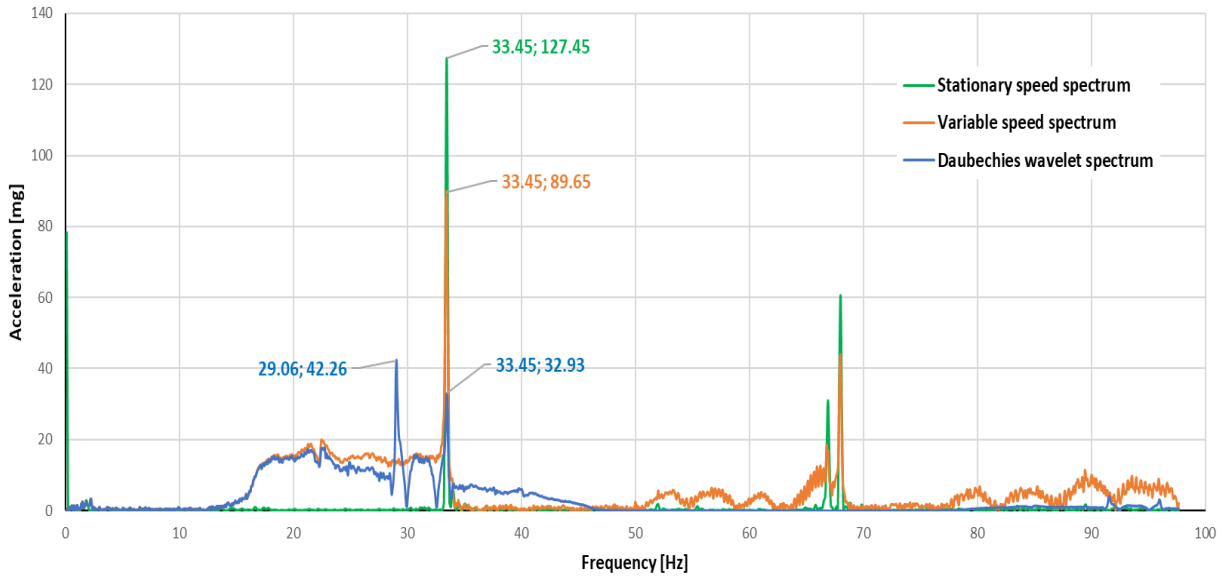

Figure 3.61. Spectra comparison of vertical acceleration on bearing 1 with mass 4.95 g on disk 1.

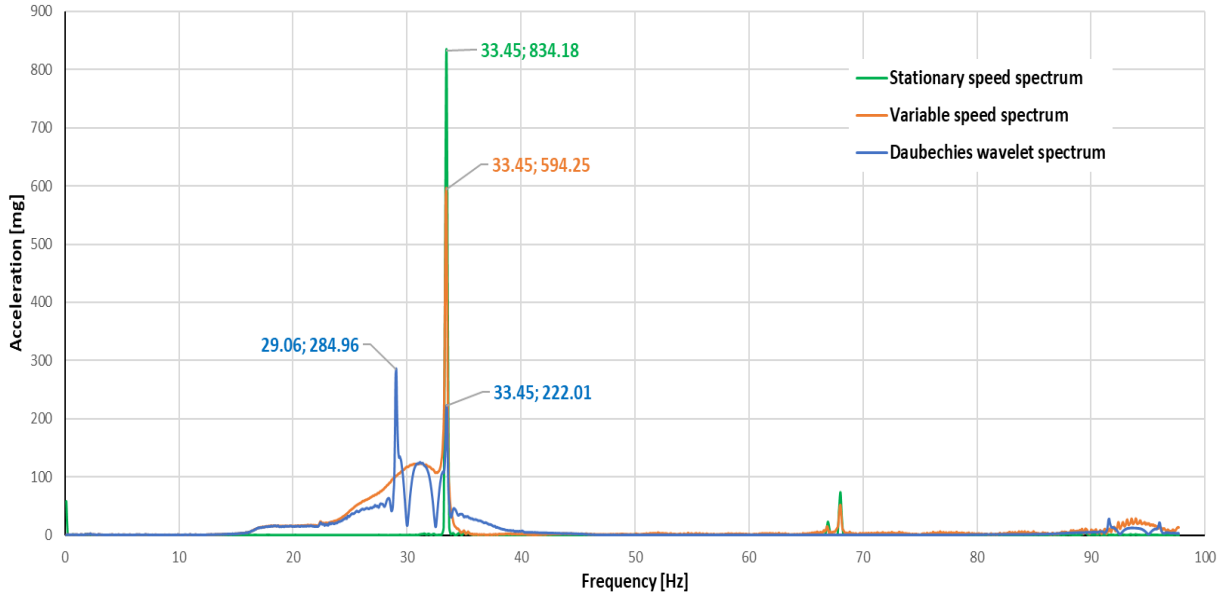

Figure 3.62. Spectra comparison of vertical acceleration on bearing 2 with mass 4.95 g on disk 1.

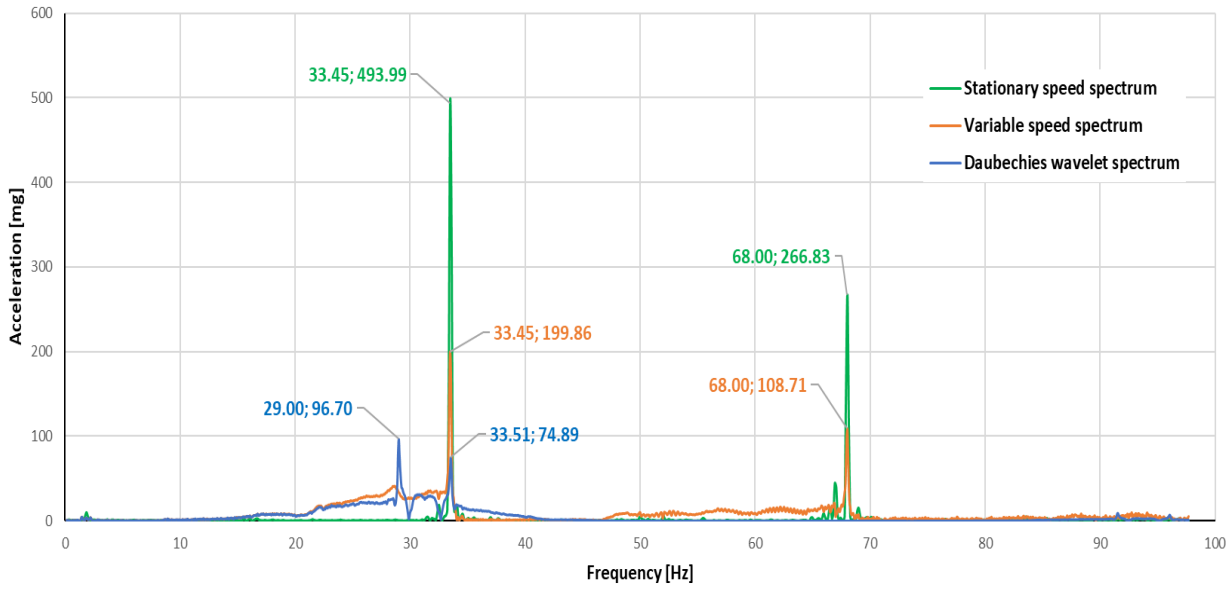

Figure 3.63. Spectra comparison of horizontal acceleration on bearing 1 with mass 4.95 g on disk 1.

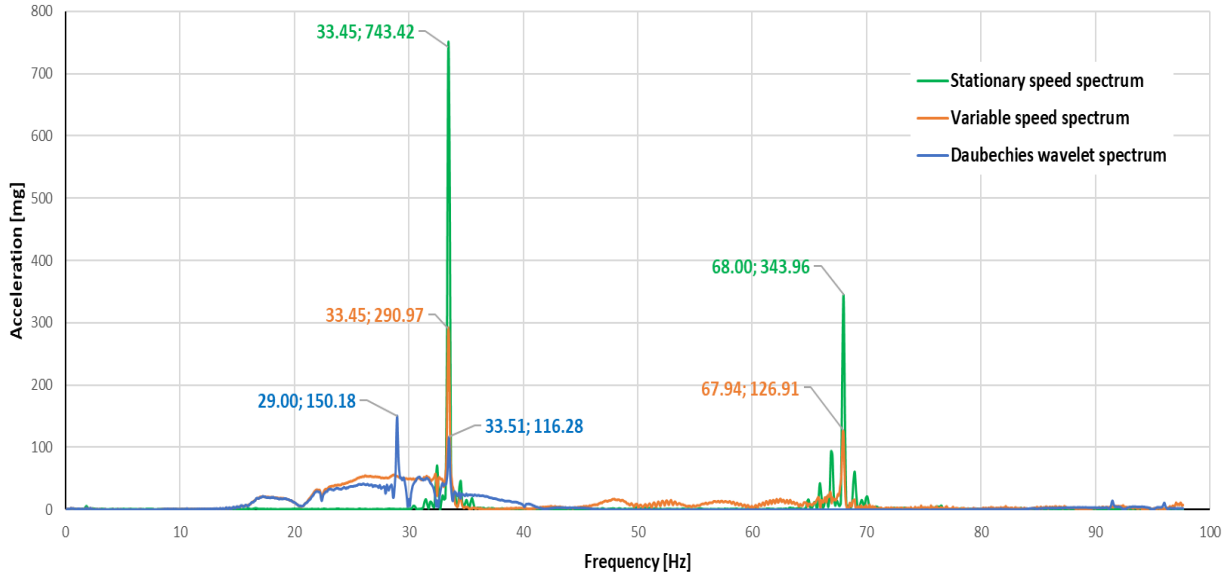

Figure 3.64. Spectra comparison of horizontal acceleration on bearing 2 with mass 4.95 g on disk 1.

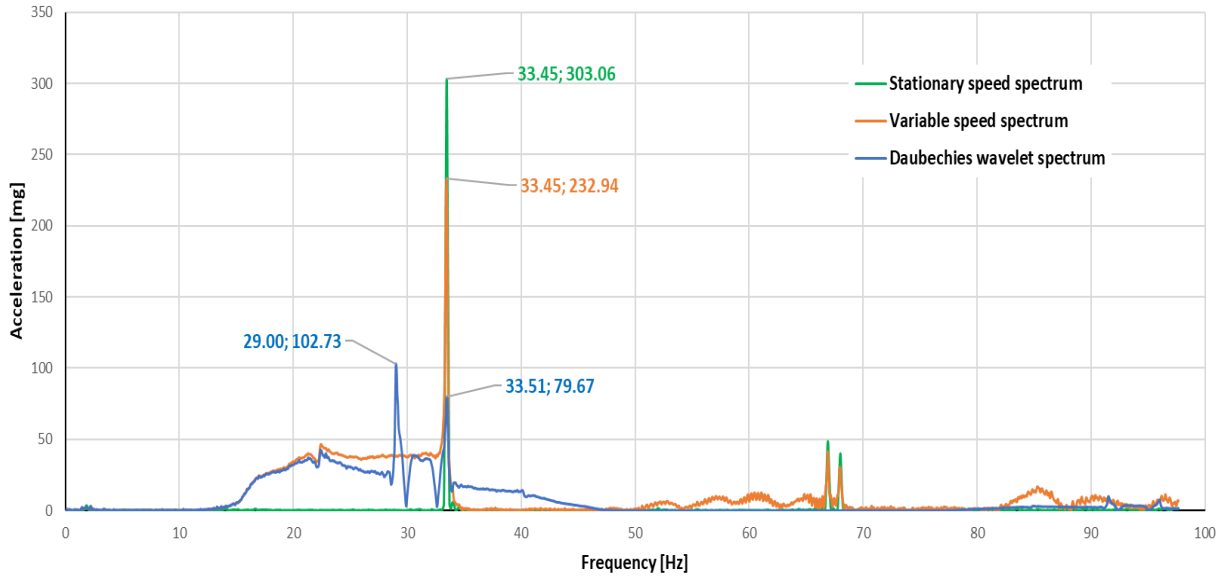

Figure 3.65. Spectra comparison of vertical acceleration on bearing 1 with masses 4.95 g on disk 1 and 2.

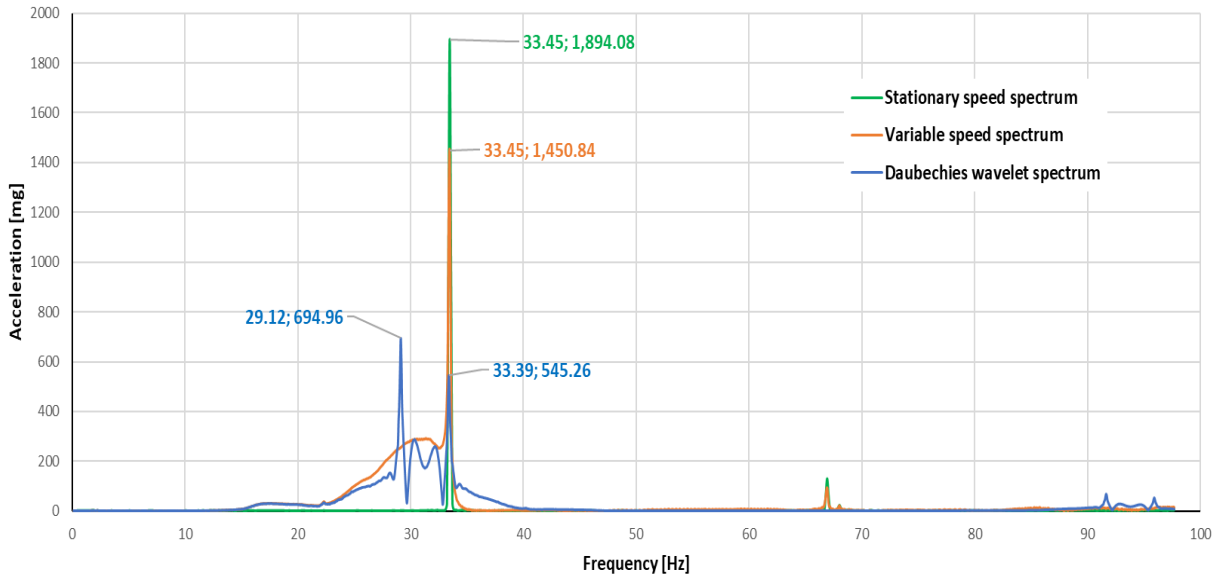

Figure 3.66. Spectra comparison of vertical acceleration on bearing 2 with masses 4.95 g on disk 1 and 2.

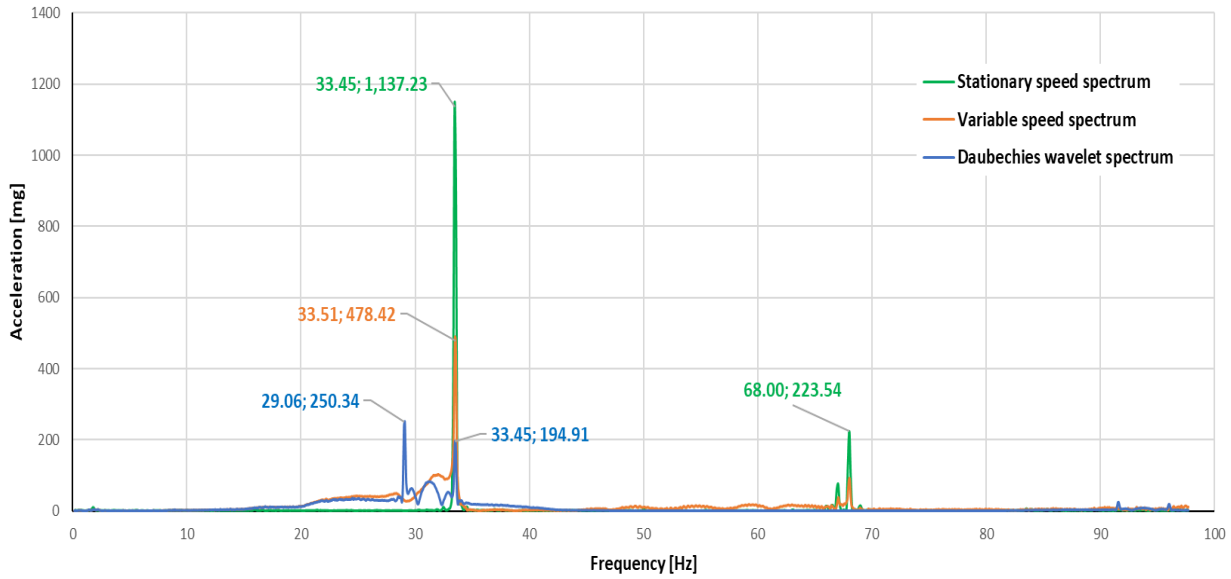

Figure 3.67. Spectra comparison of horizontal acceleration on bearing 1 with masses 4.95 g on disk 1 and 2.

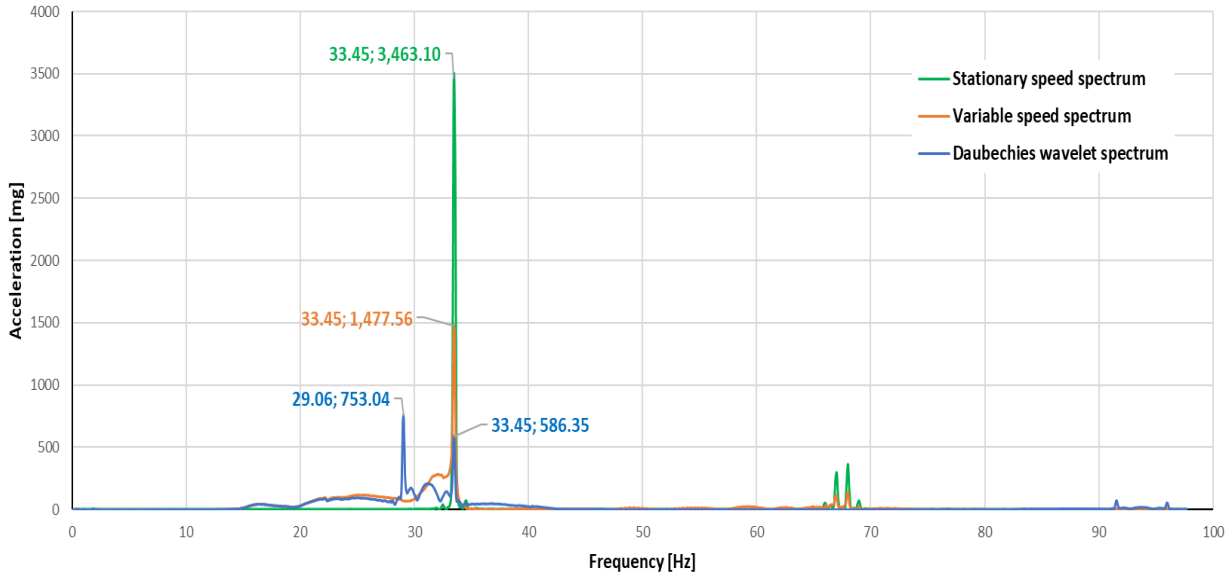

Figure 3.68. Spectra comparison of horizontal acceleration on bearing 2 with masses 4.95 g on disk 1 and 2.

General Conclusion

General Conclusion

The experiment aimed to evaluate the effectiveness of Daubechies db4 wavelet and spectrum analysis in diagnosing faults using a fault simulator under both stationary and non-stationary speed conditions. The results revealed distinct advantages for each method under different conditions.

Under stationary speed conditions, spectrum analysis demonstrated superior performance in detecting mass unbalance faults compared to the db4 wavelet. The spectrum's ability to clearly identify mass unbalance makes it a reliable tool for this type of fault diagnosis in stationary states. Additionally, the spectrum analysis showed a significant advantage in detecting misalignment faults, which were barely detectable using the db4 wavelet analysis.

Conversely, the db4 wavelet analysis exhibited a better performance in identifying resonance frequency passage, which spectrum analysis struggled to highlight. This indicates the wavelet's strength in analyzing transient phenomena and providing more detailed frequency information in certain scenarios.

Furthermore, the db4 wavelet analysis outperformed spectrum analysis under non- stationary speed conditions. The wavelet's adaptability to changing speeds allowed for more accurate fault detection in dynamic environments, showcasing its potential for applications where speed variability is a factor.

In summary, spectrum analysis is more effective for diagnosing mass unbalance and misalignment faults at stationary speeds, while the Daubechies db4 wavelet offers better resonance frequency analysis and superior performance under non-stationary conditions. The complementary strengths of these methods suggest that a combined approach might offer a more comprehensive diagnostic solution across varying operational conditions.

We suggest for future studies to process other wavelet analyzes for different defects and make a comparison between them.

Bibliography

[1]-Grossmann, A., & Morlet, J. (1984). Decomposition of Hardy Functions into Square Integrable Wavelets of Constant Shape. SIAM Journal on Mathematical Analysis, 15(4), 723–736. doi:10.1137/0515056

[2]- Daubechies, I. (1988). Orthonormal bases of compactly supported wavelets. Communications on Pure and Applied Mathematics, 41(7), 909–996. doi:10.1002/cpa.3160410705

[3]-Yaghouti, S. H., Patankar, S. S., & Kulkarni, J. V. (2012). Condition monitoring of rotary machinery using Continuous Wavelets. 2012 IEEE International Conference on Computational Intelligence and Computing Research. doi:10.1109/iccic.2012.6510266

[4]- Prabhakar, S., Mohanty, A. R., & Sekhar, A. . (2002). Application of discrete wavelet transform for detection of ball bearing race faults. Tribology International, 35(12), 793–800. doi:10.1016/s0301-679x(02)00063-4

[5]-Hocine,B., & Salah,B. &, Mohamed.S.B (2012). Application of Wavelet Transform for Fault Diagnosis in Rotating Machinery. International Journal of Machine Learning and Computing 2(1):82-87. doi : 10.7763/IJMLC.2012.V2.93

[6]- Ahamed, S. K., Karmakar, S., Mitra, M., & Sengupta, S. (2010). Novel diagnosis technique of mass unbalance in rotor of induction motor by the analysis of motor starting current at no load through wavelet transform. International Conference on Electrical & Computer Engineering (ICECE 2010). doi:10.1109/icelce.2010.5700732

[7] C. Sidney Burrus, Ramesh A. Gopinath, and ,Haitao Guo. Introduction to Wavelets and Waavelet Transforms (1998)

[8] Thakral, S., & Manhas, P. (2018). Image Processing by Using Different Types of Discrete Wavelet Transform.

[9] Haar A.: Zur Theorie der orthogonalen Functionsysteme. Math Annal. No 69, pp. 331-371. (1910)

[10] Govindan, V., Chakraborty, R. S., Santikellur, P., & Chaudhary, A. K. (2018). A Hardware Trojan Attack on FPGA-Based Cryptographic Key Generation: Impact and Detection. Journal of Hardware and Systems Security. doi:10.1007/s41635-018-0042-5

[11] Daubechies I.:"Orthonormal bases of compactly supported wavelets" Commun. Pure Appl. Math. , 41 (1988) pp. 909–996

[12] Yves M, Daubechies wavelets, Chapter 2, 1999 CRC Press LLC

[13] George Lindfield, John Penny, in Numerical Methods (Fourth Edition), 2019

[14] Mohamed E, Mirjam J, and Friso D.: R Wave Detection using Coiflets Wavelets.(2014)

[15] Elgendi, M., Jonkman, M., & De Boer, F. (2009). R wave detection using Coiflets wavelets. 2009 IEEE 35th Annual Northeast Bioengineering Conference. doi:10.1109/nebc.2009.4967756

[16] Discrete Wavelet Denoising into MFCC for Noise Suppressive in Automatic

Speech Recognition System, Article in International Journal of Intelligent Engineering and Systems · April 2020

[17] © 1994-2005 The MathWorks, Inc. symlets

[18] Jyotsna, Rajpal, N., & Vishwakarma, V. P. (2016). Face recognition using Symlet, PCA and cosine angle distance measure. 2016 Ninth International Conference on Contemporary Computing (IC3). doi:10.1109/ic3.2016.7880231

[19] Deliou A. (2013, juin 22). Extraction des caractéristiques fréquentielles des signaux biomédicaux et g acoustiques par des algorithmes basées sur des techniques temps fréquence non paramétriques. Faculté des sciences, Agadir

[20] Assous S. (2005, décembre 14). Time-frequency analysis by the S transform and interpretation of the laser Doppler flowmetry signals: clinic diagnosis applications. Ecole Nationale Supérieure d'Arts et Métiers.

[21] George N V. (2009). S Transform: Time frequency analysis & filtring. Department of Electronics and Communication Engineering, National Institute of Technology,Rourkela, India

[21] Mi, X., Ren, H., Ouyang, Z., Wei, W., Ma, K. (2005). The use of the Mexican hat and the Morlet wavelets for detection of ecological patterns. Plant Ecology, 179(1), 1–19. DOI 10.1007/s11258-004-5089-4.

[22] Matlab Official Website / wavelet families

[23] https://reference.wolfram.com/language/ref/DGaussianWavelet.html

[24] Johns Hopkins APL Technical Digest. THE CONTINUOUS WAVELET TRANSFORM: A TOOL FOR SIGNAL INVESTIGATION AND UNDERSTANDING, Volume 15, Number 4 (1994)

[25] A. N. Skodras, 'Discrete Wavelet Transform: An Introduction, Technical Report HOU-CS-TR-2003-02-EN

[26] Palle E, Myung S Comparison of Discrete and Continuous Wavelet Transforms, 2007

[27] Rhif, M., Ben Abbes, A., Farah, I., Martínez, B., & Sang, Y. (2019). Wavelet Transform Application for/in Non-Stationary Time-Series Analysis: A Review. Applied Sciences, 9(7), 1345. doi:10.3390/app9071345

[28] MATLAB Official Web